Title
THE PRODUCTION, REACTIONS AND SPECTRA OP LOW-VALENT, HIGHLY REACTIVE CHEMICAL SPECIES - WITH SPECIAL EMPHAS ON THE PHOSPHORUS-FLUORINE SYSTEM

Author
Solan, David.

Publication Date
1969-08-01

UCRL-19049

eg. I

THE PRODUCTION, REACTIONS AND SPECTRA OF LOW-VALENT, HIGHLY REACTIVE CHEMICAL SPECIES - WITH SPECIAL EMPHASIS ON THE PHOSPHORUS-FLUORINE SYSTEM

David Solan
(Ph. D. Thesis)

August 1969

AEC Contract No. W-7405-eng-48

LAWRENCE RADIATION LABORATORY
UNIVERSITY of CALIFORNIA BERKELEY

UCRL-19049

eg. I

DISCLAIMER

TABLE OF CONTENTS

LIST OF FIGURES AND TABLES

FIGURES

TABLES

and ultraviolet absorption spectra, making them readily amenable to analysis.

Radicals investigated in this work include GeH_2, SiF_2, GeF_2, PF_2, PF and CS. New compounds formed include GeH_3SiF_2H, GeH_3SiF_3(?), $GeH_3Si_2F_4H$, $GeH_3Si_3F_6H$(?), P_3F_5, and P_4F_6.

The fluorogermylsilanes were made by cocondensation of SiF_2 and GeH_4. This was shown not to be a true cocondensation reaction for it took place, to some extent upon warmup of the resulting solid.

P_3F_5 and P_4F_6 were made by the cracking of P_2F_4 at 900°C followed by the immediate condensation of the products of this cracking at 77°K. Both of these fluorides are unstable, but P_4F_6 has been stabilized in carbon disulfide solution at room temperature. P_4F_6 has been characterized through mass spectra, fluorine and phosphorus nmr spectra, infrared absorption spectra and elemental analysis.

P_2F_4 was shown to undergo heterolytic and homolytic fission, when pyrolyzed at 700°C, to form PF and PF_2 radicals. PF was identified mainly through its ultraviolet absorption spectrum, while PF_2 was identified by means of mass, infrared and epr spectroscopy. Thermodynamically, it has been shown that both of these fissioning processes are very favorable, though most likely the PF and PF_2 species are not reaching equilibrium with respect to PF_3 and phosphorus.

Photolysis of P_2F_4 in the matrix environment produces PF_3 and P_3F_5 in an unusual "excitation photolysis," wherein the reaction takes place, in the matrix environment, between excited chemical species, as opposed to fragments of excited species.

THE PRODUCTION, REACTIONS AND SPECTRA OF LOW-VALENT, HIGHLY REACTIVE CHEMICAL SPECIES - WITH SPECIAL EMPHASIS ON THE PHOSPHORUS-FLUORINE SYSTEM Thesis

David Solan

Inorganic Materials Research Division, Lawrence Radiation Laboratory,
and Department of Chemistry,
University of California, Berkeley, California

ABSTRACT

This dissertation concerns research into the production and synthetic use of low-valent, high temperature species. The radicals produced and the products they formed were identified, and their structure and bonding illucidated, by such means as mass spectroscopy, infrared and ultraviolet spectroscopy, nuclear magnetic resonance (nmr) spectroscopy, and various vacuum line techniques (such as molecular weight, vapor pressure, or melting point determination).

Reactions were carried out by means of "cocondensation reactions." In this method, high energy species are cocondensed with molecules of a reactant on a 77°K surface. Reactions proceed in the "liquid-like, intermediate, transitory" ("LLIT") state of matter formed while condensation is proceeding, and upon warmup of the resulting solid, the products being pumped off and handled in a vacuum line.

As a further means to understand the nature of the species being reacted, matrix isolation spectroscopy was utilized. Here materials are produced and quickly condensed on a nearby transparent surface at 20°K along with a large excess of inert gas. Such a process stabilizes high energy species for spectroscopic investigation and allows further treatments to be made, such as photolyses and diffusion-controlled reactions upon warmup. Also, matrix isolation has a simplifying effect on infrared

Some or all of the fundamental modes of vibration in the matrix environment have been determined for each of the following species using infrared absorption spectroscopy: PF, PF_2, PF_3, P_2F_4, P_3F_5 and P_4F_6.

INTRODUCTION

A. Production and Synthetic Use of Radicals

For the purposes of this dissertation, a "radical" will be defined as a low-valent, highly reactive chemical species, a definition which includes the species of "free radical," defined as a radical with an odd, unpaired electron. Radicals are usually the fragments of stable molecules formed under highly energetic conditions, and are usually quite short-lived.

The existence of radicals has been hypothesized for many years to explain the mechanism of a variety of reactions, but since they were regarded as transitory species incapable of being isolated for detailed investigation, many chemists remained skeptical of such hypotheses. It was not until the pioneering work of Moses Gomberg[1] in 1900 demonstrated the possibility of isolating a stable free radical [$(C_6H_5)_3C\cdot$], and showed what sort of reactions such a radical might be expected to undergo, that all doubts were expelled, and research into the production and synthetic use of radicals began to accelerate greatly (of course radicals have other peculiar properties, besides their inordinate reactivity, which make them entities of chemical importance, but this is the one property that will be emphasized in this dissertation).

Before use can be made of the high energy of radicals to synthetic advantage, they must first be produced. Therefore, a brief description of the general means used to produce radicals for synthetic purposes will now be given.

One of the earliest used sources of energy input to form radicals from stable compounds was simply the application of heat. This method

is particularly useful in the gaseous state, both because of the fast cooling rates achievable in a gas, after thermal excitation has occurred, to stabilize the products of the reaction, and because few common solvents will remain liquid at high temperatures. Furthermore, in the gaseous state, translational and rotational entropy are less for whole molecules than for the fragmentary species they are composed of, so it would be expected that at high temperatures in the gas, the $T\Delta S$ term of the free energy would predominate for the latter species making them thermodynamically favorable.

In the thermal production of radicals, we rarely have equilibrium with respect to all possible species that could form from the elements present (an exception to this rule would be the reaction, $BF_3(g) + 2B(c) \rightarrow 3BF(g)$ at 1700°C, used by Timms[2] to study the chemistry of the BF radical). Rather, the input of thermal energy causes a sequence of reactions to occur that produce intermediate, high energy products whose further decomposition is kinetically hindered, though not thermodynamically prohibited. These intermediate radicals can then be made to react with another compound to form the final products. An example of such a situation is the thermal decomposition of N_3CN to N_2 and N=C=N radicals at 50°C in solution.[3] If the solvent for this material is unreactive towards it, a resin forms. If a reactant is present that can quickly react with the NCN radicals before they engage in the more thermodynamically favored process of polymerization, new products will form.

<u>In situ</u> production of radicals by thermolysis, as is the case with NCN, is a rarely used method to produce radicals for synthetic purposes because the heat input could also destroy the reactant at the same time it was producing the radical. Therefore, in this method, the production

of the radical is usually carried out at some distance from the point of reaction, to which the radical, after formation, is quickly brought before it decomposes.

On the other hand, photochemical formation of radicals is much more amenable to in situ production and reaction. Photolysis can be a very selective means of raising the energy of just one type of molecule in a mixture. The energy absorption process can also put a much greater amount of energy into one molecule than thermal methods can. However, the very concentration of energy the procedure produces in one molecule militates against a high concentration of excited molecules at any one time (the exception being flash photolysis). Thus reactions must usually be carried out over a period of time which requires the simultaneous presence in the same space of both the radical-forming compound and the reactant, a condition which could lead to the decomposition of the reactant or the products of the reaction by the irradiating light.

The possibilities exist in photolysis that the absorbing molecule will rearrange after excitation or fragment into other species which will then undergo further reaction. Many secondary reactions can take place under such conditions because the excited molecules are very far from equilibrium. In particular, the possibility of a chain reaction exists, where a radical, usually a doublet, reacts with the reactant present in a series of reactions to form the desired product, but also to reproduce the original radical. Such a reaction propagates its own continuance as long as reactant is available and so is called a chain reaction.

Under normal photolysis conditions, a "steady-state" concentration of the radical undergoing reaction is always present, since its rate of formation would equal its rate of reaction. This concentration would be

very low, in contrast to thermolysis and to some methods to be mentioned later on.

Photolysis can be carried out in all three states of matter. In the condensed liquid or solid states, the complication of "geminate recombination" can occur. When the two highly reactive species, formed by the absorption of a photon causing the breaking of a bond, cannot move away from each other faster than the rate of quenching by their surroundings, due to the high viscosity of these surroundings, they might recombine to form the original molecule with no net reaction. This is called the "cage effect." The quenching rate of the state in which the photolysis takes place has one other very important effect. Radical reactions usually give off large quantities of energy which initially reside in the products of these reactions. In condensed media, however, the high relaxation rates quickly remove these large quantities of energy before they destroy the products of the reaction. In the gas, the quenching is reduced considerably, and therefore the probability of decomposition or secondary reaction of the products of the radical reaction is correspondingly increased.

Chemical means are one of the most common modes of radical production for synthetic purposes. In this method, a chemical reaction results in the formation of a radical which then reacts further with other materials present to form new products.

Other means of radical production include discharge (silent and spark, as well as microwave) and radiolysis. In the former method, large electric fields are used to break up molecules (silent electrical), or ion bombardment is used (spark discharge), or very rapidly oscillating fields effect a breakdown of the molecule (microwave). Radiolysis is

the use of high energy particles or ionizing radiations to promote a reaction. In such a procedure, many thousands of molecules could be fragmented or even ionized by a single photon or high energy particle. This method is highly non-uniform, produces many secondary effects, and is difficult to interpret in most cases. It is commonly used in the formation of very small concentrations of radicals in solids for epr investigation.

Once radicals have been produced, they must be identified. In most cases, spectroscopic evidence is taken as the only valid proof for the existence of a radical (C_3 in the excited triplet state might be an exception, since it has been recognized chemically, but, to my knowledge, has never been positively identified spectroscopically[4]). Since radicals are short-lived, at least in the gaseous state, flash photolysis followed by rapid scan absorption or fluorescence can be a powerful tool in their identification. A unique variant of the rapid scan technique is the phase shift method, which makes use of the correspondence of the lifetime of an excited state of a radical with the period of the amplitude modulated exciting frequency it absorbs in its ground state. Another method of spectroscopic identification, utilized in this research, involves the trapping and isolating of a radical at very low concentrations in an inert solid environment, usually at low temperatures, where it can be observed in either absorption or fluorescence at one's leisure, because of its effective stability in such surroundings.

After a radical has been identified, its synthetic characteristics can be more easily interpreted. It can be said that an investigation of the reactions of a radical is another way of identifying it, the identification being carried out through <u>chemical</u> means.

The two general modes of radical reactions are abstraction and addition. In abstraction, the radical forms a bond with one of the atoms of a molecule while a bond between this atom and the rest of the molecule breaks. In the case of doublet radicals undergoing abstraction with a reactant, the molecule formed which contains the radical within its structure can be quite stable, while the fragment left is another doublet that can undergo further reactions until chain terminations occur, (unless, of course, the reactant is in elemental form to begin with, in which case no reactive fragments are left at all, as was the case with the early "mirror method" used to detect free radicals, where the disappearance of a metallic mirror when a gas was passed over it was taken as evidence for the presence of free radicals in that gas). In the case of triplet radicals, such abstraction reactions lead to two radicals which can either combine with each other or with another radical like themselves. In addition reactions, the radical simply adds onto a stable compound, either through bond insertion (which really indicates an end result rather than a mechanistic detail) or multiple bond breaking, to form another (stable) compound. An example of the former would be the reaction[5] of $Si(CH_3)_2$ with $(CH_3)_3SiH$ to produce $(CH_3)_3SiSi(CH_3)_2H$, and of the latter would be the reaction of CF_2 with C_2H_4 to produce $F_2C\begin{smallmatrix}CH_2\\CH_2\end{smallmatrix}$.[6] Radicals which undergo addition reactions in which one old bond is broken and two new ones are formed, like the ones just mentioned, are called "carbenoids," from the similarity of their mode of reaction with that of carbenes (divalent carbon species).

The exact mechanism of bond insertion can be quite different for different types of radicals, or even different types of the same radical. For instance, two different types of bond insertion can be distinguished from one another on the basis of whether the configuration of a stereoisomeric reactant is retained after reaction or not. In the addition of NCN radical

to trans-1,2-dimethylcyclohexane as a paraffinic substrate, over 98% yields of trans-1,2-dimethyl-1-methylaminocyclohexane were produced, showing that the reaction was stereospecific. Yet when the same reaction was carried out in methylene bromide solution, a 50-50 mixture of the cis and trans isomers of this product was produced, showing that the NCN was adding here in a non-stereospecific manner.[3] Thirteen years ago Skell and Woodworth[7] proposed that the stereospecificity of a radical reaction depended on the electronic multiplicity of the radical undergoing reaction. Specifically, they maintained that triplet insertion would require a three step process (owing to spin conservation rules): single bond formation, free rotation about this bond, and deexcitation to the singlet coincident with the second bond forming; and therefore the configuration of the reactant would be lost during the second step. Singlet insertion, on the other hand, would require a single concerted step. Therefore, triplet insertion would be non-stereospecific, while singlet insertion would be stereospecific. Thus, in the example given, NCN would appear to react as a triplet in methylene bromide but as a singlet in a paraffinic substrate.

Two methods of radical reaction were used in this work. In the method of "cocondensation" a radical was formed (using thermal means in this work) separately from the reactant it was to react with. Thus the energy source did not affect the reactant. The radical and the reactant were then both directed towards a liquid nitrogen cooled surface (at -196°C or 77°K) upon which they both condensed simultaneously. The entire process was done at such low pressures that the possibility of gas phase reaction was nil, so that the reaction took place during or after the condensation process at the surface. Since rapid cooling can take place on the cold surface, secondary or chain reactions were reduced to a minimum. More will be said about this type of reaction in the next section of this dissertation.

The second method of radical production and reaction used in this work was that of matrix photolysis. This method will also be elaborated on in the next section of this dissertation.

B. Matrix Isolation Spectroscopy - A Brief Description and History

Matrix isolation spectroscopy is a technique of trapping in a solid and taking the spectrum of a molecule, usually a highly reactive species, that under normal conditions would last only a fraction of a second in the gas phase. It also aids in studying chemical and photolysis reactions. The technique consists of generating the one or more species under investigation and directing a stream of them to impinge onto a transparent target at low temperatures, while simultaneously codepositing on this target a large excess of some inert material (such as krypton, xenon, or nitrogen) introduced separately from a gas handling system. The entire procedure is done at very low pressures and low flow rates of materials. The "matrix" then formed can be investigated at one's leisure as long as the low temperatures are maintained. By convention, the species "isolated" in this way is called the "R" species (for "radical") while the gas in which it is a host is called the "M" gas (for "matrix"). The ratio which describes the dilution of the R species in the matrix is then termed "M/R". A description of the apparatus used is given in the experimental section of this dissertation, while a more detailed explanation of the advantages and usefulness of this technique is given in the next section.

One of the first investigators to do extensive spectroscopic phosphorescent, fluorescent and absorption studies of molecules isolated in a matrix was G. N. Lewis in the early 1940's.[8] Various organic dyes and radical-producing molecules were "frozen" out at low concentrations

(M/R = 1000 to 10,000) in matrices that ranged from boric acid or glucose at ambient temperatures to a mixture of ether, isopentane, and alcohol (to produce a clear glass upon freezing) at 79°K. His method of producing these matrices was simply to dissolve the R species in the M solvent and then quickly cool to solidification. Photolyses were performed at various frequencies in an attempt to form new species, including radicals, which could then be observed in absorption. Gradual warmup experiments, producing diffusion of the trapped R species, were also performed in an attempt to observe reactions of these species in the non-rigid solid medium. Photodissociation, photo-ionization, and photo-oxidation were observed by Lewis in various matrices.

Throughout the 1940's, much use was made of low temperature (or, at least, low viscosity) matrices for phosphorescent studies. The low temperatures facilitated the radiationless relaxation of the excited singlet states to the lowest lying triplet state (through internal conversion and intersystem crossing), which then phosphoresced to the ground state. Thus, fluorescence from these singlet states occurred to a lesser extent, which removed confusing light emissions. The rapid relaxation to the lowest vibrational level of the triplet state combined with the loss of rotational structure for the phosphorescent transition made these phosphorescent lines very narrow, and therefore readily amenable to theoretical analysis. Despite the fact that the low temperature solid environment promoted the radiationless intersystem crossing from the singlet to the triplet, it actually hindered the relaxation of the lowest triplet state to the ground singlet state, thereby increasing the intensity and measured lifetime of the triplet phosphorescent transition. This comes about because the solid environment prevents the diffusion of other molecules to

the excited triplet that would tend to quench its excess energy through mutual interactions.

However, few attempts were made to exploit the other benefits of matrix isolation in the 1940's. It was not till 1954 that Lewis's spectroscopic absorption studies were expanded greatly by G. Porter and coworkers[9] in England, and coincidently by G. C. Pimentel and coworkers in America.[10]

Using the same solution technique as Lewis, and irradiating various materials suspended at M/R = 5000 in frozen hydrocarbon glasses at 86°K, Porter was able to produce a whole host of radicals (C_2H_5, CS, ClO or C_6H_5), and observe their infra red and ultraviolet absorption spectra. Pimentel was concerned with producing the R species <u>outside</u> the matrix by means other than photolysis. In their initial paper, Porter and Norman suggested the "possibility or using still lower temperatures and other solvents."

Perhaps taking up this suggestion, several investigators in the late 1950's decided to try liquid hydrogen temperatures and inert or unreactive gases as the "solvent." For example, Becker and Pimentel[11] isolated HBr, HCN, H_2O and other species in various inert gas matrices and noted the varying effects of such factors as dilution and temperature of deposition on the infra red spectra and matrix shifts observed for these species. They reported warmup and photolysis experiments in the matrix a year later.[12] This is when the modern matrix isolation technique was born. If differs from the earlier techniques mentioned in that instead of freezing a homogenous solution of M and R molecules, the M and R molecules are slowly and simultaneously sprayed onto a transparent cold surface for a period of time. The R molecules used do not dissolve in a liquid rare gas and, in any event, are at times high temperature species that can only be formed in the environment of a furnace, so the freezing of solutions is impossible here. Thus the energetic species trapped can be produced outside the matrix by means

other than photolysis. The incompatibility of M and R is also a benefit, since the lack of solubility of R in M comes from the absence of any appreciable forces between the R molecules and rare gas atoms, which, in turn, means smaller complicating solvent effects in the spectroscopic properties of the R molecules.

Today a large body of scientific data has already been accumulated on the matrix phase of matter, in such fields as infra red and ultraviolet spectroscopy, epr and nmr spectroscopy, X-ray diffraction, conductivity measurements, and phosphorescence and fluorescence. It has been shown that, in general, the environment of a matrix disturbs neither the structure nor the vibrational force constants of the suspended R molecules to any appreciable extent, and has all the advantages of Lewis's and Porter's work, plus several others, some of which have been outlined in this section, and most of which will be gone over in detail in the next section.

C. Vacuum Line Work

As early as 1912, Alfred Stock and his coworkers[13] realized that in order to handle and identify the volatile, highly reactive and air-sensitive compounds formed from the action of acid on magnesium boride, MgB_2, a completely new set of chemical techniques would have to be invented. Thus Stock developed the glass vacuum line and the many devices that could be used in conjunction with it. By means of this system, he was able to characterize B_2H_6, B_4H_{10}, B_5H_9, B_5H_{11}, B_6H_{10} and $B_{10}H_{14}$. Today, vacuum technology has reached a high degree of sophistication and vacuum line techniques are used by many chemists.

A vacuum line is a system of interconnected glass and metal tubing, with valves and inlet-outlet ports, in which a high vacuum is maintained, used for the purpose of handling any material that is volatile near room

temperature (has a vapor pressure above 10 millitorr at room temperature). The materials put into the vacuum system never contact air or any other gas (unless one wants them to)and only remain in contact with glass and the stopcock materials (in Stock's work these were mercury valves). Transferral of chemicals in a vacuum line is based upon the fact that a gas expands into all the volume available to it and equalizes its pressure throughout this volume. Thus a material condensed out at a low temperature in one U-trap of the vacuum system can be transferred to a second U-trap in the system by simply allowing the first to warm while cooling the second. The usual coolant in vacuum line work is liquid nitrogen. Gases which do not condense out at the temperatures of liquid nitrogen (77°K) are called "permanent" gases and require special handling techniques in the vacuum line. Very rarely were such gases handled in this work.

Materials in the gas phase at low pressures do not flow from one spot to another by the usual viscous flow conditions we are accustomed to at atmospheric pressures. At low pressure the flow is termed "molecular," because the molecules flow virtually independently of one another (there are many more molecule-wall collisions than there are molecule-molecule collisions per unit time). Under such flow conditions, the diameter of the pumping line becomes critical in determining flow rates, and so the diameter of the glass tubing used in this work was large (about 17 mm). See Appendix B for the equations describing the flows, and the parameters they depend upon, in both the viscous and molecular flow regions of pressure and conducting tube diameter.

Various attachments can be placed on the vacuum system and connected via a stopcock so that the materials in the vacuum system can be taken off inside these attachments for measurements of their properties by some

external device. In general, any operation that can be performed in air can be performed in the vacuum system with the one stipulation that the materials used are volatile enough to be transferred around the vacuum system.

A vacuum line, to be described in detail in the experimental section, was utilized in this work because of the chemical characteristics of the materials produced.

D. Radicals Investigated

Since the carbenes have such a rich chemistry, it was first thought, in this research, that the investigation of other divalent group IV species might also prove fruitful. Consequently, the chemistry of GeH_2, SiF_2 and GeF_2 was examined. A theoretical description of the kinds of bonding and stability expected in these species will be given in the "Results" section of this dissertation.

All three of these species are stable to some extent in the gas phase due to a kinetic barrier to their polymerization in this phase, but polymerize readily in the condensed phase because their close proximity to other molecules of their kind in this phase can overcome that kinetic barrier. GeH_2 and SiF_2 polymerize irreversibly, but GeF_2 solid is ordered (into a series of parallel, F-bridged, polymer-like chains[14]) and can be reevaporated with partial decomposition to yield the monomer at 500°C in the gas.[15]

The GeH_2 radical has been hypothesized for many years as the intermediate in the formation of GeH_2 and GeH polymers.[16] Much evidence, to be presented in the "Results" section, suggests the transient existence of GeH_2 monomer or a highly unstable $(GeH_2)_n$ (n = 2 or 3) telomer under certain experimental conditions, such as in the cracking of Ge_2H_6.

Despite this evidence, and despite much work done on the synthetic properties of GeH_2, very little synthetic work ever done clearly suggested the existence of a GeH_2 reactant. An exception is Timms et al.,[17] who passed a mixture of silanes and germanes through a furnace and produced mixed silicon-germanium hydrides as well as higher germanes, but no higher silanes, a set of reactions that can be explained through the intermediacy of a GeH_2 radical.

In this work, an attempt was made to extract the GeH_2 radical from the furnace in the pyrolysis of Ge_2H_6 and react it at a 77°K surface in a cocondensation reaction. Difficulities arose due primarily to the extreme difficulty in reproducing the exact conditions for GeH_2 production, and to the concurrent production of H_2 gas in this cracking which probably prevented the GeH_2 from reacting with other species before it decomposed by itself. Though this cracking did produce some highly unstable material, its composition remains a mystery.

SiF_2, which is now a very well characterized gas phase species, was first discovered in 1958 by D.C. Pease.[18] He passed SiF_4 over silicon and silicon-containing materials at high temperatures and identified SiF_2 in the effluent gases by chemical means -- through its reaction with halogens and through the stoichiometric composition of the polymer obtained upon condensation of the effluent gases. SiF_2 has since been shown to have an enormously rich chemistry in cocondensation reactions. Some examples are: $SiF_2 + C_2H_2 \rightarrow HCCSiF_2SiF_2CHCH_2$; $SiF_2 + BF_3 \rightarrow Si_2F_5BF_2$; and $SiF_2 + C_6H_6 \rightarrow C_6H_6Si_2F_4$.[19] SiF_2 is the least thermodynamically stable silicon dihalide with respect to disproportionation to the element and the tetrahalide, yet it is the most (kinetically) stable silicon dihalide in

the gas phase with respect to disproportionation or polymerization. Its reactivity is believed to come from the fact that silicon in the tetravalent state is much more stable than silicon in the divalent state.

In this work, SiF_2 was cocondensed with GeH_4. GeH_4 was used as a reactant for two reasons: one, its low melting and boiling points meant that it would take a long time to become rigid at the 77°K surface after it struck this surface from the gas phase, thus creating a better chance for a cocondensation reaction to take place, and two, such a cocondensation reaction might lead to products containing $-SiF_2GeH_2-$ groups which might be better GeH_2 releasing agents under pyrolysis than the germanes. A reaction was noted between the two compounds, which occurred even when GeH_4 was deposited on top of the cold SiF_2 polymer. Therefore, this reaction was probably occurring, at least partially, during the warmup of the condensed solid. Some of the products formed and their characterization are discussed in the "Results" section of this dissertation and in Appendix F.

GeF_2, as mentioned before, exists as a well-defined solid which can be sublimed at 100°C and recondensed without decomposition. Above 160°C, the vapor will slowly decompose to GeF_4 and GeF polymers.

In this work GeF_2 was produced by passing GeF_4 over Ge metal in a graphite furnace at 400°C. The species exiting from the furnace were immediately condensed on a 77°K surface with another compound. Though GeF_2 was definitely being produced, it was not observed to react with any of the species cocondensed with it to produce volatile compounds.

CS was produced by an electrical discharge through CS_2 and formed C_3S_2 upon immediate condensation on a 77°K surface with CS_2. A similar experiment to produce C_3S_2 was performed in 1965 by Diallo,[23] and the compound C_3S_2 itself was known as early as 1912.[24]

Since the synthetic work on the divalent group IV species chosen seemed to be relatively unproductive, a new line of investigation with group V atoms was initiated. A study was made of the cracking of the newly discovered compound, P_2F_4.[20,21] By analogy with the N_2F_4-NF_2 equilibrium,[22] it would be expected that P_2F_4 would dissociate into PF_2 radicals under thermolysis.

In this work, pyrolysis of P_2F_4 has been shown to yield two different radicals, PF and PF_2, through heterolytic and homolytic fissioning respectively of the P-P bond. Immediate condensation of these radicals with the other species coming out of the furnace (PF_3 and P_2F_4) on a 77°K surface produces the compounds P_4F_6 and a highly unstable fluoride of phosphorus, most likely P_3F_5. Cocondensation of these radicals with other compounds did produce new compounds, but they were all too unstable to characterize.

Matrix infrared and ultraviolet studies of the products of the P_2F_4 pyrolysis proved the existence of these radicals. It was also found that P_2F_4 could readily photolyze in the matrix to form PF_3 and P_3F_5.

II. THEORY AND PRINCIPLES OF EXPERIMENTS

A. Condensation, and Cocondensation Reactions

A cocondensation reaction is a reaction between a highly reactive chemical species and one or more other reactants, taking place on a cold surface while these species and reactants are condensing on it from the low pressure vapor. In order to understand the nature of such a reaction, an investigation into the physical process of condensation is in order.

In condensation from the gas phase to the low temperature solid, great quantities of heat energy, due to the heat capacity, the heat of condensation and the heat of reaction (if any) of the condensing gases, must be released to the surface upon which the condensation is taking place. Since the heat conduction and thermal gradients at the surface would be finite, this release of energy takes time, and the question arises, what is happening to the molecules after they impinge on the surface, but while they still are in the process of losing their excess gas phase energy? A great many quantitative, microscopic, kinetic theories of physical condensation (or even adsorption) onto a solid surface from the vapor (such as Walton's condensation model) suggest that during this process an intermediate state of matter exists, wherein surface migration and diffusion of the condensing molecules occurs before final solidification. A simplified diagram showing what the process of condensation might look like on the molecular scale is shown in Fig. 1. It can be seen that between the gas state and the solid state a third state of matter can be said to exist.

Because of the evidence that will be presented, I propose to invent a new concept to stand for this non-equilibrium state that condensing matter finds itself in before it solidifies completely: the "LLIT" (for "Liquid-

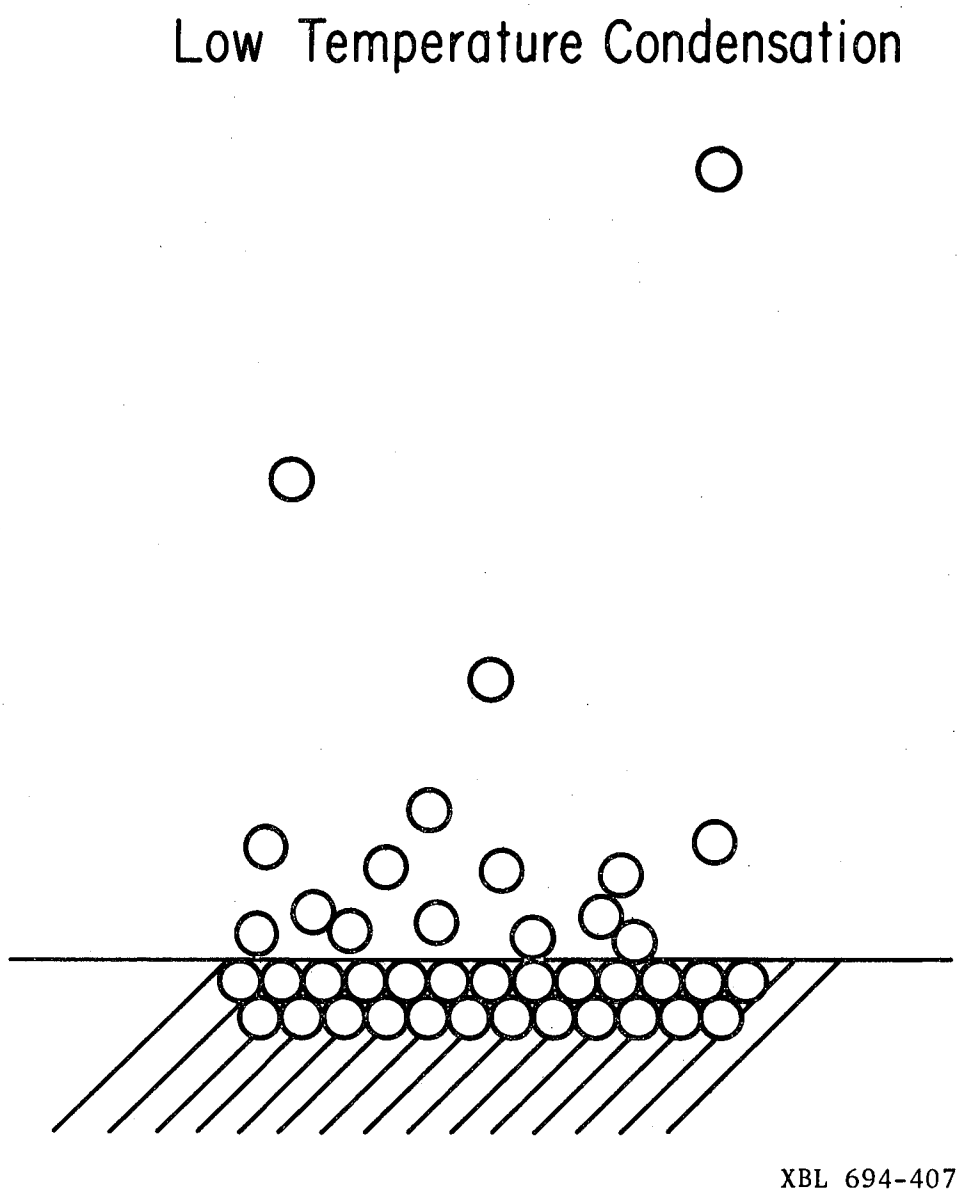

Fig. 1 Low temperature condensation

like, Intermediate, Transitory") state of matter. The LLIT state is "intermediate" because it exists in between the gas and the solid phases, in time. It is "transitory," since it only last several milliseconds, at most. It is "liquid-like" because the condensing molecules roam across the surface for some time as their energy is being taken away, and usually have no crystalline order. In order to understand the nature of the condensation process and hence a cocondensation reaction, we must look into the properties of this state.

1. The "LLIT" State of Matter in the Condensation Process

The LLIT state of matter is that non-equilibrium state in which matter exists while it is in the process of condensing from the vapor to the solid, at those temperatures at which the condensation coefficient approaches unity. The last stipulation is necessary in order to specify that: 1. We are dealing with molecular flow conditions for a completely condensible gas passing to a cold surface; 2. No reflections of the impinging molecules occur, so that all molecules that strike the surface are ultimately frozen out; 3. The surface is cooled well below the triple point of the gas, so that given the rates of the deposition involved here, the vapor pressure of the resulting solid can be considered negligible; 4. And thus, this is a non-equilibrium situation. When the condensation coefficient is not unity, and/or when the solid has an appreciable vapor pressure, the condensation process might be more complicated than in the LLIT state, nucleation becoming an extremely important phenomenon.

In the LLIT state we have extremely fast relaxation processes occurring, of all forms of energy, due to the strong interactions that exist between molecules in a condensed phase. As a matter of fact, no faster way of relaxing such larger quantities of energy in so small a volume is possible (with the possible exception of some exotic method of superfluid He II cooling).

Let us now review some of the qualitative evidence that leads one to hypothesize the existence of the LLIT state of matter.

One piece of very direct evidence comes from in situ electron microscopy of surfaces -- solids condensing on surfaces inside of electron microscopes. This work is usually done on solids at such a temperature at which the condensation coefficient is not unity, but nevertheless does demonstrate long range migration of condensing molecules on surfaces.[25]

By observing the crystallinity of the resulting solid from a condensation process that has continued for some time, one can arrive at inferences of how that solid was built up. Crystallinity, or ordering, or the extent of the microcrystals formed in the solid, can be measured in several ways, two of which will be mentioned here. First, we have X-ray diffraction, which gives powder patterns for a microcrystalline material, the half width of whose lines is proportional to the degree of disordering in the solid; the more the ordering, the narrower the lines. Second, we have measurement of the heat given off upon warmup of the resulting solid to its devitrification or annealing temperature, the more the heat given off, the more disordered the solid was before the annealing.

Both these indicators show that when depositing solids from low pressure vapors on very cold surfaces, the slower the deposition rate, generally, the less the ordering in the resulting solid.[26,27] This behavior is exactly the contrary of the process of crystal formation from melts and solutions, where the slower the crystal formation rate, the larger and more perfect the crystal formed. In the latter two cases, a condition near dynamic equilibrium exists at slow deposition rates, such that molecules are constantly adhering to the crystal and then are taken away if they have not stabilized themselves in a perfect lattice point,

this process repeating itself again and again, as the net build up slowly continues. But in the case of a gas condensing out on a surface at a pressure far from its equilibrium value, all molecules striking the surface adhere immediately (such a one-molecule-at-a-time adhering process could never be duplicated in a liquid or solution, but only occur in a gas, owing to the "infinite" divisibility of the latter). The explanation, then, of the increase of ordering from high deposition rates, must come from some factor that allows a dynamic "equilibrium-like" situation to occur at the surface in these cases -- ie. the enhancement of the LLIT state of matter. In other words the higher the deposition rate, the greater the amount of heat being given up to the surface per unit time, and so the higher the surface temperature needed to accommodate this heat flux. Therefore, the less immediate is the loss of kinetic energy of the impinging molecules as they strike the warmer surface, the larger their surface mobility and migration lifetime before they solidify, and the better their chances of finding a perfect lattice point to adhere to, promoting their ordering into equilibrium crystalline arrays.

Simply the fact that so many materials, even inert gases, do not form amorphous materials (that is, a solid with one or more dislocations every 5 nm) when deposited from the vapor at very low temperatures, suggests in itself that an intermediate phase is allowing some time for condensing gas molecules to freeze out in an ordered arrangement. After all, the cooling of a liquid can not be accomplished nearly as quickly as that of a gas in condensation, yet many liquids form glasslike solids in solidification, while many gases form crystalline solids upon condensation.

Better evidence for the LLIT state comes when we include a small amount of another, highly reactive material with the bulk of the main vapor condensing. For instance, it has been shown through X-ray diffrac-

tion that, under otherwise identical deposition conditions, pure argon deposited at 4°K is distinctly less ordered than argon with a small amount of free radicals (such as N atoms) added to it,[26] even though, in the latter case, it would be expected that the inclusion of a foreign substance, free radicals, in the lattice would increase the dislocation density and hence the disordering, since they would not fit isomorphously into the argon lattice. Indeed, admixture of foreign stable gases to the depositing argon does increase the disordering in the solid at 4°K. It is believed that the exothermic recombination reaction of free radicals produces their ordering influence. Since once the radicals are solidified in the argon, no further recombination occurs, it is quite evident that the only way that a heat release of recombination could anneal the argon crystallizing out is for it to occur upon deposition, as the energy is liberated at the surface in the LLIT state. The recombination of the radicals occurring in the LLIT state prolongs the lifetime of, and "heats," this state, so as to allow a more uniform and ordered arrangement of the argon atoms before total solidification. This effect is so strong that it overwhelms the impurity broadening of the X-ray lines. As a matter of a fact, Peiser states, "So effectively are atoms and molecules apparently knocked into equilibrium-phase positions by the recombining radicals that serious consideration should be given to this process for growing good crystals at very low temperatures."[26]

Once we deposit these high M/R matrices at low temperatures, we not only can observe the extent of crystallization of the M gas, but also the amount present and the degree of isolation of the R species, to find out more about the process of condensation itself. From purely mathematical considerations, Jackson[28] has shown that the typical maximum free

radical concentrations that could be expected to exist in a solid matrix are of the order of 10 to 14% (this assumes: 1. a close-packed configuration in the solid; 2. radicals always combine at any orientation if they are next to each other; 3. only diatomics can form after such a combination occurs; and 4. second and further nearest neighbor radicals do not combine). Yet actual maximum concentrations attainable, as measured by spectroscopic means (replying on gas phase extinction coefficients), are usually in the range of 0.1 to 1%. Since we know in many cases that a much larger amount than this exists in the gas, a great deal of recombination must be taking place during condensation, presumably in the LLIT state.

By observing the spectrum of trapped R molecules in a matrix, especially in the infrared, we can determine if they are well isolated in the resulting solid, or if they have been trapped out in the form of aggregates. In the former case, sharp lines corresponding to the fundamentals would be observed. In the latter case, broadened out lines would be observed, as well as lines that would not correspond to any monomer frequency at all. These two indicators of the degree of isolation of R, then, can lead us to important conclusions about the condensation process.

For instance, Leroi et al.[29] found that enormously high M/R ratios (from 1000 to 4000) were needed to isolate CO well in the matrix environment, yet similar behavior is not noted for many other materials. Most likely, CO molecules aggregate in the LLIT state before final solidification. High dilutions are then necessary to keep the CO molecules from each other in the LLIT state before they solidify, after which they remain isolated.

It has been shown that a lower rate of deposition of both M and R under matrix isolation conditions can increase the isolation of R. A lower rate

of deposition means a shorter-lived LLIT state, causing a decrease in the probability that one R species will touch another in this state before they solidify.

Finally, some interesting effects with the condensing temperature of the surface have been observed.[30] Using CCl_4 as the matrix gas, and various species at low concentrations added to it, it was observed that condensation on liquid-nitrogen cooled targets gave poor isolation of the dilute species. When liquid hydrogen was used as the coolant, much better isolation was obtained, but this time, upon warming the target above liquid nitrogen temperatures, the isolation remained. Thus the level surface temperatures in the first condensation must have been above those of the target material itself (77°K).

The last piece of evidence I will offer here for the LLIT state of matter occurs when the R species used is a simple, stable, volatile compound, and the deposition rates upon the low temperature surface are increased to very large amounts. Up to a certain extent, this increase is accompanied by poorer and poorer isolation of the R molecules involved, as the LLIT state becomes longer and longer lived. But beyond a certain rate of deposition, the degree of isolation of R goes up again, as measured by the sharpness of its infrared fundamental modes. This was discovered by Dr. Mark Rochkind and was termed by him "pseudo matrix isolation."[31] When gases containing a mixture of M and R are pulsed, at one atmosphere pressure, onto a cold target, the LLIT state that forms is so high in temperature it very well might be called a liquid, not "liquid like". Under these energetic conditions, two R molecules that collide have enough energy to separate again, despite the forces of attraction between them, and so these R molecules remain homogeneously distributed throughout

the LLIT state until the pulse has subsided, cooling has set in, and the entire "solution" then freezes out solid. Notice that R need not be soluble in M, so we are not really dealing with an equilibrium solution here, and that this liquid state produced is just an energetic extreme of the normal LLIT state formed under slower deposition, not something fundamentally different from it.

2. Cocondensation Reactions

The LLIT state of matter has great potentialities for synthetic usefulness in radical reactions. These reactions usually have little or no activation energy in the condensed phase and so can proceed at low temperatures, and involve the release of large amounts of energy after completion, which must be quickly taken away to prevent decomposition of the products formed. Relaxation processes are possible in both the liquid and gaseous state, but the LLIT state has the highest rate of relaxation of the three, and therefore the best chance for stabilizing an unstable intermediate in such reactions. Here, the energy released from a chemical reaction can be taken away at a faster rate than the metastable species that are forming from that reaction can distribute that energy into their weak bonds to cause their breakage and hence the decomposition of that species.

We can draw a crude analogy to a damped oscillator to illustrate, in principle, what might be occurring in the LLIT state during a cocondensation reaction. In Fig. 2 we see a hypothetical plot of the total potential energy of the triatomic system, A + B + C, as the distance between the equidistant atoms is changed (we will assume the Born-Oppenheimer approximation as well as a continuous gradation of possible internuclear distances here). Let us also assume that two compounds exist in this system, AB, which is metastable, and ABC, which has the lowest energy for the three atom system. A + B + C initially have an electronic energy of

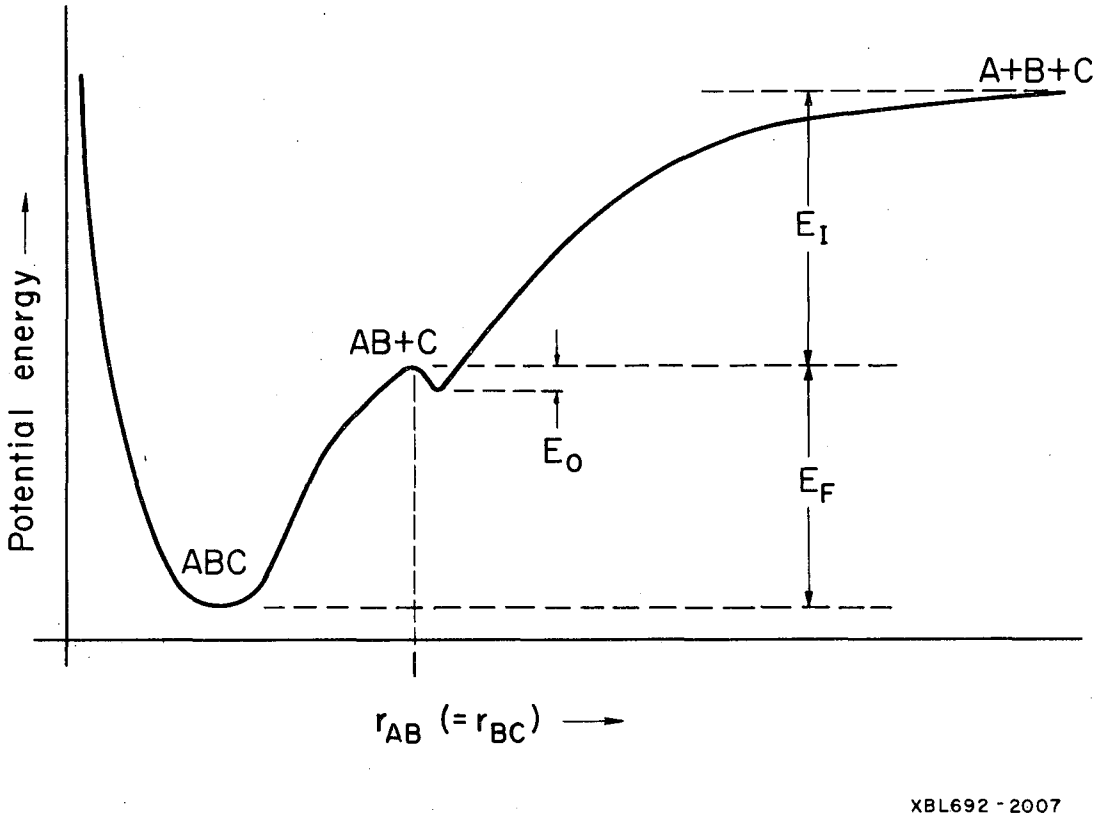

Fig. 2 Hypothetical potential curve for equidistant atoms A + B + C

$E_I + E_F$. A and C are approaching atom B from either side in the LLIT state. In coming together, they pass through a slightly stable AB + C combination (which could become even more stable if A came closer to B than to C). If the quenching processes occurring can remove the excess energy E_I (now in the form of kinetic energy) before point r = 1 is reached, AB would be stabilized with energy E_0, which could then be quickly dissipated. Even if the bump in the potential curve is passed over, the resultant ABC might be so energized that it would dissociate up the curve all over again, perhaps just to the point where AB is formed. Essentially, this is what I propose is happening in the LLIT phase to produce the highly unstable compounds observed. Needless to say, a much more complicated set of reactions could be occurring in actual cocondensation reactions, with the possibility of the further reaction of the trapped unstable intermediates upon warmup and pump off of the solid matrix at 77°K.

Notice also that the reactions taking place in the LLIT state could give off heat which would prolong the existence of that state, allowing still further reactions to take place, as was the case with the recombination of the N atoms mentioned above.

In cocondensation reactions, the radicals are produced separately from the compounds that they are intended to react with and in a different portion of the system from where the reaction takes place. Therefore, the energy source used (such as heat, microwave, etc.) to produce the radicals will not be able to also affect the reaction. Usually, we know from other (spectroscopic) experiments exactly what radicals are forming in the energy source used, so a clearer picture of the chemical reactions expected of these radicals is possible, and the new compounds identified in the final pump out might be more readily explained in terms of those reactions.

The reactive species, once formed, are then transferred in the gaseous state to the cold cocondensation surface, usually by a line of sight path at low pressures to prevent their decomposition. For very stable radicals, such as SiF_2, such precautions are not necessary, nor are they necessary for materials such as N atoms whose high energy of recombination can not be dissipated in the gas phase, and so which do not recombine very readily in the gas phase. On the other hand, for very unstable species such as $SiCl_2$, such precautions are a necessity for any reaction other than polymerization to occur,[32] and represent one of the few ways that such materials can be chemically utilized at all. Indeed, the very fact that $SiCl_2$ (and $SiBr_2$[33]) do react as monomers in cocondensation reactions, as evidenced by the products of these reactions, proves fairly conclusively that the initial reactions take place on the cold surface during condensation, not in the solid upon warmup (where all the formerly free and reactive $SiCl_2$ would be in a polymerized form already).

Simultaneously, with the deposition of the radical, the reactant (usually a stable, volatile compound) is sprayed on the cold surface, and, as both radical and reactant are condensing, the reaction takes place. In the case of the formation of P_4F_6 (and presumably P_3F_5), both the radical (PF and/or PF_2) and the reactant (PF_3 and/or P_2F_4) exit from the furnace together, but of course the principle is the same.

If very low pressures are used, few collisions will take place in the gas phase and no reaction will occur there at all. The low pressure also serves the function of allowing the radicals to be directed towards the 77°K surface so that they never hit any intermediate temperature surface along the way, which could cause polymerization, decomposition or back-reactions. For instance, Staudinger and Kreis[34] in 1925 predicted

that superheated sulfur vapor, upon condensation at low temperatures, would become a deep blue solid, due to the presence of S_2 units condensing from the vapor. Experimentally, they heated sulfur vapor to a high temperature in one end of a tube, whose other end was immersed in liquid air. Only amorphous sulfur deposited in the cold end. But when Rice and Sparrow[35] repeated the experiment, only this time placing a cold finger next to the furnace exit with continuous pumping, a deep purple material did deposit out. The difference can be attributed to the fact that in Staudinger's work, the S_2 molecules probably first struck the glass surface where its temperature was far from 77°K and where, consequently, the S_2 polymerized to S_8 readily, because of the reactivity of S_2 at these temperatures.

Some radicals used in this work would not react with other compounds at room temperature in the gas phase because of a kinetic barrier to such reaction. In these cases, paradoxically, the cold, condensed phase promotes reactions by bringing the molecules into close proximity with one another, overcoming their repulsive kinetic barrier, and removing the energy of reaction fast enough to prevent decomposition of the products back to the initial reactants. Such is the case with SiF_2 and O_2, which do not react to form any volatile compound in the gas phase, even at moderately high pressures (this was proven mass spectroscopically), yet nevertheless do form hexafluorodisiloxane, other volatile compounds, and polymers upon condensation on a cold surface.[36]

As was mentioned before, in the LLIT state at 77°K surfaces, relaxation processes are extremely rapid, and the quenching of all kinds of energy proceeds very quickly. Because of this high quenching rate, a good chance exists to form and stabilize unstable intermediates in the solid at 77°K. Since the LLIT reaction is over so soon, and takes place at such low tempera-

tures, polymerization reactions, at least upon initial condensation, are very unlikely.

An interesting example of the effect of rapid quenching is given by the reaction of C_2H_2 with oxygen atoms. At ambient temperatures, a simple oxidation takes place according to the following equation: $C_2H_2 + 5\ O^* \rightarrow H_2O + 2\ CO_2$.[37] But upon cocondensation of C_2H_2 and O atoms at 90°K, the reaction is much more complex, CHOCHO being a major product.[38] And at the greatest quenching rate and lowest temperatures attainable, in a matrix environment at 20°K, O atoms (from photolyzed N_2O) will react with C_2H_2 to form ketene, H_2CCO, coming from a rearrangement of acetylene's structure upon oxygen atom addition.[39] Obviously, the energy liberated in the O atom addition in the matrix can be removed by the environment before further decomposition takes place, but such is not the case at higher temperatures in the solid nor in the gas.

The fact that unstable compounds, which readily decompose at room temperature and above, are often pumped off after the warmup of the resulting solid from cocondensation, is further proof that the reactions in question could not have taken place in the high energy input region or in the gas phase, where these unstable compounds would have surely been destroyed. Therefore the reactions must have taken place on the cold surface. The question still remains: did these new compounds form in the LLIT phase upon deposition or in subsequent reactions upon warmup of the solid after cocondensation was completed? In the case of very unstable species (as was mentioned before) such as $SiCl_2$ or carbon atoms in the ^1S state, we can be sure that the reaction took place in the LLIT state, since these species would not have lasted any longer than that state would have. But for other species, the answer is not this simple.

One fact that always rules out the reaction of trapped radicals upon warmup, is that sometimes sequential condensation of first the radical and then the reactant does not ultimately lead to the same products obtained from the simultaneous cocondensation. This phenomena can be explained either in terms of a reaction in the LLIT state, which would only be effective in the cocondensation, or otherwise, a surface barrier to the reaction of the two solid bulk materials in the sequential condensation that breaks down when they are intimately mixed in the cocondensation.

The latter hypothesis is quite untenable. First of all, impinging radicals have been known to penetrate solids deposited out at 77°K[40] and would be expected to diffuse quite readily upon warmup and vaporization. Secondly, the radical and the reactant surfaces would be touching each other in the sequentially deposited matrix, since no adsorbed layer of impurity would exist between their surfaces. Finally, the stabilizing effect of a crystalline lattice would not be of great importance with the unannealed, vitrified, microscrystalline materials forming here. Thus, when a sequential condensation does not produce a product that simultaneous cocondensation produces, a reaction in the LLIT state can be assumed.

An excellent historical example of the failure to recognize this crucial point concerns the reaction of NH and benzene. Stewart,[41] in 1940, cocondensed NH radicals and benzene on a -185°C surface and observed the formation of aniline and p-phenylene diamine upon warmup. But when Rice, in 1951, tried to repeat the experiment by first condensing out the NH in solid form and then condensing on top of it some benzene (all at low temperatures), he observed no formation of aniline whatsoever. He concluded that his results differed from Stewart's in this respect, but in

fact they did not. Rice just did not consider the possibility of a cocondensation reaction.

Another observation that rules out the reaction of trapped radicals upon warmup as the explanation of all the resulting products from cocondensation reactions, is that the deposition rate of the two materials can sometimes have a drastic effect on the amount of reaction observed. For instance, Skell and Engel[43] found that in order to react ^3P carbon atoms deposited on the surface of neopentane at 77°K, with olefins, it was necessary to blast the olefins onto the cold surface at an enormous rate, causing momentary liquification of the neopentane substrate. It was only then that the reaction proceeded.

Finally, it is sometimes observed that the physical properties of the cocondensing reactant affect the yield of products greatly, which would suggest that the physical process of condensation had a great deal to do with what sort of reactions resulted. For instance, Skell and Engel[44] cocondensed ^1S carbon atoms with pentane, hexane, and a 50-50 mixture of pentane and hexane. The melting point of hexane is 6.5°C, while the melting point of pentane is -93°C, and that of the mixture, around -100°C. It was found that the ^1S carbon atoms reacted, by inserting into the C-H bonds, readily with pentane, almost not at all with hexane, and about equal amounts with both the pentane and the hexane in the mixture cocondensation. Since these two compounds have fairly similar C-H bonds, the difference in their reactivity must come from another source. That source seems to be their different melting points, as evidenced by the mixture cocondensation. Thus, in contrast to the pentane and the pentane-hexane mixture cocondensation, the LLIT state in the case of pure hexane is extremely short-lived because of the tendency of hexane to solidify very rapidly

after striking the surface, and the carbon atoms have no time to react with it before the hexane is in the solid state, after which, presumably, they become unreactive towards it.

Of course none of this means that no reactions at all are occurring during the warmup after a cocondensation reaction. On the contrary, the very fact that the initial reactions have taken place in the LLIT state of matter means that highly unstable materials might have formed, which would then be expected to decompose when raised in temperature. I believe, for instance, that P_3F_5 is formed in the P_2F_4 "cocondensation," but vaporizes, after warmup and pump out, to condense and form only polymeric materials in the U-traps of the vacuum system.

B. Infrared and Ultraviolet Spectroscopy

All molecules absorb characteristic electromagnetic radiation. In the infrared, these absorptions usually correspond to transitions between the vibrational levels of the various modes of vibration that the molecule possesses. Using a simple mechanical model, an infinite number of frequencies (and amplitudes) of vibration are possible for a molecule, but quantum mechanically it is found that only a few discrete modes of vibration of any molecule are infrared active (called the "normal modes"). In the ultraviolet-visible portion of the spectrum, the absorptions correspond to transitions between electronic states, which would have different electronic orbits and different internuclear distances. In atomic spectra, these absorptions occur as strong, sharp, well-separated lines. In the spectra of diatomics, the rotational-vibrational energy levels for each electronic state cause a series of bands of lines to appear, numbering in the many hundreds or thousands for each electronic transition. However, in the matrix, rotation is stopped, and vibrational

excitation in the ground electronic state is quenched to the lowest level, so the full intensity of the absorption, for each electronic transition, goes into a regular series of fairly sharp peaks corresponding to each vibrational level of the excited electronic state. In polyatomic molecules, several different modes of vibration are possible, thus spreading out the intensity of any electronic absorption throughout these different modes. And since these transitions to different vibrational modes in the excited state would overlap in the matrix, only one broad peak would be observed for electronic transitions in these types of molecules.

1. Quantitative Spectroscopic Analysis, Oscillator Strength and the Linear Curve of Growth

When radiation passes through a substance and is absorbed, several terms are used to quantitatively describe the process according to certain laws of absorption. Given that I_o = incident radiance of the radiation, I = transmitted radiance, l = path length of the radiation, and c = concentration of the absorber in that path length, we have the Beer-Lambert Law,

$$I = I_o e^{-klc} \qquad (1)$$

where, k = constant and e = base of natural logarithms (2.71828---) This law holds exactly for most gases at low pressures at any one particular wavelength, so that k is a function of frequency only.

The extinction coefficient, ϵ, is defined as,

$$\epsilon = (1/lc)\log(I_o/I) = 0.434\ k \qquad (2)$$

and values of ϵ are usually expressed for the maximum peak heights in electronic absorptions.

Transmittance, T, is defined as the ratio of I/I_o, and percent transmittance, %T, the value plotted directly by the infrared spectrophotometer used in this work, is defined as $100I/I_o$.

Absorbance, A, the value plotted directly by the ultraviolet-visible recording spectrophotometer used in this work (in the gas phase absorption studies), is defined as $\log(I_o/I) (= \log(100/\%T))$, and as such, is directly proportional to the concentration of the absorbing species at any one particular wavelength, if Beer's Law holds.

At first glance, one might believe that absorption spectroscopy would be an ideal tool for gas analysis, since the peak heights obtained would be proportional to the amount of material present. But the basic point is that the radiance of a beam of light can never be measured at exactly one frequency, but only across a band of frequencies, in order to have a finite amount of light to measure. The slit width required for a particular spectrometer limits the resolution of the absorption spectrum obtainable with that spectrometer. Thus, for infrared gas phase work, $I = I_o e^{-klc}$ holds exactly for individual rotational lines, or, more specifically, small frequency increments of individual rotational lines. But rotational lines for most compounds are <u>much</u> finer than the best resolution obtainable from the instruments available. Therefore, the "wide" slit used can never give a true line shape for each rotational line, but only a form of "integrated" intensity over many rotational lines.

This "integrated" intensity will follow equation (1) only in the so-called "linear curve of growth" region of the % transmittance, where the exponential of klc closely equals 1 + klc for each individual rotational line. Below a point of about 80% transmittance for the individual lines, detailed assumptions about rotational line shapes would have to be made in order to obtain quantitative concentration data from the low resolution absorption curve . These assumptions would become more and more difficult to make as the % transmittance became smaller. Thus the linear curve

of growth region of a gas phase absorption line spectroscopically observed is the only region in which absorbance ratios measured will correspond to concentration ratios, with low resolution instruments. Later on, it will be shown that this is generally not the case for matrix absorption lines due to the inherent broadening of these lines in the matrix.

The oscillator strength or f-value of an electronic transition is defined as the ratio of the quantum theoretical and classical contributions of the transition in question to the refractivity (n-1).[45] The f-value, as defined here, is proportional to the Einstein transition probability of a transition (B_{mn}), and hence is a measure of its absorption intensity. For each electron in a molecule, the sum of f-values of all its transitions to all its excited states equals one. Usually, the Rydberg states, that is, the very high energy states which can be viewed as a lone electron orbiting about a polynuclear core, have a very high intensity, so that the f-values of the other transitions in the near ultraviolet are in the range of 10^{-5} to 10^{-1}. f-values can be determined from absorption or emission.

An f-value calculation for the 260.6 nm gas phase absorption of P_2F_4 is done in Appendix A, using the equations given in Herzberg.[45] A plot of $A(\omega)$ from the ultraviolet machine is the primary data, and from this plot we can obtain B_{mn}. f^{nm} is then obtained by multiplying B_{mn} by the appropriate constant.

In calculating B_{mn}, we must calculate the integral, $\int(1 - e^{-2.303A(\omega)})d\omega$ over the entire absorption corresponding to the transition in question. This integration must be carried out over each and every rotational component of this absorption band. But, as was the case with concentration measurements, complications arise here because of the relatively poor

resolution of the instruments available, which is nowheres near enough to separate the individual rotational lines. What is actually recorded, is the single, smeared out, "integrated" absorption, and the integral, mentioned above, calculated using this machine-generated $A(\omega)$ is not the same as the integral in the resolved case, which is really the sum of the integrals over each rotational component. This difficulty is obviated in the linear curve of growth region where the absorbance is small, for then the exponential e^{-x} can be approximated by 1-x, and it can be shown mathematically that the smeared out absorption integral of $1 - A(\omega)$ will be close to the value of the sum of the separate integrals of $1 - A(\omega)$ over each resolved rotational line. Thus, in the linear curve of growth region, both the height of the absorption can be used to measure concentration, and its area can be used to measure f-values.

Though the above reasoning can apply both to infrared and ultraviolet absorption spectroscopy, quantitative values for relative concentrations were only obtained in the infrared in this work, with the exception of gas phase ultraviolet spectra taken with the recording spectrophotometer.

2. Normal Vibrational Modes in the Infrared

In the infrared, line absorptions are usually due to changes in the energy of a molecule that correspond to "vibrational" energies as analyzed quantum mechanically. Molecules in the matrix do not rotate, so rotational levels are not superposed on vibrational levels here as they are in the gas.

In the matrix, the infrared transition observed is the v=0 to v=1 transition in the ground electronic state. From quantum mechanics, we can show that each transition of this type will correspond to a classical

normal mode of vibration for the molecule as a whole.[46] The energy of each of the vibrational levels in a normal vibrational mode, given an harmonic oscillator approximation (where there are only quadratic terms in the potential energy) is;

$$E_i = h\nu_i(v_i + 1/2) \qquad (3)$$

where, $\nu_i = (1/2\pi)\sqrt{\lambda_i}$, h = Planck's constant and v_i = the vibrational quantum number, 0,1,2,3... Thus, transitions where $\Delta v = 1$ (the allowed transitions in this case) will correspond to a frequency of the absorbed photon that is equal to the classical vibrational frequency. Assuming a classical model of the molecule as a group of nuclei held together along their "bonds" by weightless springs, this frequency, in turn, can be related to the various presumed force constants in the molecule along these bonds. In this basically classical analysis, the expression of the potential energy of the molecule, which is to be related to the vibrational energy transitions, is done in terms of displacement coordinates for the nuclei of the molecule in a normal vibration, the constants of the expression being the force constants in question.

Unfortunately, the number of potential constants (or force constants) thereby derived is usually far greater than the number of fundamental frequencies observed for the molecules (at least those molecules for which no isotopic data is known), so that the former can not be derived from the latter. The next step, therefore, in obtaining these force constants, is to make certain simplifying assumptions as to how restoring forces act in the molecule in order to reduce the number of potential constants required to specify its motion in the normal modes of vibration. If the molecule has symmetry, as does XY_2, this simplification can be aided considerably.

In what follows, we will use certain nomenclature. We will assume we have the molecule XY_2 as depicted in Fig. 3, with the Y-X-Y angle being 2α. m_X and m_Y stands for the masses of the X and Y atoms, respectively (in amu), and k is the symbol used for a force constant. The 1 and 2 subscripts on k stand for the two X-Y bonds or the two Y atoms, the 3 subscript stands for the X atom or the Y-Y "bond," and the α subscript stands for the angle between the two X-Y bonds. Only harmonic forces will be considered (so that the potential energy will be expressed in second order terms of displacement coordinates). The value, λ_n, is defined as,

$$\lambda_n = 4\pi^2 c^2 \nu_n^2 K \qquad (4)$$

where, c = velocity of light in vacuo, ν_n = frequency of the normal vibration in Kaisers (ν_1 = symmetric stretch, ν_2 = bend and ν_3 = anti-symmetric stretch), and K = mass conversion factor from amu to grams (1.66028×10^{-24} gm/amu). This expression comes to, $\lambda_n = 0.058091 \times \nu_n^2$.

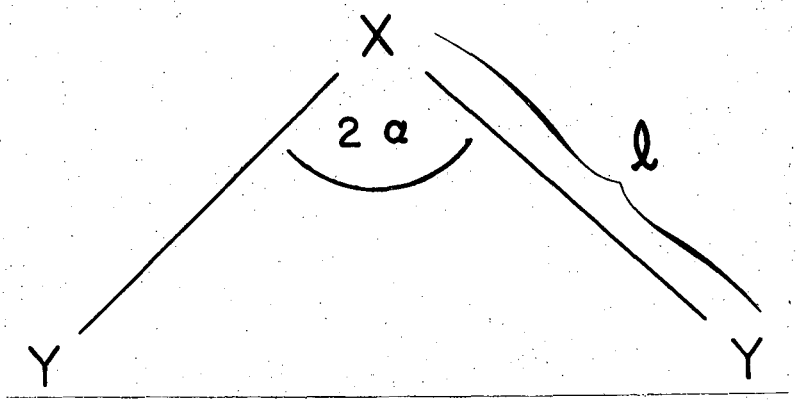

Fig. 3 The XY_2 molecule

The assumption of central forces is that forces act only between atoms (bonded or non-bonded) in a molecule on a line joining their centers. This is equivalent to assuming that the potential energy has no cross terms in it -- that it is a pure quadratic function of the displacement

coordinates between the nuclei. For XY_2, in Fig. 3, we may assume just two central force potential parameters, since two of the bonds would be identical, k_1 and k_3. The formulas derived[46] are,

$$\lambda_3 = (1 + (2m_Y/m_X)\sin^2\alpha)(k_1/m_Y) \tag{5}$$

$$\lambda_1 + \lambda_2 = 2k_3/m_Y + (k_1/m_Y)(1 + (2m_Y/m_X)\cos^2\alpha) \tag{6}$$

and,

$$\lambda_1\lambda_2 = 2(1 + 2m_Y/m_X)\cos^2\alpha\,(k_1k_3/m_Y^2) \tag{7}$$

Instead of central forces, we can have the assumption of the so-called "valence forces". In this assumption, a restoring force exists only between those atoms that are bonded in the molecule, as well as between any two valence bonds joined to the same atom in terms of the angle between them being displaced from its equilibrium value. The formulas derived[46] are,

$$\lambda_1 + \lambda_2 = (1 + (2m_Y/m_X)\cos^2\alpha)(k_1/m_Y) + (2/m_Y)(1 + (2m_Y/m_X)\sin^2\alpha)(k_\alpha/l^2) \tag{8}$$

$$\lambda_3 = (1 + (2m_Y/m_X)\sin^2\alpha)(k_1/m_Y) \tag{9}$$

and,

$$\lambda_1\lambda_2 = 2(1 + 2m_Y/m_X)(k_1/m_Y^2)\,(k_\alpha/l^2) \tag{10}$$

Here, l is the length of the X-Y bond, and the force constants associated with the restoring force on the angle are given in terms of it to keep their units the same as the other force constants.

Valence bond coordinates yielding the above equations give good agreement with the normal frequencies of many XY_2 molecules. This agreement is measured by calculating k_1 and k_α/l^2 using the first two of the above equations and then substituting them into the third equation to check the agreement in it.

We can also introduce an additional force acting on one Y atom when the distance of the other Y atom from X is changed, into the valence force system, to produce a complex valence force set of equations as follows,[46]

$$\lambda_1 + \lambda_2 = (1 + (2m_Y/m_X)\cos^2\alpha)((k_1+k_{12})/m_Y) + 2(1 + (2m_Y/m_X)\sin^2\alpha)(k_\alpha/m_Y l^2) \quad (11)$$

$$\lambda_3 = (1 + (2m_Y/m_X)\sin^2\alpha)((k_1-k_{12})/m_Y) \quad (12)$$

and,

$$\lambda_1 \lambda_2 = 2(1+2m_Y/m_X)\ ((k_1+k_{12})/m_Y^2)(k_\alpha/l^2) \quad (13)$$

There is a yet more generalized valence force system which includes cross terms in both the linear bond stretching and angle, bond stretching interactions. The expression for the potential energy in this system is,

$$V = 1/2\ k_1(\Delta l_1^2 + \Delta l_2^2) + 1/2\ k_\alpha(\Delta\alpha)^2 + k_{12}\Delta l_1\Delta l_2 + k_{l\alpha}\ (\Delta l_1 + \Delta l_2)\ \Delta\alpha \quad (14)$$

and the formulas derived[47] are,

$$\lambda_1 + \lambda_2 = (1 + (2m_Y/m_X)\cos^2\alpha)((k_1+k_{12})/m_Y) + (2/m_Y)(1+(2m_Y/m_X)\sin^2\alpha)(k_\alpha/l^2) - (k_{l\alpha}/l)((8 \sin\alpha \cos\alpha)/m_X) \quad (15)$$

$$\lambda_3 = (1 + (2m_Y/m_X)\sin^2\alpha)((k_1-k_{12})/m_Y) \quad (16)$$

and,

$$\lambda_1\lambda_2 = ((2 + 4m_Y/m_X)/m_Y^2)[(k_1+k_{12})(k_\alpha/l^2) - 2(k_{l\alpha}/l)^2\ ] \quad (17)$$

In this system of coordinates, we have one more force constant than frequency, so an added condition must be included to determine all the

force constants uniquely. According to Linnett and Heath, the best value for these constants will have a low value for the bending constant, k_α/l^2. Thus, the minimization of this constant can be considered to be the fourth condition, if no isotopic data are available.

Another means to remove this fourth condition is by extrapolating a known stretching force constant for the X-Y bond from another molecule to the one in question, and substituting this value into the above expressions.

The v=0 to v=1 transition gave the frequencies substituted into the above expressions in this work. Since all molecules are anharmonic oscillators, to some extent, better values for the force constants would have been obtained if the hypothetical zero-order frequencies were used. These frequencies come from an analysis of several vibrational levels and more closely approximate the harmonic oscillator frequencies that would be compatible with the harmonic force assumption in all of the above expressions.

3. Point Group Symmetry, the Normal Modes and Site Symmetry

If a molecule has n atoms, it will have 3n degrees of freedom, 6 of which (for three-dimensional molecules) will correspond to translational and rotational movements, and the remainder to vibrational movements (the normal modes). The question arises what effect will the symmetry of a molecule have on the kind of normal modes of vibration these 3n-6 degrees of freedom will correspond to (especially, what effect in the infrared absorption spectrum)?

The symmetry of a molecule is defined by the numbers and kinds of symmetry operations that can be performed on it while returning it to a configuration identical in every respect with the original one it had.

All molecules can be classified, according to these symmetry operations they possess, into classes known as "point groups." The following method is used to obtain the symmetry of a molecule's normal vibrations given the point group it belongs to and its molecular structure. See Cotton[48] and Davydov[49] for the details.

We can describe each of the symmetry operations that can be performed on a molecule in a certain point group by a $3n \times 3n$ matrix. We form this matrix by setting up three cartesian coordinate vectors on each atom of the molecule, with each atom at the respective point of origin of each of these sets of three vectors, and then expressing the effect of a single symmetry operation on each vector in terms of a linear sum of the $3n$ original vectors, writing the coefficients of these $3n$ sums in a $3n \times 3n$ matrix.

The group of h traces of each matrix (for each symmetry operation), where h is the number of symmetry operations for the molecule, forms a reducible representation of the symmetry of all the molecular movements of the molecule in its normal modes. This reducible representation can then be reduced to the irreducible representations that correspond to the symmetries of each of the molecular motions of the molecule, and which belong to the point group the molecule belongs to. Eliminating those representations that have symmetries that apply to rotation and translation of the molecule as a whole, we are left with the symmetries of the normal modes of vibration in terms of the irreducible representations of the point group.

When we say that a normal vibration is of a symmetry type A, where A is an irreducible representation in a point group, we are saying that the normal vibration is a linear combination of symmetry modes of vibration which transform according to A, not necessarily that the normal

vibrational displacements themselves transform like A. By now looking up the irreducible representations corresponding to the normal vibrations, in the character tables under the point group in question, we can determine which normal vibrations are infrared (and/or Raman) active (infrared active modes transform as first powers of x, y or z, so that the transition moment integral of the transition is non-zero for dipole radiation), and the degeneracy of each normal mode (the dimensionality of the representation gives the degeneracy of the normal mode corresponding to it, where A and B representations are 1 dimensional, E are 2 dimensional, and T types are 3 dimensional).

For the isolated molecule, therefore, its symmetry will determine the selection rules for its vibrational energy transitions and the degeneracies that might be associated with any of these transitions. Once such a molecule is placed in the environment of a solid, however, as in the case of matrix isolation, the point group symmetry of the site as determined by the symmetry of the neighboring M atoms, the so-called "site symmetry", need not share the symmetry elements that the molecule possesses. If it lacks certain symmetry elements relative to the molecule, that is, if it is an "asymmetric site," it can effectively reduce the symmetry of the molecule as far as its selection rules and degeneracies are concerned. Selection rules will break down and degeneracies will be split into their components to the degree to which an interaction takes place between the atoms of the site and the molecule in it. For instance, a vibration may be inactive in the high symmetry of the isolated molecule, yet become active, to some extent, in the lower symmetry that a matrix site might produce (as in the case of S_2, mentioned on page 59). Or, a vibration that has an E representation and therefore is doubly degenerate, could be split in a site symmetry that had no representa-

tion of order greater than one, thus indicating that it corresponded to an E mode of vibration, something the gas phase spectrum could not tell us.

C. Thermodynamics

Thermodynamics has been called a teleological science, since it is a science that purports to explain the behavior of matter, which is composed of molecules, yet does not delve into the nature of individual molecules themselves, but only deals with the end effects of many billions of molecules on a macroscopic scale. In order to understand the energy changes going on in transformations of matter, thermodynamics postulates certain variables that can be given definite values for an equilibrated, macroscopic system, among them "state functions", which are always a single constant for a system under certain conditions, no matter what path was used to get to that system under those conditions. The two most elementary state functions are E, the internal energy, and H, the enthalpy. These terms are defined in any thermodynamic textbook.

Another very important state function is entropy, S. Entropy is a measure of the number of quantized energy levels possible for a system as a whole at a certain temperature. For a gas, it is a measure of the number of quantized energy levels for the individual molecules it contains, weighted to the lower-lying levels. Entropy is said to be an indicator of the "disorder" of a system, the number of ways the molecules can arrange themselves into various energy levels, and still have the same energy and temperature. If two states of a system have the same enthalpy, but one of them has many more microscopic ways of being than the other, then this state will be more probable than the other and have a higher entropy.

Another factor determining the relative probability of different macroscopic states of a system is their total energies (in terms of H). The higher this energy, the less probable it will be that the system will rearrange by taking up extra energy to reach this level. The two factors determining the likelihood of any one state can be combined into one factor, the free energy, F.

The free energy state function is set equal to H - TS, and for an isothermal change in a system,

$$\Delta F = \Delta H - T\Delta S \qquad (18)$$

The free energy change for a reaction, which varies with the concentrations of the reactants and products, among other things, gives us a measure of the driving force on the reaction for an isothermal system (the more negative it is, the greater the driving force). ΔF°_{T} for a reaction is defined as the free energy change when one mole of reactants, in their standard states, go to one mole of products, in their standard states, at the temperature T. Through thermodynamics, we can show that,

$$\Delta F^{\circ}_{T} = -RT \ln K_{p} \qquad (19)$$

where, K_p is the equilibrium constant for the reaction expressed as a product of pressures (in atmospheres) of the species involved.[50] One must always remember that this standard state molar free energy change is not the free energy change of the reaction in general.

Because of the great number of molecules present in any macroscopic system, and because of their constant state of motion and interaction, probabilistic considerations can be applied to these molecular motions and interactions to obtain a connection between their net effect for the system as a whole and the thermodynamic variables describing the system. This application is called "statistical thermodynamics,"

and connects ordinary thermodynamics with the molecular level, with which it must be consistent. Knowing the quantum mechanical nature of matter on a molecular level, and using the formulas of statistical thermodynamics, one can derive certain formulas expressing the state functions of macroscopic ideal gases in terms of several different microscopic properties of the molecules composing the gas.[50] These formulas could then be used to estimate or determine the thermodynamic functions for gases from estimated or determined microscopic properties of the molecules composing them.

The various motions of the molecules of a gas, as well as the contributions of these motions to the entropy and enthalpy content of the gas, can be divided into three components to a very good approximation: translation, rotation and vibration. The following formulas have been derived for these three contributions to the third law entropy of a gas, as shown in reference 50.

For the translational entropy, S°_{tr}, we have,

$$S^\circ_{tr} = (2.303R/2)\times(3\ \log M + 5\log T) - 2.315 \text{ cal/deg mole} \qquad (20)$$

where, R = universal gas constant, M = molecular weight of the molecule and T = temperature.

For the rotational entropy, S°_{rot}, we have,

$$S^\circ_{rot} = R\,[1/2\ \ln(D\times 10^{117}) + 3/2\ \ln T - \ln\sigma] - 0.033 \text{ cal/deg mole} \qquad (21)$$

where, D = product of the principal moments of inertia of the molecule ($D = I_a I_b I_c = I_x I_y I_z - 2I_{xy} I_{yz} I_{xz} - I_x I_{yz}^2 - I_y I_{xz} - I_z I_{xy}^2$) and σ is the rotational symmetry factor.

For the vibrational entropy, S°_{vib}, we have $S^\circ_{vib} = \sum_u S^\circ_{vib_u}$, where,

$$S^{\circ}_{vib_u} = R\left[\frac{u}{(e^u-1)} - \ln(1-e^{-u})\right] \text{ cal/deg} \qquad (22)$$

where, $u = 1.4387\ (\nu/T)$ and ν = one of the normal vibrational frequencies of the molecule.

For the difference in the enthalpy content of a gas at T°K from its enthalpy content at 298°K, we have,

$$H^{\circ}_{tr} - H^{\circ}_{tr_{298}} = 5/2\ R(T-298) \text{ cal} \qquad (23)$$

$$H^{\circ}_{rot} - H^{\circ}_{rot_{298}} = 3/2\ R(T-298) \text{ cal} \qquad (24)$$

$$H^{\circ}_{vib} - H^{\circ}_{vib_{298}} = RT\left[\frac{u_1}{(e^{u_1}-1)} - \frac{u_2}{(e^{u_2}-1)}\right] \text{ cal} \qquad (25)$$

where, u_1 is the value of u at T and u_2 is the value of u at 298°K (u is as defined above).

All these preceding formula ((20) through (25)) have been programmed into the computer program "ECOM", listed in Appendix D, whose output will be used in chapter S of section IV.

D. Matrix Isolation Spectroscopy

One of the most important experimental tools used in this research was matrix isolation spectroscopy. The experimental technique was described briefly on page 8 of this dissertation, and will be described more thoroughly on page 82.

1. The Advantages of Low Temperatures

Matrix isolation spectroscopy is especially useful when studying highly reactive, transient molecular species or fragments. Usually, such materials are formed using large amounts of energy input, resulting in highly excited gaseous molecules which tend to have very complicated

absorption spectra, owing to the many vibrational and electronic states they are distributed throughout. Indeed, many important gas phase species, such as CaO, have not had their ground states definitively determined as of yet. Furthermore, a large amount of Doppler broadening can occur at high temperatures. But under matrix conditions, rapid relaxation to the ground electronic and vibrational levels occurs, while maintaining isolation of the species under investigation. In absorption spectroscopy, this means that only v"=0 transitions will be observed. In ultraviolet fluorescence spectroscopy, the fact that the matrix phase is a low temperature solid means that the quenching time of the excited vibrational levels of the excited states produced via irradiation in the matrix, might be shorter than the lifetime of these electronic states themselves, so that fluorescence can often occur exclusively from the v'=0 level of the excited state. This greatly simplifies the observed spectrum, eliminating confusing arrays of light emissions from many different states. And of course, in the low temperature solid, Doppler broadening is eliminated.

The inertness of the M atoms combined with the low temperatures employed chemically stabilize species for long periods of time, especially through the absence of diffusion at these temperatures which keeps the trapped R species isolated for a period of time. This stabilization is ideal for observing highly reactive materials that usually require such complex and sophisticated techniques as steady-state, phase shift or rapid scan spectroscopy, to be observed in the gas phase before they disappear.

2. Narrowing and Broadening of Absorption Lines

In gas phase spectra, even at low temperatures, bands usually extend over an appreciable range of frequency because of the many rotational levels possible for each state involved. Structure, such as P, Q, and R branches, are often observed. But rotation is stopped in a matrix. For infrared spectroscopy, this usually means that only one strong, sharp feature will be observed for each vibrational fundamental, and resolution of accidentally degenerate peaks becomes feasible. In ultraviolet spectroscopy, if splitting of excited states with different total angular momentum does not occur, a similar narrowing is noted for electronic levels. The disadvantage of this narrowing is that rotational analyses cannot be performed, and that parallel and perpendicular absorptions cannot be distinguished from one another. Actually, some investigators have hypothesized restricted rotation or libration of species trapped in the matrix to explain certain spectral features observed, especially the existence of multiple lines, the broadening of lines, and the relative values of $g_{\parallel}$ and $g_{\perp}$ in epr spectra.[51] Mostly, only small molecules, such as SiH_3, CH_4 or other hydrogen-containing species, have been postulated to librate. In this work, no evidence for rotation of the phosphorus-fluorine species trapped in the matrix was observed.

The narrowing of absorption lines in the infrared in the matrix environment has practical importance in separating the vibrational modes of fragmentary species from similar modes of the parent compound. For instance, let us look into the case of the NH species. When the products of HN_3 passed through a silent electrical discharge are quickly condensed on a 77°K surface, a paramagnetic, blue solid is formed.[52] Mador and Williams[53] performed the experiment with both a 77°K and 4°K transparent surface and

reported that all infrared absorption bands could be attributed to HN_3 and NH_4N_3 (the usual materials formed on warmup). A year later Dows et al.[54] using conditions of deposition that improved resolution, reported infrared bands assigned to $(NH)_2$ and $(NH)_x$. Finally, in 1957, Becker et al.[12] were able to resolve the NH stretch from the overlapping HN_3 and NH_4N_3 bands by matrix isolation of the products of discharged HN_3. This advantage of matrix isolation was used in this work to resolve the phosphorus-fluorine stretches in the 800-900°K region of the infrared of the following compounds: PF, PF_2, PF_3 and P_2F_4.

Of course, in the pure solid R material at low temperatures we also have relaxation to low energies, the absence of diffusion, and the quenching of rotation. But,in general, intermolecular interactions between like molecules in a pure solid (or liquid, or high pressure gas) have two undesirable effects, which are reduced to a minimum in the matrix environment. First, there is the possibility of chemical interactions, such as that which would occur in the recombination of two doublet species. Secondly, a total wave function for a system of two or more identical particles in close proximity has certain quantum mechanical symmetry requirements impressed on it which lead to drastic changes in this wave function (from a simple product of individual wave functions to a determinant of wave functions) and hence in the common energy levels of the two or more particles involved. And slight changes in the separation or interaction between these identical particles will change this quantum mechanical "resonance" effect greatly. Thus, the net effect will be a large amount of broadening (as well as shifting) of the energy levels of these particles, much larger than for the same species isolated in the matrix, with inert gas atoms surrounding it.

However, due to such factors as multiple sites, vibronic coupling with the phonons (the quantized lattice vibrations) of the solid, long range R-R interactions and libration, all of which give rise to a spectrum of differing interactions between the trapped R species and the matrix cage, there still exists some broadening of lines in the matrix environment. And it is this small amount of broadening that gives an unexpected bonus to matrix spectroscopy, as it may allow quantitative concentration measurements from peak heights beyond the linear curve of growth region of absorbance. As was pointed out on page 35 of this dissertation, the individual rotational components of a gas phase band are much too fine to be resolved by the infrared spectrometers in use, and therefore both peak heights and areas recorded are those of the smeared-out, "integrated" rotational lines over a comparatively wide slit resolution. Since the formulas for radiance only hold for each individual rotational line, the peaks of the wide slit spectrum do not obey these formulas beyond the linear curve of growth region. All this changes in matrix isolation spectroscopy. Here the true line shape is obtained at a slit opening of 0.2-1.0 K, which is obtainable with the instruments used, and so the maximum peak height should obey Beer's Law intensity equation, $I = I_o e^{-kc}$. Therefore, accurate measurements of absorbance ratios may be accomplished for matrix-isolated species by the simple measuring of peak heights, even at absorbances far from the linear curve of growth.[55]

A very important method of narrowing matrix lines is through recourse to higher M/R values. At some value, the concentration of the R species in the condensing vapors will be so small that its rate of diffusion in the LLIT state will be unable to bring an appreciable number of R species together before solidification occurs, thereby eliminating R-R interactions.

The ability to vary the M/R ratio over a wide range could be used to quantitatively study the interaction or chemical reaction of various species in the matrix environment.

3. Matrix Shifts

One of the more theoretically interesting aspects of the effects of matrix isolation on the spectrum of the molecule isolated, matrix shifts, can also be of great practical value.

The frequencies of absorptions of molecules in the matrix are always shifted from their gas phase values, unless two oppositely directed effects accidentally cancel out. These shifts have various causes. In the infrared, for stretches and other high frequency modes of vibration, the "dielectric shift" is of paramount importance. This red shift is caused by van der Waals attractive forces between the M atoms and the atoms of the R molecule that are moving in the normal vibration under consideration. This attractive force varies as $1/r^7$, and in the excited vibrational state, the vibrational motion takes the atoms of R a little nearer to the surrounding M atoms where this attractive force will be more powerful than in the ground vibrational state, thus lowering the energy of the excited state more than the ground state. This van der Waals force can be viewed as an "instantaneous polarizability" or "induced-dipole, induced-dipole" force, that causes a shift due to changes in the distances from one another of the electronic systems involved, not their polarizabilities.

The dielectric effect exists for lower frequency motions such as bends and torsions as well, but in those cases, where large amplitude vibrational motions are involved, repulsive "anti-exchange" interactions come into play, as the electron clouds of the M and R molecules' atoms get very close to each other. This raises the energy of the excited vibrational

state and produces a blue shift in the infrared absorption frequencies. The extent of these two shifts depends largely on the type of motion involved in the vibrational mode as well as the geometrical compatibility of M and R molecules. Usually, the larger diameter inert gases will produce a larger red shift due to their increased polarizability (which increases the van der Waals attraction) and their increased distance from the R molecules (which reduces the repulsive forces).

The actual shifts noted can sometimes give us useful information. For instance, Pimentel[56] has ascribed the anomalous 25 K blue shift of the symmetrical bending mode of NH_3 at 975 K in an N_2 matrix to the inversion of the NH_3 structure accompanying this bending.

In the ultraviolet absorption spectrum, the main shifts also come from polarizability or van der Waals interactions, causing unequal negative energy perturbations in the ground and excited states of the R molecule. The red shift noted in the matrix environment for most molecules, is due to the greater polarizability of their excited states versus their ground states, which is due to the facts that electrons are less tightly held in excited states and that nuclear distances usually are larger in these states. This polarizability difference far outweighs any changes in van der Waals forces generated in the excited state due to changes in the distances between M and R. The more polarizable the inert gas surrounding the isolated R molecules, the greater the red shift, so the red shifts here, as in the infrared, increase as we go from argon to xenon.

There also exists a blue shift in ultraviolet spectroscopy, which is manifested much more in atomic than molecular spectra, due to the fact that the polarizability of atoms is about equal in their ground and excited states. This shift is caused by the increased radius of the

electronic volume in the excited state versus the ground state, causing an increase in the M-R repulsive interaction in the excited state. Here again, as in the infrared, the larger diameter inert gases produce the least blue shift, for they are the ones that provide the largest cavity for the R molecule to be trapped in (in monosubstituted sites), and so allow the greatest amount of outer electron orbital expansion with the least repulsion.

This blue shift becomes very apparent for all types of R species trapped in the matrix for highly excited vibrational levels of electronic states. In effect, the potential well in which the atoms of the R molecule find themselves, is steeper in the matrix environment.

Matrix shifts in matrices other than inert gases can sometimes be very different than the above, due to bonding effects or energy transfer between M and R. No such matrices were used in this work.

Matrix shifts have the disadvantage of displacing frequencies from their gas phase values. Nevertheless, this shifting can be quite useful in other respects. As was mentioned, the amount and direction of the shifts sometimes can give us information as to the trapped species and its environment, especially when trends are set up. Furthermore, using various M gases for isolation can serve the function of removing accidental degeneracies, since the relative shifts of two lines can be different in two different matrices.

4. Photolysis and Diffusion Experiments

Many molecules have been dissociated into two or more fragment radicals upon photolysis in the matrix. At the time of the radical formation, large local energies exist which can cause momentary diffusion of the species formed, thus separating each of them in an inert cage and making geminate

recombination impossible. If a second R molecule is added to the matrix, the radicals formed upon photolysis can diffuse to it to initiate a reaction. Because of the high relaxation rates under such conditions, secondary photolytic reactions, beyond fragmentation and initial reaction of fragments, are usually stopped, so that the primary process can be examined in more detail. Also, an isolated molecule in the solid has a much better chance of fissioning into constituent radicals upon photon absorption than one in a solid environment of many similar molecules, which could react with the fragments formed.

Diffusion is virtually non-existent at 20°K in the solid for most materials, and indeed, it is this property which allows the isolation of highly reactive materials in the matrix environment. But warmup, after deposition is complete, can allow controlled diffusion to take place, which could lead to chemical reactions whose intermediates could be stabilized and spectroscopically identified. This matrix reaction could then be compared with the analogous cocondensation reaction at 77°K.

Using this method, relative rates of low energy of activation reactions can be measured in the matrix environment. Furthermore, such diffusion can be used to anneal the M gas, tending to reduce the number of dislocations and other high energy defects in the solid structure, thereby creating a greater uniformity of sites and narrowing the absorption lines.

5. The Matrix Phase

The formation of the matrix phase, as with all solids condensed out from the vapor, must go through the LLIT state of matter. What happens in this state, therefore, determines, to a large extent, the nature of the built up solid.

As I have noted, increasing the M/R ratio will decrease the chances for two R molecules to pass near each other in the LLIT state and freeze out together, thus reducing broadening of lines and complication of the spectrum due to aggregate peaks. Deposition rate also affects the LLIT state. The higher this rate, the longer the LLIT state lasts and the more voluminous it is in the steady state. These conditions also promote the formation of aggregates, and the broadening of absorption lines. This occurs despite the fact that the more quickly deposited the matrix, the greater the ordering and crystallinity of the M solid. However, if the R molecules are trapped in dislocations or grain boundaries, the greater defect density in the more slowly deposited matrix would provide a greater number of sites in which to trap individual R molecules.

Adjusting the temperature of the target relative to the triple point of the matrix gas used can change the lifetime of the LLIT state on the surface of the target before solidification, affecting the isolation of the R radicals. For instance, xenon deposited at 20°K usually gives a very translucent material suggesting a very quick condensation, and indeed, xenon gives much better isolation than krypton deposited at these temperatures.

All rare gases are close-packed in the solid phase. Though theoretical calculations point to a greater stability for the hexagonal close-packed structure for the pure solids, only cubic close-packing (face centered cubic) has actually been observed. However, slight impurities in the solids readily shift the entire structure over to hexagonal close-packed. This would then be the most probable structure for the highly ordered inert gas plus radical matrix solid. In such a solid, each atom would have

twelve equivalent nearest neighbors (if there were no defects in the structure of the solid solution, nor any chemical interactions between M and R).

Numerous x-ray studies have been performed on solid low-boiling gases condensed out from the low pressure vapor. It has been shown that a polymicrocrystalline solid is formed from such condensation having short range ordering of linear dimensions around 10^{-4} to 10^{-6} cm.[26] Amorphous materials rarely, if ever, form. As a matter of fact, the rare gas microcrystallites do not even have a random orientation texture, but usually show a preferred orientation relative to the plane of the target. This has also been demonstrated by epr studies showing anisotropic orientation of free radicals in a matrix environment.[57]

Vapor deposited, low temperature solids, though crystalline, often occur in modifications different from those obtained by cooling the same substance from the melting point, because the LLIT state of matter does not last long enough to produce a stable structure. A sharp increase in the temperature at some point in the warmup,[27] as well as x-ray evidence,[26] suggest the existence of these high energy structures. These phase changes could cause a large amount of momentary diffusion of any R species that happened to be present in the frozen gas. After the heat is released, appreciable changes are seen in the x-ray spectra.

In the matrix, R molecules can substitute for M atoms ("solid solution"), or lie in the interstices between M atoms, or lie on the grain boundaries between two microcrystals, that is, in a defect (such as a dislocation or vacancy). This last alternative is a distinct possibility, since a rare gas deposited from the vapor has many defects in its structure, and the addition of a foreign material to this solid will increase

the number of these defects. If most radical trapping did occur in dislocations, sites in the matrix would not be homogeneously dispersed throughout the solid. Such a set of sites could explain the diffusion of R molecules upon warmup or in photolysis reactions: the diffusion would readily occur along two-dimensional surfaces that were defined by the boundaries of the microcrystallites (instead of three-dimensional random diffusion).

Due to the possibility of multiple stable sites, splitting or broadening out of lines can occur in the matrix. While this splitting can create spurious complicating effects, it can also be of some use, as was the case with S_2 isolated in a matrix.[58] Matrix isolated S_2 shows a progression of v' lines in its ultraviolet absorption. Though it should have no infrared spectrum, a small absorption is observed in the infrared assigned to the S_2 stretch (at a highly displaced value from the first vibrational transition deduced from the fluorescence spectrum). This has been attributed to a small fraction of the S_2 molecules lying in a highly asymmetric site, removing the symmetry prohibition for the infrared stretching mode of these molecules. Indeed, this second type of S_2 was seen weakly in the ultraviolet absorption spectrum along with the "normal" lines mentioned above.

Site symmetry effects, as those for S_2, would be expected to be different for different sites. For radicals lying in substitutional sites in the close-packed structure, with twelve equivalent nearest neighbors all around them, no great asymmetry of the environment would be expected. On other other hand, if there were one or more vacancies lying next to the substitutional site in which the radical was trapped, or if the radical were so large so as to require two or more adjacent M atom sites, large

amounts of asymmetry would result. If radicals were trapped in dislocations, where two differently oriented crystals would exist on either side, large asymmetries might well be expected (especially of a C_n or C_{nv} type). The effect of asymmetric sites on the infrared absorption of molecules trapped in them was reviewed in Chapter B, part 3 of this section.

III. EXPERIMENTAL PROCEDURES AND APPARATUS USED

A. The Vacuum System

Much of the reactions, analyses, and general handling of the chemicals used in this work were done in a vacuum system -- a set of valves, traps and other devices connected together and sealed from atmospheric leaks in which pressures are maintained at usually below one millitorr by an attached pumping system. A schematic diagram of the vacuum line, without the pumping attachments, is shown in Fig. 4. The entire system was designed so that it could be readily cleaned (using a solution of 10% HF which proved a very effective cleaning agent), owing to the tendency of many of the materials used in this work to decompose and deposit as polymers on the inner surfaces of the line.

The pumping system consists of a Marvac vacuum pump (with a speed of 4 cubic feet per minute) connected to a water-cooled mercury diffusion pump connected to a liquid nitrogen vacuum trap connected to the system. The diffusion pump has a bypass for pumping large quantities of permanent gas. The limiting pumping diameter here is a 15 mm bore greased stopcock. After every several weeks of work, the trap must be taken off the system and its contents allowed to evaporate in the hood, before being cleaned and replaced for operation.

Pressure measurements are done with a manometer connected to an ampule system (to be described below), a thermocouple gauge and a McLeod gauge. The thermocouple gauge is based on the principle that a hot filament will lose some of its heat to any surrounding gas colder than it (which will, in turn, transfer that heat outside the vacuum system) at a rate proportional to some power of the pressure of that gas. For a given electrical current through the filament, its temperature will be dependent

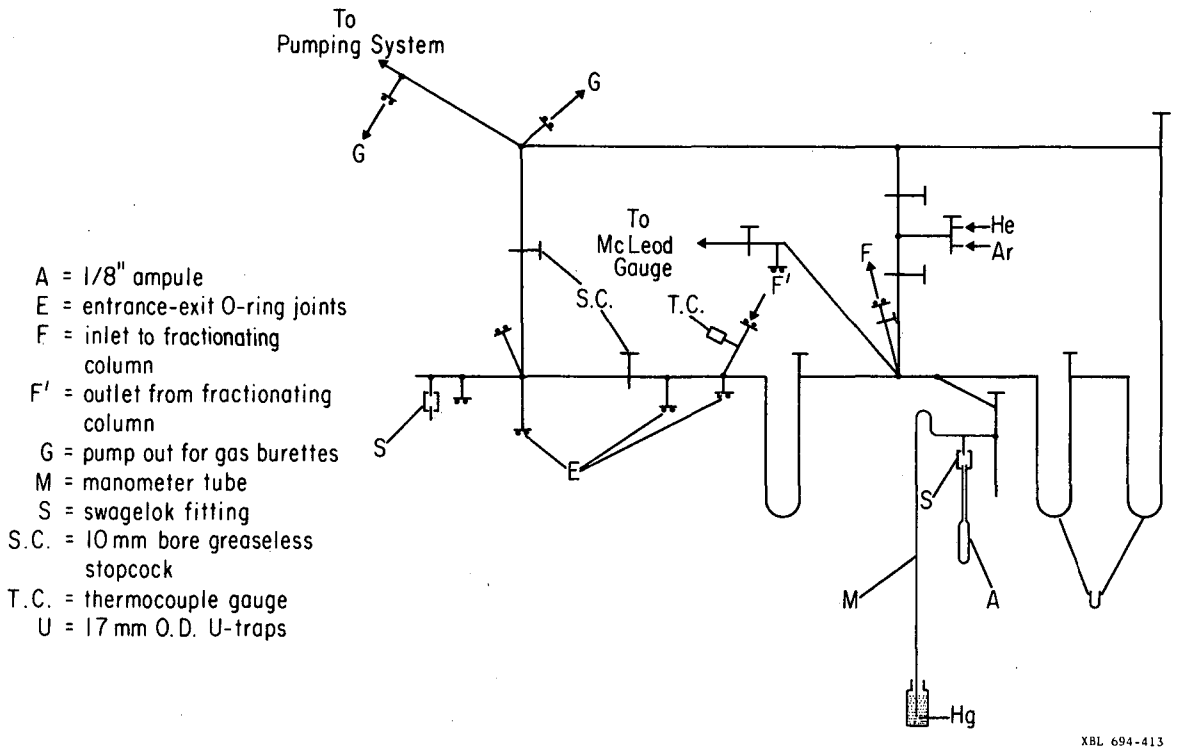

A = 1/8" ampule
E = entrance-exit O-ring joints
F = inlet to fractionating column
F' = outlet from fractionating column
G = pump out for gas burettes
M = manometer tube
S = swagelok fitting
S.C. = 10 mm bore greaseless stopcock
T.C. = thermocouple gauge
U = 17 mm O.D. U-traps

Fig. 4 A schematic diagram of the vacuum line

upon the amount of heat being conducted away from it by the surrounding gas, which, in turn, will be proportional to the pressure of that gas. Therefore, if a thermocouple is attached to the filament, its temperature and EMF output will rise in a reproducible manner as the pressure is lowered, so that the reading of this thermocouple becomes a measure of the pressure in the system.

A McLeod gauge is based upon Boyle's law. In its operation a given constant volume of the gas from the system, V_2, is compressed with a mercury column into a much smaller volume in a capillary, and its new pressure is then measured by simple manometric procedures. Using $P_1V_1 = P_2V_2$, and measuring both P_1 and V_1, we can obtain P_2, the pressure of the gases in the system (other than mercury, which condenses into the mercury column upon compression).

The vacuum system itself consists of pyrex glass tubing (17 mm outside diameter) fused together wherever possible. Entrance-exit O-ring joints are placed throughout the system allowing the connection of more complicated apparatuses to the line as well as the admitting and taking off of chemicals from the line. The seal on these joints consists of a viton O-ring very lightly coated with Kel-F grease [a per-(fluorochloro) hydrocarbon]. The valves used are 10 mm bore Westglass greaseless valves. The body of these valves is made of teflon, and the vacuum sealing is done also with slightly greased viton O-rings. All sources of mercury vapor can be closed off from the main system so that mercury vapor would not interfere with the vacuum line work either as a chemical reactant, or as a blackening agent making it impossible to see what is occurring inside the vacuum system (mercury vapor deposits out black on 77°K surfaces).

Once materials are placed in the vacuum system at a point, they are transferred to any other point by allowing them to condense on a surface at that point which is submerged in liquid nitrogen. This is done with pumping whenever the 77°K cooled surface is along the only route by which the condensible gases can be pumped out to the vacuum trap, but must be done with a closed-off system when transferring a condensible to one of the inlet-outlet joints. After a substance has been frozen out anywhere in the system, it can be allowed to warm and reevaporate to be condensed anywhere else in the system. In this way, transferral of materials from one U-trap to another, to external storage, to reaction flasks, to infrared cells and various other places can be readily accomplished.

Two open-ended 1/4 in. O.D. tubes are also used as inlets and outlets. These are fitted either with ultra-torr Cajon high vacuum fittings (using viton O-rings to make the vacuum seal) or with Swageloks using teflon or nylon ferrules to make the vacuum seal. Actually, most of the materials let into or taken out of the vacuum system are sent through the unique ampule system that is shown in the middle of Fig. 4. The sample to be taken off the line is first condensed into the large diameter tube in this ampule system, and then the valve connecting it to the rest of the system is closed off. The sample is next transferred to the glass ampule (which has an 1/8 in. stem and a 3/8 in. diameter body) kept at liquid nitrogen temperatures. Now while the system is pumped on, the ampule is sealed off at the 1/8 in. stem with a small oxygen-gas flame. From now on the ampule must be kept near liquid nitrogen temperatures or its contents would warm and explode it. Since the ampules are so small, a great number of separate samples can be stored in individually labeled ampules in a single large storage dewar. To remove the ampule

from the system and place another empty one on, helium is let in to fill up a portion of the vacuum line plus the ampule system, and when the internal pressure is slightly above one atmosphere, as indicated by the bubbling mercury at the bottom of the manometer in the ampule system, the Swagelok is opened to remove the ampule. An empty ampule is now attached and the Swagelok tightened. In this way, no air or water has a chance to adsorb onto the internal surface of the vacuum system, since the helium is constantly flowing out of the system during the operation to prevent back diffusion.

If it is desired to release the contents of an ampule into the system, the following method is used. First a scratch is placed on the 1/8 in. glass stem below the sealed portion for subsequent easy breakage. Next, while the helium is flowing out of the system, the ampule, still at 77°K, is broken in a stream of argon that comes from a tube surrounding the 1/8 in. stem. Then the ampule is quickly taken out of the liquid nitrogen, removed from the argon flow and attached to the system. In this way, helium is coming out of the system while argon is coming out of the ampule (argon condenses at liquid nitrogen temperatures) as the connection is being made, so that no air can enter the ampule or system whatsoever.

Separation in a vacuum system can be done by the process known as trap-to-trap distillation (as well as by fractional distillation discussed below). In this fairly crude process, the first trap of a series of three connected traps has the mixture to be separated in it (at 77°K). The second trap is cooled to some intermediate temperature between 25°C and 77°K, and the third trap is cooled to 77°K. When the first trap is allowed to gradually warm while pumping on the third trap, the mixture to be separated passes to the third trap, but a portion of it condenses

out in the second trap. Thus a separation is effected through the properties of low temperature vapor pressure as well as nucleation rate. Now the contents of the second trap can be transferred to the ampule system and taken off (vide supra). This method is also useful in removing exceptionally volatile impurities from a mixture by leaving the third trap at room temperature, and pumping on the second trap, after which is a thermocouple gauge to measure the pressure. When the pressure has gone down, one knows that all the exceptionally volatile materials have been removed through the pumping operation. Separation of permanent gases from condensible gases is achieved by warming a mixture of the two in a closed volume till it vaporizes, then freezing it out and pumping on it, repeating the process as many times as necessary to pump away all the permanent gases.

A fractional distillation column, of an unpublished design developed by R. Schaeffer and Arlan Norman at the University of Indiana, and diagrammed in Fig. 5, is used for separations of materials whose boiling points are close to each other. It was especially useful to separate PF_2I from P_2F_4, since PF_2I is a liquid at low temperatures while P_2F_4 is a solid, and PF_2I is less volatile than P_2F_4, so that it would move up the column behind P_2F_4 and continually drip down to remain behind it while the P_2F_4 was being taken off. The distillation column is three feet long and consists of a vacuum jacket around two vertical,concentratic,glass tubes. An axial temperature gradient is maintained in the inner tube by flowing a controlled amount of cold nitrogen gas (produced by placing a heater in a dewar of liquid nitrogen and controlling the heat input into the dewar down the center of this tube. Since some heat losses of the gas do occur as it travels down the tube, the top of the column becomes colder than the bottom. The material to be fractionated is allowed to

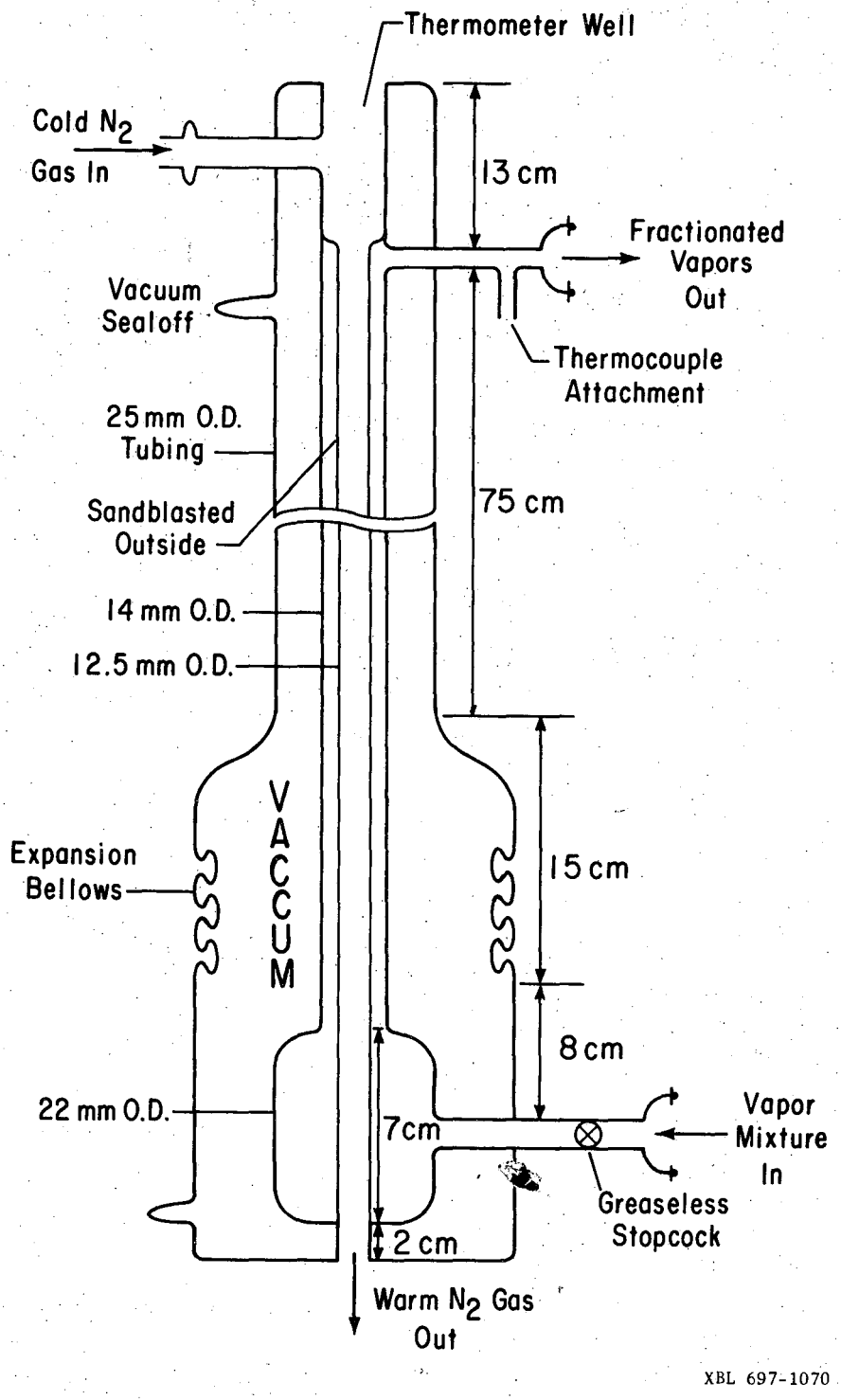

Fig. 5 Low temperature, low pressure fractional distillation column

enter the column from the bottom in the annular space between the two tubes while the nitrogen flow is maintained at a very fast rate so as to cool the entire column to a low temperature. Therefore, the material condenses out on the bottom of the column. Now the bottom stopcock to the column is closed, and the column gradually warmed by slowing the flow of cold nitrogen. The material in question then slowly moves up the annular space between the two tubes under vacuum, separating into its various components. These components eventually come off the top of the column one at a time, and are detected by a thermocouple gauge situated at the exit of the column. As each component is detected, it is trapped in a different U-trap of the system, thereby effecting a clean separation of these components.

Separations of components are also done off the vacuum line on an Aerograph Model A-90-P Gas Chromatograph. The packing material is a liquid substrate, 20% Silicone (GE-SF-96), on a firebrick solid support. This chromatograph system uses helium as the carrier gas and has a leak tight, detachable trap connected to it for the transferral of materials from and to the vacuum system.

Melting points are obtained with a Stock-type dropping needle apparatus. In this device, the sample is condensed in a narrow tube around a thin glass rod suspended in the tube (by a magnetic assembly). The device is now filled with helium to prevent evaporation of the sample. The entire tube is slowly warmed as its temperature is carefully taken. The temperature at which the sample becomes mobile enough to be incapable of supporting the glass rod, which drops in the tube noticeably, is considered the melting point of the sample.

Vapor pressures and densities are measured in the ampule system.

The sample is condensed into the vertical tube on the right side of the ampule system and the system is closed off. Null readings and readings at various temperatures of the sample's pressure are taken by observing the level of the manometer (sometimes with a cathetometer), differences in its level being a measure of the pressure. After the volume of the ampule system has been calibrated, including the added volumes of the small ampule used to condense the sample in, and of the inside of the mercury manometer that arises as the pressure inside the ampule system increases, vapor densities can be determined. The method consists simply of condensing a known volume and pressure of sample into a small, weighed ampule, sealing off the ampule, and reweighing it (making a correction for the original weight of air within the ampule). The gas equation, PV = nRT, can then be used to calculate the molecular weight of the unknown. This method cannot be used for very volatile or unstable materials, since the pressure buildup in the ampule in those cases could explode it at room temperature in the weighing operation.

1. Vapor Pressure Plots

Vapor pressure versus temperature plots for pure compounds yield useful information about the kinds of forces between molecules in the condensed state.

Due to thermodynamic relationships that apply to the vaporization process, we can derive a formula relating the change of pressure with temperature to the heat of vaporization (the Clapeyron-Clausius equation) which applies approximately to a great many compounds:[50]

$$\frac{d\ln(P)}{dT} = \frac{\Delta H_{vap}}{RT^2} \quad . \qquad (26)$$

Thus, by taking vapor pressure measurements, we can obtain the heat of vaporization (sublimation or evaporation) of the substance under consideration.

From the heat of vaporization, the entropy of vaporization at the boiling point can be obtained, by using the formula:

$$\Delta S = \Delta H_{vap}/T_b \qquad (27)$$

where T_b is the atmospheric boiling point of the compound.

This entropy of vaporization from the liquid to the gaseous state is a fairly constant number for a great many compounds and is termed "Trouton's Constant" (discovered by Trouton in 1884). This is so because entropy can be considered a measure of disorder, and the change in disorder in going from the liquid state to the gaseous state at one atmosphere (or any other pressure) is approximately the same for all materials owing to the nature of these states. And if a certain material gives an anomalous value for Trouton's constant, far from the usual value of 22 cal/deg, this is a sign of some peculiar property it possesses. The constancy of this change in disorder in transitions of state is less valid for solid to gaseous transitions, and still less valid for solid to liquid transitions.

2. Absorption Spectroscopy in the Infrared and Ultraviolet

Gas phase infrared and ultraviolet absorption spectroscopy are very useful in the quick identification of small amounts of materials being manipulated on the vacuum line, especially when such materials are one of a number of compounds all of whose spectra have been previously taken and recorded. Since such spectroscopic absorptions are additive, a mixture of several components can be qualitatively analyzed in a matter of minutes this way.

The instruments used are two Perkin-Elmer Infracord Spectrophotometers that cover the infrared range from 4000 K to 400 K and an Applied Physics Corporation Cary Model 14 Recording Spectrophotometer which covers the range from 185 nm to 800 nm. The infrared frequencies reported in this work are purposely uncorrected to vacuum.

An infrared gas cell can be conveniently connected to the line to take off small samples to have their spectrum taken. This cell has a greaseless stopcock, a small side arm to condense the gas sample in, and two No. 25 back-to-back O-ring joints, upon which two infrared transmitting plates (NaCl, KBr, or CsI) are placed and fixed by four pressure screws placed around the circumference of the plates. A small detachable ultraviolet cell with a greaseless stopcock was also constructed. This cell can completely fit into the light-sealed compartment of the Cary Spectrophotometer. Also, a one liter photolysis cell was constructed, consisting of a large quartz plate black-waxed onto the cell which also has a cold finger and a greaseless stopcock.

Because of the lack of vibrational coupling, certain bonds in compounds have characteristic stretching and bending modes in the infrared which can be used to identify certain structural features of a new compound, as well as determine the presence of certain elements. For instance, if one had a phosphorus compound with no absorptions above 1500 K, one could be quite sure that no hydrogen was attached to the phosphorus in the compound. Also, low frequency bending modes below 700 K are usually unique for each compound examined, and this portion of the spectrum, called the "fingerprint region," can be used for identification of several related compounds all of which have approximately the same stretching modes at higher frequencies. For many stable compounds with only high lying energy

levels, such as PF_3, ultraviolet-visible spectroscopy is entirely useless, since no absorptions occur in the air region (185-800 nm). However, it would be expected that some of the unstable materials formed in this work might have an ultraviolet absorption within this range because of the high energies of their ground states, and perhaps because of partial multiple bonding in these states.

B. Cocondensation Reaction Procedure

Several different types of apparatus are used to carry out the cocondensation reactions. For the GeH_2 and SiF_2 research, it was believed that immediate condensation by a line of sight path was not necessary to transport considerable quantities of these radicals to the cold surface, so they are produced at some distance from the liquid nitrogen cooled portion of the apparatus and have to travel around a bend in order to reach it. A diagram of the SiF_2 producing and reacting system used is shown in "Preparative Inorganic Reactions"[19] on page 70, and a similar apparatus is used for GeH_2 production, with the exception that the furnace in this case has a constricted tip to allow high pressures of germane to build up in the furnace upon the rapid injection of the germane into it. For the GeH_2 and SiF_2 furnaces, Nichrome wire and Kanthal wire are used, respectively, both of which can withstand air oxidation at high temperatures.

However, for other species, most notably those arising from the pyrolysis of P_2F_4, immediate condensation is a prerequisite for any reaction (besides simple polymerization) to take place at all. After several trials, the apparatus shown in Fig. 6 was developed (which is a modification of the apparatus used by Timms to study the chemistry of the BF carbenoid[2]). A modification of this apparatus with a graphite furnace instead of a quartz one is employed in the GeF_2 research.

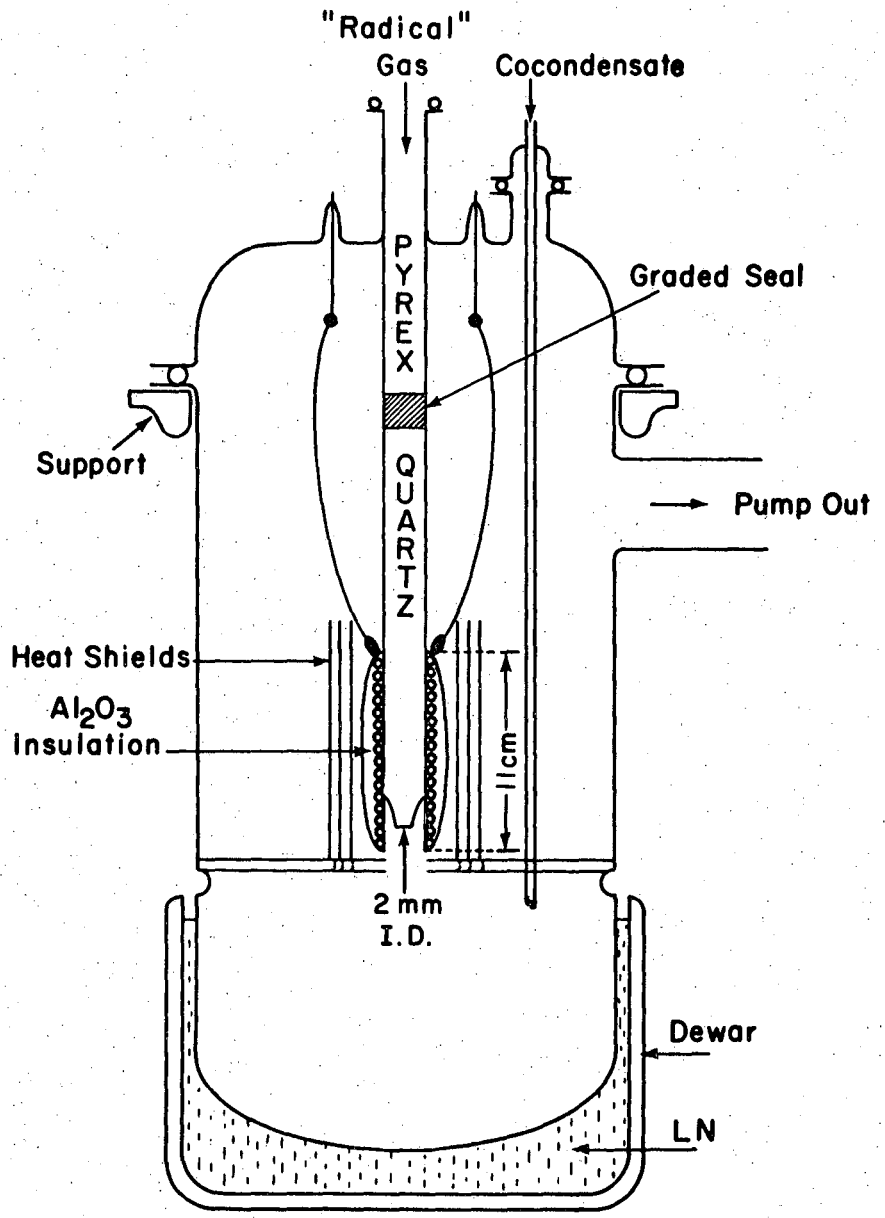

Fig. 6 The reaction vessel

The furnace in Fig. 6 is wound with 20 mil tantalum wire (since it is situated within a vacuum, air oxidation cannot occur in this case) and is insulated with Al_2O_3 cement. The heat shields are made of 2 mil tantalum sheet. It was found that tantalum wire is better than molybdenum or tungsten wire for heating to moderate temperatures because of its high rate of change of resistivity with temperature. At high temperatures, high voltages (20-40 volts) can be put across the furnace windings without blowing out the fuse in the transformer because of excessive currents.

The furnace is made of quartz which was found to be a suitable material for phosphorus-fluorine work, though references can be found which claim that PF_3 etches SiO_2 at elevated temperatures. For instance, Booth and Bozarth[59] claim that PF_3 reacts with SiO_2 above 500°C at one atmosphere pressure in the following manner: $4PF_3 + 3SiO_2 \rightarrow 3SiF_4 + 3O_2 + 4P$, because they found traces of SiF_4 and phosphorus in their products The glass they were using was soda-lime, not quartz.

Since the pressures are low in the apparatus, the species exiting from the furnace travel straight down to the cold surface, and since there is such a large surface available, very high cryogenic pumping rates are thereby effected. It was estimated that the species exiting from the furnace spend less than $\frac{1}{2}$ millisecond in the gas phase before striking the cold surface and condensing out on it. With the chemicals used in this work, the molecular probability of condensation on a 77°K surface (the condensation coefficient) is unity. Furthermore, due to the low flow rates and hence low pressures involved, the condensation process is truly unimolecular as it starts, since the probability of two distinct gas phase species striking the surface "together" and simultaneously is virtually zero. The inlet labeled "cocondensate," which

leads down the concondensate sprayer tube, is used to simultaneously condense some normal volatile compound with the radicals.

Temperature calibration of the furnace (with the liquid nitrogen in place) is done before reaction by heating the furnace with a thermocouple placed down its center and accurately recording the amperage and voltage through the furnace windings for several different temperatures. Reproducing these same amperages and voltages when the furnace is operating during a cocondensation reaction was then believed to reproduce these same temperatures. Ideal temperatures for P_4F_6 production (after the pump out) were found to be 900°C, though still higher temperatures do seem to increase the yields slightly.

Experiments with sulfur vapor passing through the furnace suggested that the tip of the furnace is at a lower temperature than the body, since when the central portion measured 800°C, no appreciable amounts of S_2 (which is colored purple at 77°K) were noted condensing on the cold surface, yet S_2 should form at temperatures as low as 550°C at the low pressures in this furnace. Thus the S_2 forming in the center of the furnace was repolymerizing at the nozzle of the furnace. This temperature gradient, however, would not be expected to affect the P_2F_4 pyrolysis greatly, since the rate of reverse reaction of PF and PF_2 is probably quite small.

In a cocondensation reaction, great care must be taken to purge the materials to be reacted of all permanent gas, since a very slight amount of this gas could raise the pressures during the deposition considerably, thereby making a line of sight path for the radicals much less probable. The permanent gas concentration is reduced by the method mentioned previously.

For the SiF_2 reactions, the flow of SiF_2 plus SiF_4 is started before

the flow of cocondensate starts and ends after the flow of cocondensate is stopped, so that back diffusion of the cocondensate into the furnace from which the SiF_2 is emerging is avoided. Flows for cocondensation reactions in general are in the range of 0.1 to 2.0 mmoles/min, a much faster rate than that for matrix isolation (see below). Using the equations of Dushman [60] for viscous flow, and given a flow rate of 0.6 mmole/min through an orifice of 2 mm bore and 1 mm length, we can calculate the back pressure in the furnace in Fig. 6 at 900°C to be 0.5 torr (Appendix B). It has been experimentally observed by Mr. Ralph Kirk[61] that these equations predict consistently low results, which can be partially due to the effects of non-ideality of the flowing gases, back pressure, and restriction to flow along the entire length of the furnace. Thus, my estimate of the actual furnace pressure here would be about 2.0 torr.

C. Mass Spectroscopy

Mass spectroscopy is a very powerful tool in initial identification of new materials (or radicals) formed in cocondensation reactions. In mass spectroscopy, an electron current inside a vacuum chamber is used to ionize the unknown molecules injected into it. The impinging electrons eject other electrons from the molecules they strike, and give up so much energy into the various bonds of the resulting ion that its dissociation ensues. The ion of the parent molecules, as well as the ions of the various fragments, are immediately accelerated as they are formed in the ionization process and then analyzed for their mass. From an output containing the mass of each of these ions, we can usually obtain a very good idea of the molecular weight of the parent molecule, as well as its mode of dissociation upon electron bombardment. Knowing the original elements that had to be present in the parent molecule, we can usually arrive at its

detailed formula. Knowing its mode of decomposition, we can sometimes arrive at its structural characteristics as well.

By varying the energy of the electron ionizing current, that is by varying its accelerating voltage, we can use mass spectroscopy as a tool to measure "appearance potentials" of ions. The lower the electron voltage, the less the chance of fragmentation upon ionization, and, at a certain point, ionization itself becomes thermodynamically impossible, since all the kinetic energy of the ionizing electrons is not enough to eject one electron from the molecule. This critical accelerating potential for the electrons, below which they will not ionize the parent, is called the appearance potential and is usually a measure of the ionization energy of the parent molecule. Due to the extremely wide range of energies that the ionizing electrons had in the machines used in this work, combined with their low sensitivity, accurate appearance potentials were not measured here, but nevertheless moderately sharp cutoffs of the intensities of certain ions can be observed by reduction of the electron energies employed.

Due to the low pressures needed in mass spectroscopy, the identity of unstable species in gases at high pressures is not readily determined by it. But it can ionize and detect extremely unstable gaseous species at low pressures, since they only need exist for a few milliseconds to get into the ionization region.

One of the most important points to emphasize in mass spectroscopy is that the fragmentation pattern observed tells us of the properties of ionized species, <u>not</u> the thermodynamic properties of the neutral parent molecule. Furthermore, the relative abundances of the ions observed may be mainly kinetically controlled, so that thermodynamics would not apply here at all.

Other points that might lead to spurious results in mass spectroscopy are the following. First of all, the heat generated in the ionization region, or some other factor, might decompose the compound you wish to ionize before it reaches the electron current itself, so that the mass spectrum you observe will be that of the compound's decomposition products. In this work, this effect is minimized by warming up samples, connected directly to the mass spectrometer, from liquid nitrogen temperatures till the point at which they just have enough pressure (about 10^{-5} torr) to produce a noticeable spectrum and then directing their vapors into the ionization region through a glass tube. In this way little chance for decomposition is possible. Another danger, especially when using the above method, is that a volatile impurity component of a mixture of chemicals might volatilize first, while the material you wish to volatilize will not do so until all the impurity has been evaporated. If you do not wait long enough, the mass spectrum you will record will be that of the impurity, not the sample you want. Finally, it is assumed that the highest mass peak observed is the parent ion peak. In general, this is true, but not always. Sometimes, one can only deduce the parent peak from a detailed examination of the remainder of the spectrum, since it itself does not appear.

Mass spectrometers are distinguished from each other mainly on the basis of the method they employ to analyze the ions, accelerated from the ionization region, for their mass spectrum. According to this classification, two different mass spectrometers are used in this work: a Bendix Model 1400 time-of-flight machine and a Quad 250 Quadrupole Residual Gas Analyzer (manufactured by Electronics Associates, Inc.). The time-of-flight machine is based upon the fact that after each ion is accelerated through a definite potential, it will have a definite kinetic energy, but

its velocity would be dependent on the inverse of the square root of its mass. The machine produces a very short burst of ions at one end of a tube, down which these ions are accelerated, and has a detector at the other end of the tube that is able to resolve the time duration of flight across the tube that each ion took. The record of these times is then printed out on a chart or viewed on an oscilloscope.

The quadrupole analyzer principle is really quite complicated, but can be explained simply as follows. The mass filter after the acceleration section consists of four equally spaced axial poles charged with a constant D.C. voltage (diagonally opposite poles having the same polarity). A complicated R.F. voltage is impressed upon this voltage. As the ions travel down the space between the four poles to the detector, they undergo complex, spiralling, oscillatory trajectories. For all but one mass peak, the amplitude of these trajectories diverges with time. Thus, in all but this case, the ions spiral out and collide with the poles of the analyzer, whereupon their charge is neutralized and they deposit out on these poles in the form of a polymeric coating. The one type of ion that does get through then gives a signal that is amplified and recorded on chart paper or displayed on an oscilloscope. By continuously changing the R.F. frequency over the range which allows, successively, all the ions from mass 1 to mass 500 to get through the analyzer and reach the detector, we obtain an output that is a scan over the entire mass spectrum.

To sum up, mass spectroscopy is of enormous use in the initial identification of products. After taking the mass spectrum of an unknown mixture, the products in it that are of value can be further purified and investigated with some knowledge of what sort of materials are being worked with.

D. Nuclear Magnetic Resonance

Some basic principles of nuclear magnetic resonance will be mentioned here. A few long-lived nuclei have a permanent magnetic dipole moment. In a magnetic field, the component of this magnetic moment along the axis of the field is quantized, with different energy levels associated with different components along the field's direction. The presence of a radio frequency electromagnetic wave passing by the nucleus whose quantum exactly equals the energy difference between these "nuclear precession" levels, can cause absorption of this quantum and excitation of those levels. When these levels then decay again, due usually to stimulated emission caused by random fluctuations of the magnetic fields of neighboring paramagnetic nuclei in the liquid, they emit the exact same frequency they absorbed, which can be picked up and monitored by a receiver, whose signal is amplified and recorded as an absorption. In this way we have a tool that can give us information about local magnetic fields at nuclei and how they differ from the macroscopic fields applied, due to electronic shielding by the chemical environment these nuclei find themselves in. This tool is more valuable if there is more than one non-equivalent magnetic nucleus in the same molecule. In this case, magnetic coupling between nuclei can result, which splits lines into very unique patterns that are of value in determining the number, arrangement and equivalence of the nuclei involved.

NMR spectroscopy is useful for hydrogen, fluorine and phosphorus nuclei, all of which have a spin of 1/2 and therefore have no quadrupole moment. A quadrupole moment of a nucleus, in an electric field gradient generated by the surrounding electrons, can cause the nucleus to "flip" prematurely, thus broadening its energy levels, or the energy levels of

another nucleus it is coupled with. Such a broadening effect is not noted with these three nuclei (the only ones investigated in this work), making them well-suited for high resolution nmr spectroscopy.

In practice the technique consists of glass blowing a 1/4 in. stem to an nmr tube so that it can be attached to the ampule system and pumped out. A small amount of the material to be investigated is then condensed into this tube; sometimes with a solvent to spread the material out throughout the length of the magnetic field (when only small amounts of material are available), and sometimes with an unreactive reference compound that has the nucleus under investigation in it for the machine to "lock" on. The nmr tube is then sealed off and warmed to the melting point of its contents. Mostly, low temperature nmr is taken, with the probe just above the melting point of the sample.

The amount of material needed for nmr spectroscopy, and the sensitivity of the signal detection, is usually greater than that required for infrared or ultraviolet absorption, because the energy differences in nmr are much smaller than in infrared, making the absorption coefficient for nmr much smaller.

Some of the machines used are: a Varian A-60 proton spectrometer, a Varian A 56/60 spectrometer for fluorine and hydrogen (at 54.4 and 60.0 megahertz), and a Varian HR-100 proton, fluorine and phosphorus spectrometer (at 100, 94.1 and 40.5 megahertz). The epr machine used for taking the spectra reported in this research is a Varian EPR spectrometer.

In this work, nmr spectroscopy proved of great value in confirmation of the structures proposed for the compounds discovered.

E. Matrix Isolation Technique

A thorough discussion of the theory of matrix isolation has been given in the last section. In this section we shall discuss the actual experimental apparatus and procedures used.

The complete apparatus consists of a cooling dewar (cryostat), furnace attachment, a vacuum and gas handling system adjacent to the dewar to allow the flow of various gases into it, and the peripheral spectroscopy equipment. Except for the power supply and the spectroscopy equipment, everything else is mounted on a single movable cart (always kept in a room specially designed to protect against hydrogen explosions).

A diagram of the matrix isolation cryostat itself plus the furnace attachment is shown in Fig. 7, with the target (T) in the viewing position. A picture of the same apparatus with the peripheral equipment attached is shown in Fig. 8. The outer vacuum casing is made of brass and the inner dewar (A) of stainless steel. The pump-out port (V) for the cryostat is connected through a ball valve to a metal cold trap and then to a two inch oil diffusion pump, which can achieve a static vacuum of 10^{-7} torr, and an operating vacuum, with krypton flowing, of about 2×10^{-5} torr.

The stainless steel dewar is radiation-insulated with aluminized Mylar (J). It is soldered at its base to a cylindrical copper block insert (I). The target (either sapphire or CsBr in this work, measuring 40 mm × 20 mm × 3 mm) is clamped in the copper target holder between indium sheet gaskets to insure proper thermal contact. Sapphire is far superior to CsBr (and to a lesser extent, even to copper) in heat conducting abilities at these low temperatures (about 400× better than CsBr), but unfortunately could not be used for the infrared work due to its absorptions in this region of the spectrum. Both sapphire and CsBr crystals

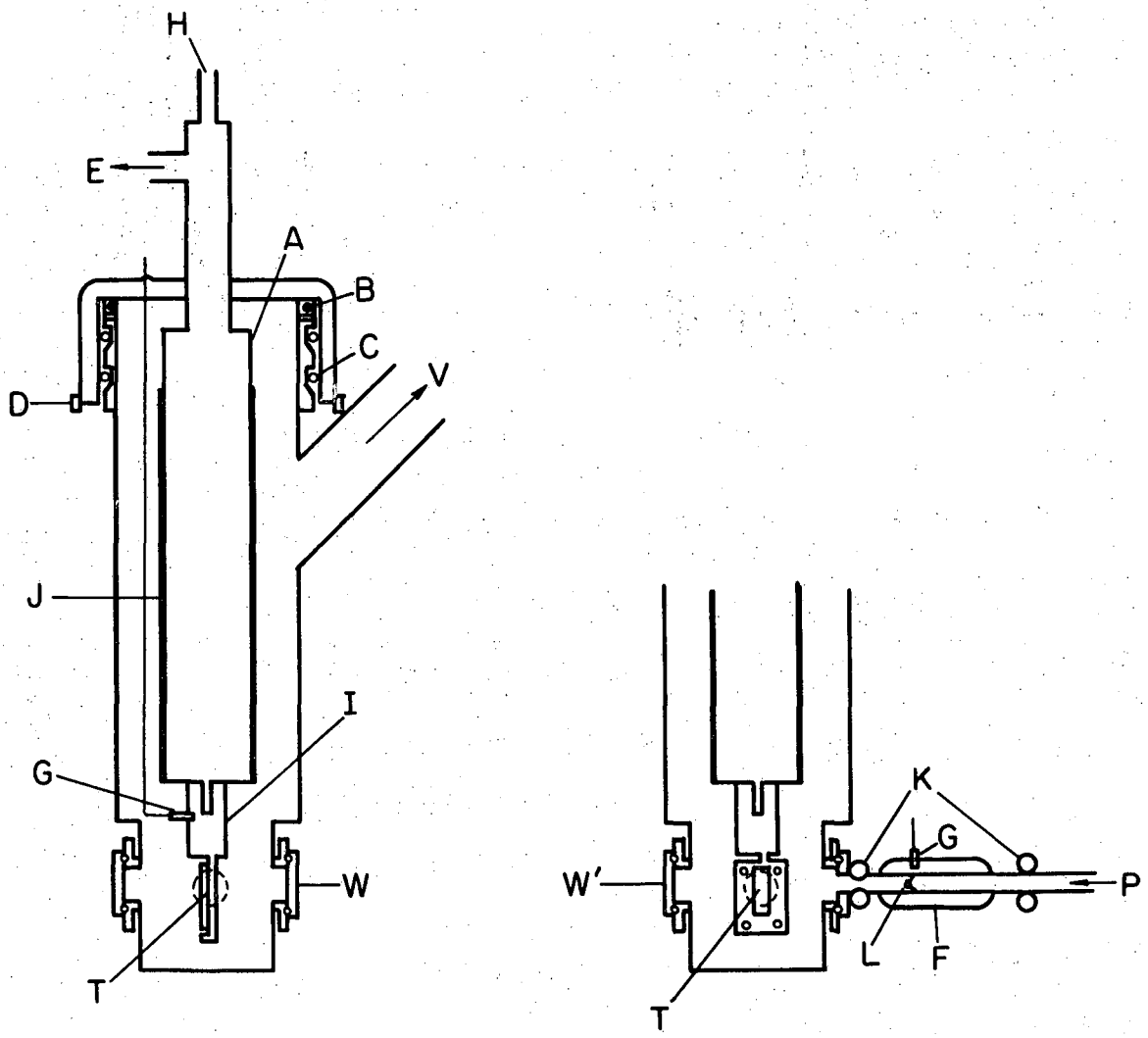

MATRIX APPARATUS

XBL692-2006

Fig. 7 The matrix isolation cryostat.

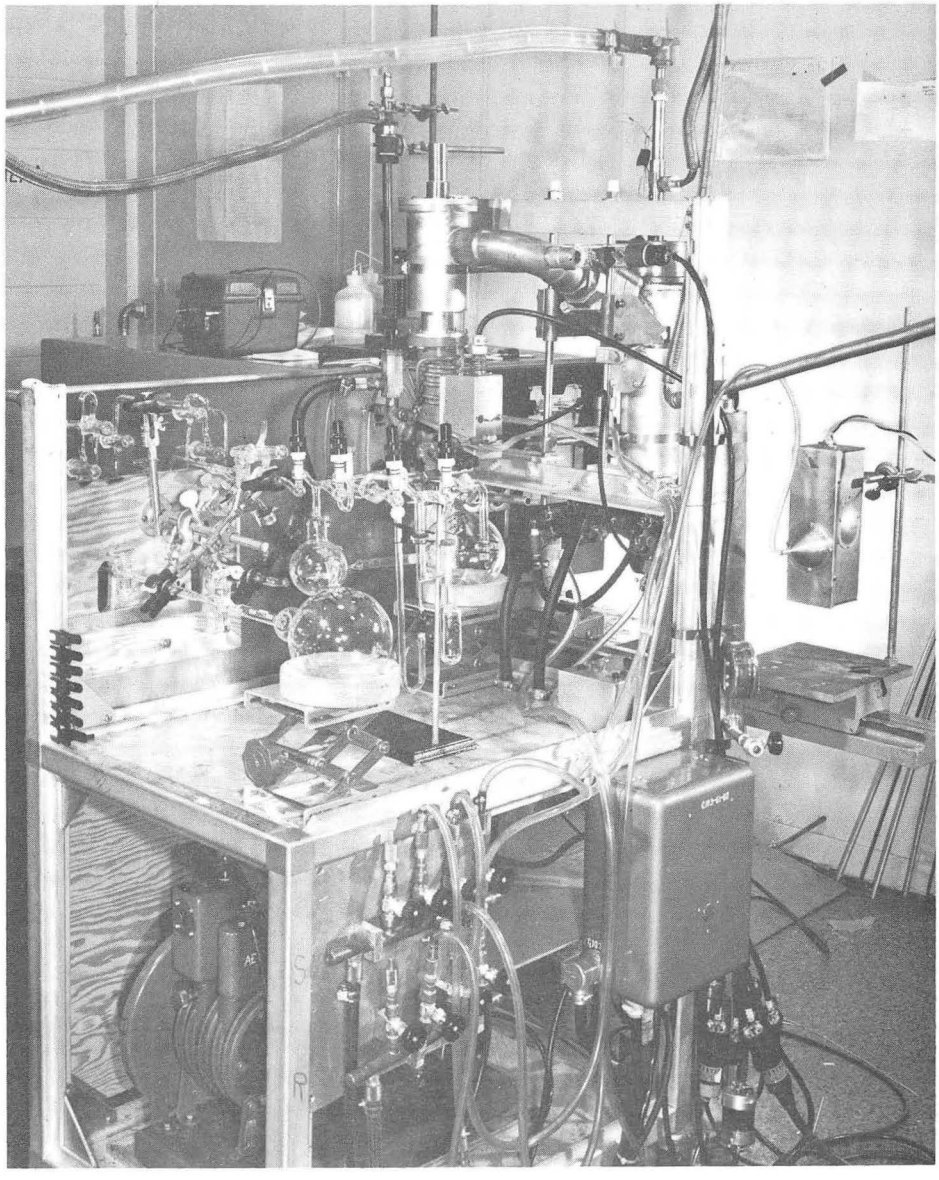

CBB 682-883

Fig. 8

can withstand great thermal stresses without breaking, which is due, in the case of CsBr, to its coordination number of 8 (instead of 6) which makes it extremely easy for it to glide or plastically deform under stress. Indeed, this plasticity gives it very good thermal contact with the copper block to which it is connected, which partially makes up for its low thermal conductivity.

It is observed on initial deposition of the M gas layer that the center of the target first becomes violet through the interference of reflected light, while the edges of the target remain colorless. Then, as the center progressively becomes blue, green, yellow and red-violet, the edges progressively become violet, blue, green and yellow, the process repeated through the spectrum several times with the edges gradually lagging further and further behind the center in the color spectrum. This is due, most likely, to the lack of perfect collimation of M as it leaves the jet built into the flange. If there were a large thermal gradient on the target, such that the center were not as cold as the edges, the condensation coefficients would differ for the center and edges, and the above behavior would not have been observed. In any event, after the matrix has been deposited for a while, the heat conductivity is limited not by the target material, but by the matrix itself, since solid krypton or xenon are extremely poor conductors of heat.

Liquid hydrogen is added to the dewar (after it has been flushed out with helium gas) through a tube that is placed through H at the top. The outlet (E) is connected to a long explosion-proof line that leads to a special one-way vent on the roof of the building. The target temperature is measured using a thermocouple [copper-gold (2.1% cobalt)] or thermistor

(G) attached either to the copper block or directly to the target (in both cases, the temperature measured proves to be about the same). The thermocouple emf is transmitted directly to a chart recorder, thus allowing a time-temperature history of the sample to be made during a warmup experiment. Typically, the dewar, which has a capacity of approximately 1500 cc, has to be refilled once every five hours during an experiment, during which time the temperature remains constant at 22°K (liquid hydrogen's heat of vaporization is quite large, 106 cal/gm).

Four ports fitted with vacuum flanges were cut at right angles to each other in the bottom of the outer shell of the cryostat. Two collinear ports carry sapphire or CsI windows (the latter being polished with chamois cloth), labeled W in the diagram, and serve as the optical path in absorption spectroscopy. A third port serves as a viewing and fluorescence window (W') and the fourth port has the furnace attachment (F) secured to it through which the reactive species exit (from the sides of this port comes the M gas which is also directed onto the target).

A thin matrix film is laid down with the target facing the beam squarely. A heat shield with a magnetic bottom (not shown in diagram) is also inside the dewar at the bottom and can be used to stop the flow of species from the furnace directly striking the target. After deposition, the dewar is rotated 90 degrees to the position shown, on ball bearings (B) by means of a gear arrangement (D), and the spectra taken. Two large diameter greased viton O-rings (C) prevent any leakage during this rotation.

Spectra are obtained in the infrared with a high resolution, Perkin-Elmer Model 421 Infrared Spectrophotometer equipped with a Dual Grating interchange for the 4000-650 K region, and a separate CsBr interchange for

the 700-300 K region. Frequencies are accurate to ±1.0 K, with a resolution of 0.2 K, in the 2000-650 K range, and are accurate to ±3.0 K, with a resolution of 3 K, in the 700-300 K range. Visible-ultraviolet spectra are photographed with a 0.75 meter focal length Jarrell-Ash f/6.3 spectrograph fitted with a 2160-line/mm grating blazed for 3000 Å and giving a dispersion in the first order of 5 Å/mm. The continuum is provided by a hydrogen discharge tube. The film used is Polaroid type 57 (3000 speed) packets for quick spectra, and the plates used for accurate work are Kodak 103-aO and SWR (short wave radiation) plates. A standard line spectrum is provided by a General Electric gemicidal mercury lamp. The plates, after exposure and development, are first recorded on a Jarrell-Ash Recording Microphotometer, and from the graphs this machine produces, measurements are carried out.

Warmups can be done with this cryostat, though inconveniently, and it was found that it took several minutes to warm the target to 50°K, above which krypton starts to come off quite rapidly. The cryotip, to be mentioned later on, is much more convenient for controlled warmup diffusion experiments.

The flow system for the rare gas (the M gas), that allows its controlled deposition on the target, has a connection directly to the mechanical pump for high speed pump-outs, a one liter storage bulb for the M gas, a mercury manometer that can be isolated during deposition so that no appreciable amounts of mercury vapor can condense on the target (this is important only for visible-ultraviolet spectroscopy), a stainless steel Nupro low-flow metering valve with teflon vacuum connections, a low-flow Fischer-Porter flowmeter made of glass with a sapphire float and attached to the system with black-waxed standard tapers, and a flexible,

vacuum-tight rubber tube connected to the M gas inlet of the furnace flange. This inlet terminates with a 40 mil bore jet, 150 mils long, built into the furnace flange to the left of the central furnace inlet and positioned so that the M gas molecules are collimated onto the center of the target plate from the side. Except for the low-flow valve, this system has only greased vacuum valves and ball and socket joints, which were not expected to chemically interfere in any way.

The matrix gases used are Linde high-purity gases or their equivalent (without further purification). Only krypton (melting point -157°C, 1 torr pressure 74°K) and xenon (melting point -112°C, 1 torr pressure -168°C) are used as matrix gases. One would expect the LLIT state to last longest for krypton, and more broadening of lines in krypton matrices was observed (this might have also been due to the lower condensation coefficient of krypton). Because of the high melting point of xenon, it forms very small microcrystallites and large, random, short range refractive index fluctuations in the solid upon condensation at 20°K, which result in a highly scattering matrix that makes ultraviolet spectroscopy difficult.

Another flow system allows the passage of P_2F_4 gas through the furnace (P) and straight onto the target. It consists of a small volume (about 70 cc) to which is directly attached a mercury manometer, a large diameter, closed-off, vertical tube for condensing out the P_2F_4, a P_2F_4 liquid-nitrogen cooled storage container (with a stopcock) for storing P_2F_4, a combination mircroflow valve and flowmeter (Matheson, Low-Flow Flowmeter with Model 150 Microflow Valve and No. 610 Metering Tube) for monitoring the extremely low P_2F_4 flow rates, and a large bore Westglass greaseless vacuum stopcock in parallel with the microflow valve assembly

for quick evacuation of the system (through the furnace attachment). The Matheson unit has only greaseless connections, is made of stainless steel and glass, and has a sapphire float to measure flows. Because of the minimum measurable flows possible with this flowmeter, and the maximum flows of M gas permissible for the refrigerant, (given the limited heat conductivity of the target plus holder) to be able to handle the load, the maximum M/R ratios attainable using this set-up are about 200. However, predilution of the P_2F_4 (or other "R" material) with the inert gas can increase this number several times over. The entire P_2F_4 flow system is greaseless, has teflon ferrule Swagelok and viton O-ring Cajon fittings, and is made of glass and stainless steel tubing.

A third system, which was only used once, can admit another gas onto the matrix through a jet built into the flange to the right of the central furnace input.

The furnace itself is also shown in Fig. 7. It is made of nichrome wire wound around a quartz body and insulated by a large amount of asbestos, in which is imbedded a chromel-alumel thermocouple (G). Water jackets (K) at both ends of the furnace make it easily heated in the system without fear of thermally decomposing any vacuum connections. The exit jet (L) is 1.3 mm bore and is placed within the furnace so that its tip would be just as hot as the rest of the furnace. Radiation from the furnace onto the target has been calculated to amount to a small percentage of the total heat received by the target,[62] most of which comes from the heat of cooling and condensation of the inert gas.

If the target becomes too warm during deposition, or the M gas layer on it becomes so thick as to act as an effective insulator, so that the condensation process then becomes inefficient, pressure measurements will

not give a good idea of this inefficiency of the condensation process. This is because a large cold surface exists above the cold target, so much of the M gas that does not condense on the target, nevertheless condenses on the upper cold surface, never reaching the ionization gauge by the diffusion pump to be recorded. Thus the pressures read are much less than the pressures in the vicinity of the target. This is partially overcome in the cryotip apparatus, where only a small portion of the central insert is at liquid hydrogen temperatures. Besides measuring the target temperature, another way of determining whether the M gas flow rate is too quick is to examine the transparency of the matrix (not to mention the final isolation of R as measured by the broadening of spectroscopic lines). A quickly deposited matrix will look opaque.

1. Procedure for Matrix Deposition and Spectroscopy with P_2F_4

The actual step-by-step procedure for depositing and working on a matrix was as follows:

1. Pump down entire system with target in place. Place heat shield between target and furnace inlet.

2. Allow about one torr of P_2F_4 (fractionated beforehand) from the storage vessel into the flow system.

3. Place a -135°C trap around the vertical tube of the P_2F_4 flow system and then pump on this system to a steady low pressure. This removes PF_3 and PF_2OPF_2 impurities. Close P_2F_4 system and keep the P_2F_4 at 77°K. Measure vacuum pressure in the P_2F_4 system on manometer.

4. Open M gas storage bulb to previously pumped out section of the M gas flow system containing the manometer to measure amounts of M gas added.

5. Heat up furnace to degas.

6. Add just enough liquid nitrogen to the cryostat dewar to cool it down to 77°K.

7. Flush cryostat dewar with helium and then add liquid hydrogen until it overflows the dewar (as evidenced by liquid air condensing on the outside of the vent tube).

8. Take a blank spectrum. Turn target to face furnace inlet. Move heat shield out of the way.

9. Turn on M gas flow for a 15 minute predeposition of pure M. This flow should be between 300-3000 micromoles/hour. Then measure the M gas pressure.

10. Warm the P_2F_4 and take its pressure (difference from vacuum to all evaporated).

11. While depositing the M gas, start the flow of P_2F_4. This flow should be about 20 micromoles/hour (a flow less than 15 micromoles/hour cannot be readily measured with the Matheson flowmeter).*

12. Deposit for the length of time desired. During this time, temperature and pressure measurements can be made.

13. Shut off P_2F_4 flow and furnace and measure the final M gas pressure and P_2F_4 pressure (again, difference from vacuum to all evaporated).

14. Continue M gas flow for another ten minutes to form a protective layer.

15. Turn the target into optical alignment with the two windows and take the absorption spectrum.

16. If desired, a photolysis can be done. This is accomplished with a high pressure mercury, AH-6, water-cooled lamp placed no nearer than 4 in.

* Using Dushman's equations (see Appendix B) for molecular flow and assuming a flow rate for P_2F_4 of 20 micromoles/hour through a 1 mm bore orifice 1 mm long at 900°C, we can calculate a back pressure within the furnace of 0.0025 torr of P_2F_4 (which would be expected to be somewhat higher if the P_2F_4 dissociated in the furnace).

from the outside window of the cryostat (to prevent warming up the matrix).

17. If desired, diffusion experiments can be tried using the emf output of the thermocouple attached to the chart recorder to give a continuous readout of the temperature. Pressures must also be watched to insure that the entire matrix is not destroyed.

18. If desired, fluorescence experiments can be performed. The AH-6 lamp is placed close to a Bausch and Lomb monochromator whose emitted light is shown on the target. The fluorescing radiation is focused with lenses onto the slit of the spectrograph.

The use of the cryotip apparatus changes this procedure somewhat. The cryotip reaches low temperatures by first cooling high pressure hydrogen gas to below its inversion point by passing it through a liquid nitrogen trap, and then free expanding it through a nozzle into a much lower pressure region. It gives less cooling than the liquid hydrogen dewar is capable of, but has an extremely useful variable temperature capability. Pumping on the hydrogen beyond the nozzle can lower temperatures to 13°K, and reducing the hydrogen flow rate while increasing the back pressure can raise the temperature to any value up to 70°K.

In cooling down the cryotip, one thousand lbs/sq in. of hydrogen is needed backing up the dewar. After 20°K temperatures have been reached, the pressure can be reduced to 600 lbs/ sq in. Increasing the pressure at this point will not decrease the temperature nor increase the rate of heat flow from the target -- because of the construction of the cryotip, it will merely cause excess liquid hydrogen to form in the well on the bottom which will be blown out of the exit line in the form of a spray.

F. Preparation of the Materials Used

The germanium and silicon used were obtained in very high purity, above 99.9%. It was found that after three runs of SiF_2 production, the silicon remaining in the furnace became inactivated due to a film of polymer forming on it, and had to be taken out to be cleaned. The method employed was to swish the dirty silicon in a Nalgene beaker with concentrated HF solution to which a few drops of HNO_3 were added. The silicon was now washed, swished in concentrated Na_2O_2 solution for several more minutes, washed again with HF solution, and then finally distilled water. This treatment brought the silicon back to a highly activated state. All of the other solid chemicals used had a purity above 99% and were obtained through standard laboratory supply houses. The magnesium germanide, used to produce the germanes, was formed from the reaction of finely powdered magnesium (greater than 99.9% purity) and germanium in a 2.05:1 mole ratio in a graphite crucible in an inert atmosphere at 750°C.

Many of the gases used were bought in lecture bottle cylinders (SiF_4, PF_3, HI, C_2H_2, $(CH_3)_2NH$, N_2F_4, etc.) and were further purified through trap to trap distillation before use. Others were prepared from more elementary starting materials: C_2F_4 was obtained from the pyrolysis of teflon chips at 500°C; C_2D_2 was prepared from the hydrolysis of CaC_2 in heavy water; GeH_4, Ge_2H_6 and Ge_3H_8 were prepared from the hydrolysis of magnesium germanide (Mg_2Ge) in 10% HF solution; GeF_4 was produced from the pyrolysis of $BaGeF_6$ at 800°C; $PF_2N(CH_3)_2$ was produced from the reaction of PF_3 and $(CH_3)_2NH$ in the gas phase for several days; and PF_2I came from the reaction of this $PF_2N(CH_3)_2$ with HI.

The preparation of P_2F_4 was so odd that I will go into it in detail, as well as mention some other attempts at its preparation which proved unsuccessful.

The only mode of preparation of P_2F_4 discovered to date involves the reaction of PF_2I and Hg. The compound PF_2I at less than 100 torr pressure is placed in a large flask with a small amount of mercury (which nevertheless, amounts to a 50-fold molar excess) and the flask is rotated end over end with the mercury sloshing about inside. After four hours, appreciable yields of P_2F_4 and Hg_2I_2 are obtained (this method is analogous to the preparation of N_2F_4 from NF_2Cl and mercury[63]). What is so unusual about the reaction is that the pressure must be kept low or else complete decomposition to PF_3 and PI_3 ensues, and the desired reaction can only occur under violent agitation of liquid mercury. PF_2I vapor does not react with mercury vapor to form P_2F_4 in the gas phase nor does PF_2Br nor PF_2Cl react with liquid mercury under agitation. Amalgamating the mercury with cadmium, copper or sodium decreased the yields of P_2F_4. Recently, PF_2I and mercury were reacted in the presence of excess CH_2I_2 in a similar manner as above to form $CH_2(PF_2)_2$,[64] so the method seems to have distinct usefulness for introducing PF_2 groups into molecules.

After purification on the fractionating column mentioned earlier in this section, the P_2F_4 was checked by its infrared and mass spectra and found to be at least 98% pure for the most carefully fractionated samples. It had a melting point of -85.5°C. P_2F_4 is a colorless, spontaneously flammable, unpleasant-smelling gas at room temperature.

G. Phosphorus-Fluorine Analyses

All the phosphorus analyses were done in the same way. The material to be analyzed was dissolved (either in conc. H_2SO_4 + HNO_3 or in Na_2O_2) in water solution, acidified, and precipitated with sulphate-molybdate reagent to form ammonium phosphomolybdate, which was accurately weighed.

Analysis of the polymer for fluorine was done in the following manner. The polymer was dissolved in a hot concentrated Na_2O_2 solution to form a clear solution. Since this solution could contain the fluorine in various forms, such as F^-, PF_6^- or $PO_3F^=$, it was thought desirable to remove the fluorine from it all in one form for further analysis. So 9M H_2SO_4 plus chips of glass were added to this solution and the mixture distilled at 135°C to remove all the fluorine as H_2SiF_6. This method not only breaks up complex ions, but also separates the phosphorus from the fluorine, so that fluorine tests can now be run that would be interfered with by phosphorus (such as the zirconium alizarin lake method). The distilled H_2SiF_6 is allowed to drip into 0.1 N NaOH. The resulting solution is then neutralized and concentrated, and an aliquot is taken to be tested for fluorine content by the peroxytitanic acid colorimetric method (known as Steiger's Method[65]). In this method a carefully prepared orange stock solution of H_2O_2 and $Ti(SO_4)_2$ (about 0.02 molar in each) and acid has its 415 nm absorption band measured, by itself and with various known concentrations of fluoride added. The absorbance at this wavelength decreases drastically, though unfortunately not linearly, with added fluoride. A calibration curve of absorbance versus fluoride concentration is plotted. The unknown is then added to the orange solution, the decreased absorbance measured, and the concentration of fluoride read off the curve. This method is sensitive to temperatures of the solution, but is not interfered with by phosphorus.

Analyzing the polymer left in the reaction vessel after PF_3 plus P_4 were passed through the quartz furnace at 900°C, showed it to contain less than 3 weight % of fluorine, indicating that the material emerging from the furnace was not a phosphorus-fluorine species, but most likely a

phosphorus-silicon-oxygen species. This polymer did have 62 weight % phosphorus. The phosphorus-fluorine polymer that forms on the walls of the vacuum system when the materials from the condensation of the products of the P_2F_4 pyrolysis are condensed on these walls was analyzed for fluorine, and surprisingly, showed little if any fluorine present (less than 5 weight %). Perhaps the polymer does contain fluorine initially but reacts with the moisture of the air and then the glass it is next to, to produce SiF_4 which evolves removing the fluorine, and leaving phosphorus-oxygen polymers only.

A P_4F_6 sample was prepared for analysis by dissolving it in acetonitrile at low temperatures and allowing the solution to warm up to room temperature. At about 0°C, decomposition to P-F polymers and PF_3 gas ensues. The PF_3 is thoroughly removed from the solution and its amount measured. The liquid plus solid precipitated residue is transferred to a Na_2O_2 solution for dissolution of the polymer. Part of this polymer dissolves immediately, but a colorless material remains (perhaps phosphorus?) that requires heat and added Na_2O_2 to finally dissolve. The solution is then analyzed by the above methods. About 46 mg of P_4F_6 gave 23.3 mg of phosphorus and 18.9 mg of fluorine in the polymer and 3.68 mg of PF_3 given off. This means that about 21 mole % of the original P_4F_6 decomposed to PF_3. After correcting for a systematic error in the fluorine analysis of the polymer that gives 5% too low values of fluorine, the mole ratio of F/P in the original compound is calculated to be $(0.1254 + 1.045)/(0.0418 + 0.752) = 1.475$, or $P_4F_{5.9}$.

IV. EXPERIMENTAL ATTEMPTS AND RESULTS

A. Bonding and Stability in the Group IV Divalent Species

All group IV elements can form tetracoordinated compounds. Without exception for carbon, silicon and germanium, these compounds are covalently bonded and the bonded groups are tetrahedrally situated. According to the valence bond approach, and ignoring d orbital bonding (either through filled or empty d orbitals), these four-valent compounds can be viewed as forming by first having the ground ns^2np^2 outer electronic configuration of the group IV atom (hereafter referred to as "G") excited to an $nsnp^3$ configuration, which then hybridizes to form four equivalent sp^3 orbitals which then form the bonds observed. The stability of the resulting compound comes from the formation of four new bonds, in this approach, which offsets the amount of promotional energy required to form the sp^3 hybrid to begin with.

Yet from the actual ns^2np^2 outer electronic configuration of the G atoms, we would suppose that only divalent species could form, from the np^2 electrons, even though only two new bonds are formed in this case. Indeed, as we go down the periodic table, the stability of divalent group IV species goes up until Sn^{++} compounds are quite common. In order to understand the relative stability of divalent versus tetravalent species in group IV, and the relationship of this stability to the bonding, structure and multiplicity of the resulting species, we will now rely on a theoretical picture of this bonding that will explain it in approximate terms.

The stability of a molecule comes from three sources: electron-nucleus (or electron-core) attraction, reduction of electron-electron repulsion,

and reduction of nucleus-nucleus (or core-core) repulsion (this last factor not being too important here), all of which depend on time-averaged distances of the electrons and nuclei of the molecule from each other.

The first energy term, electron-nucleus attraction, can be divided into two or more parts depending on which of the two or more nuclei of the molecule the electron in question stays near (to increase this attraction). If it is the nucleus or core of the atom attached to the central G (group IV) atom, then G's orbitals must be concentrated in the directions of these other atoms so as to bring the shared pair of electrons close to them. s orbitals have no preferred direction, but due to the fact that p orbitals have a planar node, hybridization of p and s orbitals do concentrate the electronic charge of the resulting hybrid in certain directions. The more the p character, the better the directionality, and pure p orbitals have the most concentration of electronic charge in one direction. This relationship has a more pronounced effect in the larger radii G atoms, where directionality to and overlap with attached atoms further away from the core becomes crucial in forming a strong bond. Thus, larger radii G atoms tend to have more p character in their bonding orbitals so that the electrons in these orbitals can get close to the core of the other atom, while smaller radii G atoms tend to have more s character in their bonding orbitals so that the electrons in these orbitals can get close to the core of the G atom. Since divalent group IV species use pure p orbitals in bonding, while tetravalent species use sp^3 orbitals, and since the two p orbitals possessed by the larger radii G atoms in their ground states give a much better overlap than the four sp^3 orbitals, as just stated, it would be expected that these larger radii atoms would more readily form divalent species. Also p orbitals have a smaller angle

between them than do the sp hybrids, so it would be expected, both from this effect and steric hindrance, that the larger radii G atoms would have smaller angles between their bonds (approaching 90°). These effects would be enhanced by attached electronegative groups, and thus would explain the stability and angle of the divalent species CF_2, SiF_2 and GeF_2 relative to the tetravalent species CF_4, SiF_4 and GeF_4, versus the similar relationship between their hydrogen analogs.

The electron-nucleus attractive term can also stabilize non-bonding electrons if these electrons are situated near the G atom core. Such electrons tend to lie in orbitals with a large amount of s character, for these orbitals reduce the second energy term mentioned above, the electron-electron repulsion, while they bring the electrons close to the core of the G atom.

This stabilizing effect on non-bonding electrons is sometimes called the "inert pair effect," which refers to the fact that electrons in s orbitals become progressively less reactive as each group in the periodic table is descended, and therefore these elements tend to have their two outer s electrons unshared in compounds they form. Applied to the species of group IV atoms, this means that the unshared pair of s electrons in the <u>divalent</u> species become progressively more stable as we go down the group.

The inert pair effect is illustrated in the $s \rightarrow p$ transitions of the monatomic, gas phase group IV atoms. Table I lists the energy of these transitions for the G atoms.

The inert pair effect is due to two sources. First of all, lone pairs tend to s character because they are not bonded to any other atom and need no directional characteristics. Their stability comes from their

Table I. Energy of the $G(s^2p^2)(g) \rightarrow G^*(sp^3)(g)$ transition for group IV atoms[66]

G	E(kcal/mole)
C	96.5
Si	95.3
Ge	119.9
Sn	113.3

proximity to the nuclear core and s orbitals meet this requirement. Furthermore, as we go down the periodic table to larger radii atoms, the further the s electrons can stay away from each other, the less their mutual repulsion and so the lower their energy (this is not true to any significant extent for p orbitals).

However, the larger the core the smaller the electron nucleus attraction, and thus the weaker the stabilizing effect of this attraction. This brings us to the second factor in the inert pair effect -- the poor shielding power of d and f electrons. In the atoms further down the periodic table, filled d or f orbitals are present neutralizing the nuclear charge for the outer electrons. But since these orbitals are so diffuse, the outer s electrons can penetrate them, thus experiencing more of the positive nuclear attractive force and lowering in energy. Most probably it is this effect alone which is the cause of the sharp rise in the energy of the $s \rightarrow p$ transition for germanium seen in the above table.

It must be reemphasized that all these considerations are inaccurate simplifications and do not adequately describe the extremely complex situation that is occurring in any atomic system. For instance, the above considerations cannot adequately explain the anomalous drop in the

energy of excitation for silicon and tin seen in Table I. However, to the extent to which they reflect reality , they would predict a greater stability for divalent species of atoms lower in the periodic table.

Another factor which could come into play here from the second energy term, electron-electron repulsion, is steric hindrance between the atoms attached to the central G atom. This hindrance would destabilize a small angle between these attached atoms, especially in the smaller radii G atoms. This, in turn, would destabilize both the tetravalent species and also the singlet divalent species (which would use two p orbitals in its bonds, that have an angle of 90° between them in the free atom - see below) in the smaller radii atoms. Thus this steric hindrance effect might have the net result of not changing the above conclusions for divalent-tetravalent stability, unless triplet divalent species could form, in which case it would stabilize the divalent species of smaller radii G atoms.

Once we have formed a divalent species, stable or not, the same valence bond approach used above can predict whether its ground state will have singlet or triplet character. A singlet would have an unshared pair of electrons in a single orbital in the ground state, and this orbital would be an s orbital from what was said before. Therefore, a singlet would definitely have two p bonding orbitals at an angle not far from 90°. A triplet could not have its two unshared and unpaired electrons in a single orbital, so one would predict one of the following two configurations for it: a linear species with two sp bonding orbitals and two lone p electrons; or a nearly linear species with two sp^2 bonding orbitals and one long sp^2 electron and one lone s electron.

Hund's Rule, which states that triplets lie lower than singlets of

the same configuration, of course does not directly apply here since the triplets and singlets are not of the same electronic configuration. Nevertheless, repulsion between s electrons will destabilize the singlet relative to the triplet. This effect decreases for largèr radii, so singlets would be expected for the larger radii divalent species of group IV.

Triplets are also destabilized by: the s → p promotion required for triplets of the first kind mentioned above, and which is greatest for the larger radii G atoms; the fact that non-bonding orbitals generally tend to s character as mentioned before, especially for species further down the periodic table; and electronegative groups attached to the G atom, which tend to put more p character into the bonding orbitals and more s character, consequently, into the lone pair, stabilizing the singlet. Thus, in general, only small radii group IV divalent species with nonelectronegative groups attached would be expected to have a stable triplet ground state. Indeed CH_2 is one of the very few of these species that has been shown to have a very low-lying triplet state.[67]

Besides the carbenes, which are known to exist as transient intermediates in solution work and have been inferred to exist in certain pyrolysis reactions in the gas phase (CF_2 and CH_2 have actually been the only carbenes spectroscopically observed in the gas phase), several other divalent group IV species have been either predicted or identified in various chemical transformations. The three I have worked with and will be discussing here are GeH_2, SiF_2 and GeF_2. Silicon and germanium compounds in the IV oxidation state are usually quite different from their carbon analogs in terms of a great many properties. Thus it would be expected that differences would also arise in their divalent species that could be very informative.

B. GeH_2 -- An Attempt at Production in Preparative Amounts

1. Evidence for GeH_2 Formation

GeH_2 has been hypothesized as a transient intermediate in many previous studies. In 1955 Fensham et al.[68] showed that GeH_4 has both a zero order and first order component to its decomposition rate at high temperatures in the gaseous state in contact with germanium metal, corresponding to decomposition at the surface of the metal and in the gaseous state, respectively. The first order component predominates at high temperatures, and of course, high pressures. This homogenous decomposition, by means of various isotopic substitutions, was shown to involve, as the rate determining step, the decomposition of GeH_4 to GeH_2 monomer and H_2 gas.

Glarum and Kraus[69] reacted phenyl bromide with $NaGeH_3$ in liquid ammonia and obtained a very unstable white solid (believed to be Ge_2H_4) which decomposed slowly at -33°C, after all the ammonia had been pumped off, to n/2 molecules of GeH_4 and $(GeH)_n$ polymer. The same sort of decomposition reaction was hypothesized by Dennis and Work[16] in the reaction of GeH_3Cl with liquid NH_3 to form NH_4Cl and other products, though no unstable intermediate was isolated in this case. More recent liquid ammonia work on the decomposition of ammonia solutions of Ge_2H_6 at low temperatures[70] showed the intermediacy of an unstable material partially soluble in NH_3, whose nmr spectrum gave three distinct peaks. This material, thought to be a lower hydride of germanium, could not be isolated, nor reacted with other materials.

Amberger[71] showed that the pyrolysis of higher germanes (Ge_3H_8 or Ge_4H_{10}), under abrupt heating, yields still higher germanes and polymeric germanes of formula $(GeH_2)_n$, suggesting the formation of a monomer in the

gas state which then polymerizes.

Timms et al.[17] showed that Ge_2H_6 and Ge_3H_8 in a stream of hydrogen passed through a heated tube containing glass wool formed a mixture of higher germanes as well as decomposition products, a result very similar to Amberger's work. However, they also showed that when a silane, such as Si_2H_6, is mixed with the germanes, mixed silicon-germanium hydrides come out of the furnace with the structure, $Si_2Ge_nH_{(6+2n)}$ (the Ge's all bonded together), and no others (such as $SiGe_2H_8$). This strongly suggests that a GeH_2 radical is forming under these conditions which has a long enough lifetime to reach and insert into the Si-H bond or Ge-H bond of a silane or another germane, respectively.

Unlike the pyrolysis of the aliphatic hydrocarbons, which are presumed to go through free radical intermediates such as CH_3 or C_2H_5,[72] the pyrolysis of silane, Si_2H_6, which has been analyzed kinetically, has been interpreted to go through the SiH_2 intermediate,[73] though the evidence is not certain for this. Thus Ge_2H_6 might also go through such an intermediate in its cracking.

We might expect GeH_2 to be a stable gas phase species from extrapolations of other divalent group IV species. CF_2 has a half-life of about 0.5 seconds at 0.05 torr pressure,[74] SiF_2 has a half-life of about 2.5 minutes at 0.1 torr pressure (being destroyed on the walls of the container),[75] and GeF_2 solid is stable. Thus a trend towards greater stability for the divalent species as we go to heavier group IV atoms is noted, as was predicted above. One of the factors increasing the gas phase stability of GX_2 is the increased electronegativity of X. Thus, CH_2 has a half-life of only 50 microseconds at 0.1 torr pressure[67] (electronegativity of H < electronegativity of F) and $SiCl_2$ has a half-life

of a few milliseconds at 0.01 torr pressure[32] (electronegativity of Cl < electronegativity of F). Though these extrapolations applied to gas phase lifetimes are quite crude, we would predict by means of them that GeH_2 is much less stable than GeF_2, but not much different in stability than GeI_2 (electronegativity of I ≈ electronegativity of H), which is known to be stable in solution and to react as a carbenoid monomer with C_2H_2 (and other acetylenic compounds) at high temperatures and pressures[76] to form:

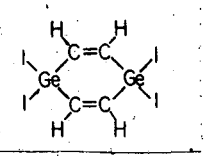

Thus, the evidence for the transient existence of GeH_2 suggests attempting to produce this radical in high yields and to quickly cocondense it with another compound to effect a reaction.

2. Work on GeH_2 Production and Reaction

An attempt was made to produce GeH_2 by the thermal cracking of either Ge_2H_6 or Ge_3H_8. It was found that at low pressures of the germanes in the furnace, or at slow flow rates of the germanes through the furnace, nothing but simple decomposition to Ge, GeH_4 and H_2 inside the furnace occurred. Neither higher germanes nor unstable materials were produced to any significant extent. However, by injecting the germanes at high flow rates (about 0.15 mmole/sec) through a 10 cm long 450°C furnace with a 1 mm bore restriction at the end, observations were made which suggested the presence of some unstable intermediate. These high pressure, high flow rate conditions were very exacting -- temperatures, shape of furnace, flow rates, and other variables had to be controlled within strict limits to produce the GeH_2.

In the case of the Ge_3H_8 cracking, the production of GeH_2 was considered to be at a maximum when a dark brown, tenacious, coherent solid

(later found to be mostly Ge metal) condensed out in greatest yields on the liquid nitrogen cooled surface beyond the furnace. It was found that the effluent gases from the furnace could be passed many feet within the vacuum system and still this solid would have the same appearance. This solid is completely different from the Ge mirror deposited in the furnace by the surface reaction of compounds decomposing at high temperatures. It is also different from the germanium metal soot that exits from the furnace at slightly higher temperatures.

The cracking of Ge_2H_6 was completely different. In this cracking, which was actually run at higher pressures and flow rates than the Ge_3H_8 cracking, the following materials were identified upon warmup of the condensed material (besides the H_2 given off): Ge, GeH_4, Ge_2H_6, Ge_3H_8, Ge_4H_{10}, higher germanes, $(GeH_2)_n$ polymer (a viscous liquid) and also some highly unstable material that decomposed to higher germane polymers (which were left on the walls of the U-traps in the form of tiny, high viscosity droplets) as it was transferred around the vacuum system. Little of the dark brown condensate that appeared for Ge_3H_8 was seen. This unstable material formed in <u>higher</u> yields when the effluent gases from the furnace were passed down a long tube before condensation, so that it would appear to be a gas phase reaction product of the species exiting from the furnace. Attempts at isolating this unstable material in -120° to -140°C traps resulted in its complete decomposition (as evidenced by the absence of any more polymeric residue being left on the traps of the system as the material was passed from one of them to another).

After condensing the effluent gases just once, they were slowly re-sprayed from the trap in which they were condensed onto a salt window at -196°, and an infrared spectrum of the solid film formed was taken. Two lines were noted that belonged to none of the germanes up to Ge_4H_{10}: a small one at 725 K and a larger one at 750 K, both in the H-Ge-H bending region. These lines did not appear when the contents of the trap were first warmed to -140°C, with pumping, before the spraying took place.

Attempts were made to react Si_2H_6 with the radical produced. In duplicating the experiment of Timms (passing Ge_2H_6 + Si_2H_6 through the furnace together) it was found that higher yields of Si_2GeH_8 could be obtained under conditions of maximum radical production. However, all attempts to produce Si_2GeH_8 outside the furnace in a cocondensation reaction or gas phase reaction proved failures. Cocondensation of the Ge_2H_6 cracking products with C_2H_2, C_4H_8 and C_2F_4 all proved to be failures as well.

Interestingly, cocondensation of the Ge_3H_8 cracking products with C_2H_2 did produce strange results, though no new compounds. First of all, much less H_2 was given off in this cocondensation than was usual for Ge_3H_8 cracking by itself. Secondly, a great deal of high boiling polymeric droplets of $(GeH_2)_n$ were left all over the vacuum system as the products of the cocondensation reaction were passed around it. Yet no sign of compound formation, as judged by infrared spectroscopy and mass spectroscopy of the products of the reaction, was found.

Assuming that some sort of reactive species is being produced here, there are several reasons for the failures noted. First, there is simply the experimental difficulty of reproducing the exact conditions for cracking. Secondly, GeH_2 or Ge_2H_4 might be extremely unstable species by themselves, yet quite unreactive with the other materials I cocondensed them with. Thirdly, the presence of H_2 in all these reactions could interfere with the cocondensation reaction at 77°K or could decompose the reactive monomer

in the gas phase.

Nevertheless, a very tentative explanation of the observations made can be given. In the Ge_3H_8 cracking, lower pressures and flow rates were used than in the Ge_2H_6 cracking. This fact, combined with the nature of the Ge_3H_8 molecule, might result in a much lower concentration of GeH_2 forming in the hot zone here than in the Ge_2H_6 cracking. This smaller amount of GeH_2 would also exist in the furnace for a longer amount of time, giving it a better chance to decompose into Ge metal and hydrogen. Because of the low concentration of GeH_2, and its higher temperature, it would be less likely to dimerize to form a Ge_2H_4 gas phase species, either within or beyond the furnace. Then upon condensation (or even in the gas phase), it could decompose to the germanium metal observed. Addition of C_2H_2 might indeed promote a reaction with this GeH_2 monomer, thereby reducing its decomposition and the H_2 formed, but the adduct so formed could be so unstable as to further decompose, upon warming, back to C_2H_2 and a $(GeH_2)_n$ polymer.

The higher pressures and flow rates of the Ge_2H_6 cracking, combined with the stability of GeH_4, could readily cause a much higher concentration of GeH_2 forming here than in the Ge_3H_8 cracking. This would account for the high yields of higher germanes produced by this cracking. These GeH_2 radicals could dimerize, either within the furnace or beyond it, to form the highly unstable, but also unreactive, Ge_2H_4 species (seen in the infrared), or perhaps a $(GeH_2)_x$ telomer. This dimer or telomer would not decompose to Ge metal and hydrogen upon condensation, but rather polyermize to higher polymers, and it might partially survive one or two transferrals around the vacuum system.

Mass spectroscopy was not used to determine the presence of GeH_2 or higher telomers in these crackings for several reasons: one, the cracking of the germanes to produce radicals required high pressures, which could not be easily accommodated by a mass spectrometer; two, the hydrogen present in the cracking products would tend to increase the pressure in the ionization region of the mass spectrometer beyond the allowable limits; three, the short time required for the cracking would necessitate a very quick, low resolution, mass spectrometric scan; and four, germanium has five naturally abundant isotopes, which would make the Ge^+ - GeH_4^+ mass envelope very complex to analyze. Neither could matrix isolation spectroscopy be utilized to solve this difficulty. The hydrogen being produced would increase the pressure within the cryostat to the point where heat conduction would make the maintainance of 20°K temperatures impossible.

C. The Reaction of SiF_2 With GeH_4

Though SiF_2 was first discovered in 1958,[18] it was not till 1965 that its potential as a radical reactant in cocondensation reactions was realized.[75] In almost every reaction of SiF_2 in cocondensation, it has been observed that the reactive species at the cold surface is Si_2F_4 or higher telomers of SiF_2, though the only gas phase species is SiF_2 monomer. This has been attributed to strong chemical forces between SiF_2 groups, immediately dimerizing the monomer as it strikes the surface, the dimer then reacting as a carbenoid subsequently.[77] Most likely all this takes place in the LLIT state of matter. The reason for the stability of Si_2F_4 could very well be due to a partial double bond between the two silicons in it (as is the case for P_2F_4).

An attempt was made to react SiF_2 with GeH_4 in a cocondensation reaction. GeH_4 gas was admitted to a stream of SiF_2 plus SiF_4 emanating from a furnace (in a 2:1 molar ratio of SiF_2:GeH_4) and the entire mixture condensed at liquid nitrogen temperatures further downstream (a line of sight path was not required here due to the gas phase stability of SiF_2). The reaction proved a success. A description of the reaction and the products it formed has been published,[78] and a reprint of this article is given in Appendix F, so that only a few details will be mentioned here along with some major points of interest.

After formation via cocondensation and warmup of the solid resulting from the SiF_2-GeH_4 reaction, a foaming, flammable, liquid polymer is left in the reaction vessel in which most of the silicon from the SiF_2 is trapped. This behavior is markedly different from SiF_2 - SiF_4 condensation by itself where only solid residues are left. This liquid polymer reacted readily with aqueous HF to form extremely unstable gases, violently explosive in

air. These gases were not investigated further. However, a small amount of volatile compounds also resulted from this cocondensation, and it was these compounds that constituted the yield. Upon low temperature, low pressure fractionation of these volatiles, three distinct fractions were obtained (besides fractions attributable to simple perfluorosilanes which almost always form to some extent in SiF_2 reactions).

The least volatile fraction was composed of highly unstable compounds difficult to characterize and was not worked on very much (it was believed, through mass spectroscopy, that some $GeH_3Si_3F_6H$ was present in this fraction). The other two fractions were found to be the first two compounds in the homologous series, $GeH_3Si_nF_{2n}H$. They were identified through molecular weights, mass spectroscopy, infrared spectroscopy and hydrogen and fluorine nmr spectroscopy (see Appendix F). Neither of these compounds was ever obtained above about 95% purity, and further attempts at purification using gas chromatography at 35°C resulted in their total decomposition. As a matter of a fact, the GeH_3SiF_2H was believed to have a small amount of a slightly more volatile GeH_3SiF_3 impurity that could never be completely separated from it.

The nmr spectra taken (at low temperatures to prevent decomposition) showed a general first order form which was readily interpretable in terms of the compounds previously mentioned. They are shown in Fig. 9.

In interpreting the nmr chemical shifts observed, some comparisons should be made with analogous compounds that have been studied more carefully. Table II lists some of the chemical shifts of related silicon, germanium, fluorine, hydrogen compounds.

We see from the table that the addition of one fluorine to silicon reduces the shielding of protons attached to that silicon a great deal, but the addition of a second or third fluorine after this actually

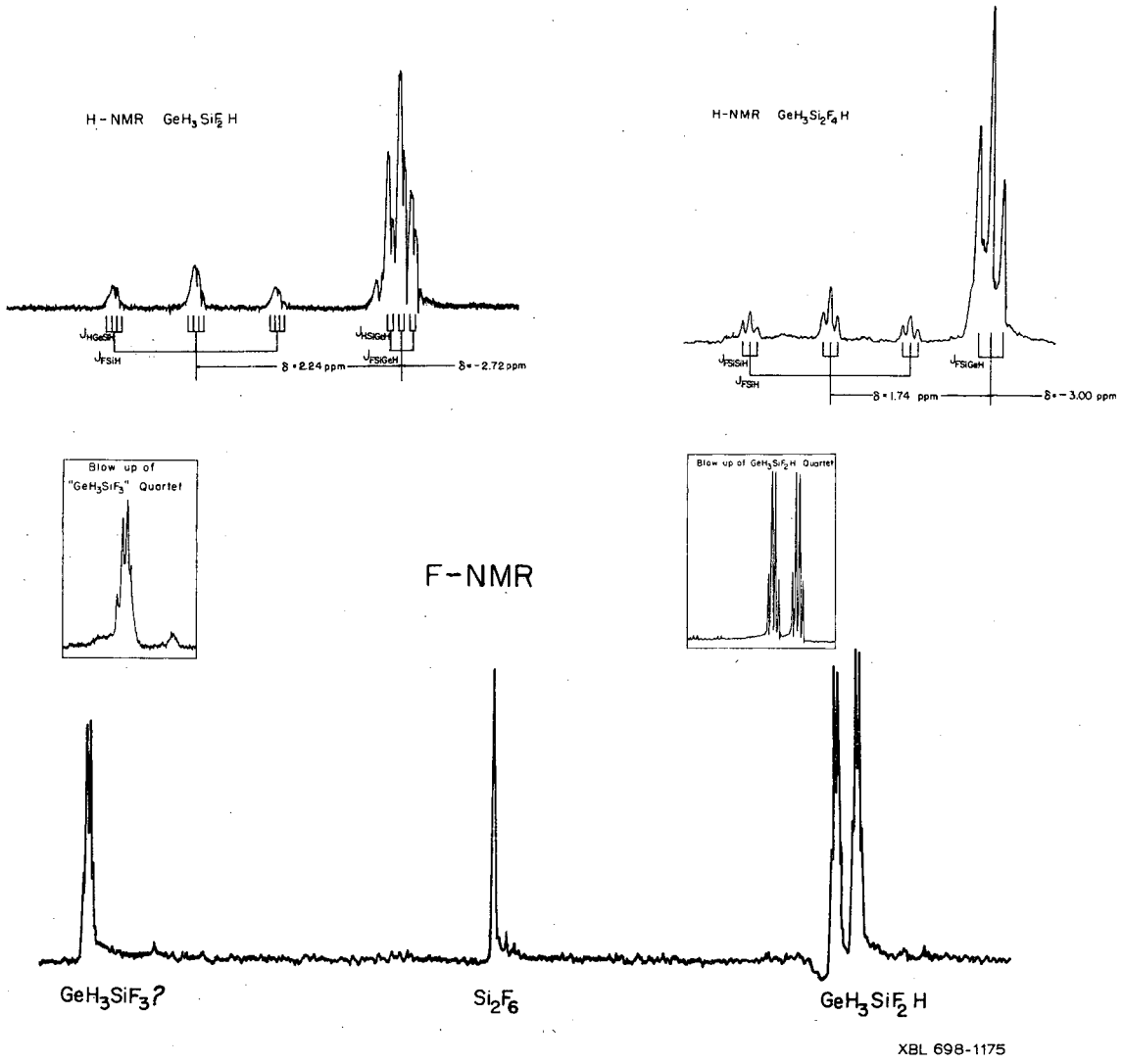

Fig. 9 NMR spectra of GeH_3SiF_2H and $GeH_3Si_2F_4H$

Table II

NMR Chemical Shifts[a] of Some Compounds Containing Si, Ge, F and H[b]

Compound	Proton Spectrum (Si-H)	Fluorine Spectrum (Si-F)
SiH_4	+7.0	-
Si_2H_6	+6.5	-
SiH_3F	+5.24	+218.5
SiH_2F_2	+5.29	+152.5
$SiHF_3$	+5.47	+111
SiF_4	-	+160.1
Si_2F_6	-	+117.9
GeH_3SiF_2H	+5.04	+126.6
$GeH_3Si_2F_4H$	+5.26	?

[a]All proton chemical shifts are expressed in ppm and are in terms of tau values = 10 - δ, where δ is the chemical shift relative to TMS; fluorine chemical shifts are relative to CCl_3F standard.

[b]Data taken from R. B. Johannesen, T. C. Farrar, F. E. Brinckman and T. D. Coyle, J. Chem. Phys. 44, 962 (1966), reference 79, and this work.

increases the shielding a slight amount. Obviously, the first fluorine is acting through the inductive effect due to its electronegativity. It has been suggested[79] that the cause of the inability of further added fluorines to increase this effect still more is the existence of back-bonding from these fluorines to the empty silicon d orbitals, which overcomes the inductive effect when two or more of them are added to the silicon. The chemical shifts of the Si-H protons in the two compounds I have formed are fairly close to the values of the mixed fluorosilanes, suggesting that fluorine backbonding is occurring in these compounds as well. Also, the Ge-H protons in these two compounds are at a slightly higher field than usual, which could come from electron donation into the GeH_3 groups. Finally, this backbonding effect in the fluorine nmr is noted in many of the fluorosilanes (with the exception of SiH_3F, where, as noted before, the inductive effect takes precedence), as well as GeH_3SiF_2H, where the fluorines show deshielding relative to SiF_4.

As was mentioned in the Experimental Section (see page 69), vapor pressure plots can lead to values of the heat of vaporization (ΔH_{vap}) and Trouton's Constant for a compound. Extrapolations of such curves can also give an approximate boiling point. Though the two compounds formed were slightly impure, the impurities present were not expected to change the slope of the log P vs 1/T plots very much. In Table III are listed the Trouton's Constants and melting and boiling points of several known silicon, germanium, hydrogen, fluorine compounds along with two discovered here.

It is seen that the replacement of some of the hydrogens in GeH_3SiH_3, or all of the hydrogens in the silanes, by fluorine, has a very large effect on the melting points, but little (though opposite) effect on the boiling points of these compounds. This would indicate that fluorination

Table III. Melting points, boiling points, and Trouton's Constants of some compounds containing Si, Ge, F and H

Compound	Melting Point (°C)	Boiling Point (°C)	Trouton's Constant (cal/deg mole)
Si_2H_6	-133°	-14°	20.6
Si_3H_8	-117°	53°	22.4
SiH_3GeH_3	-120°	7°	21.36
$Si_2H_5GeH_3$	-113°	X	X
Ge_2H_6	-109°	31.5°	20.5
Si_2F_6	--19°	-19°	25.6
Si_3F_8	-1°	42°	27.8
GeH_3SiF_2H	-77.5°	13°*	18.6
$GeH_3Si_2F_4H$	-4°	86°?	X

Data taken from P. L. Timms, R. A. Kent, T. C. Ehlert and J. L. Margrave, J. Amer. Chem. Soc. 87, 2824 (1965); E. J. Spanier and A. G. MacDiarmid, Inorg. Chem. 2, 215 (1963); reference 17; and this work.

* extrapolated; ? estimated; and X unknown

has a pronounced effect on the crystal structure of these compounds, but not on the intermolecular forces in the liquid.

It is unusual that GeH_3SiF_2H should have such an anomalously low Trouton's Constant. This indicates a high entropy in the liquid state (which would exist if a large amount of GeH_3SiF_3 impurity were dissolved in the liquid.)

One of the compounds that formed here, GeH_3SiF_2H, had only one SiF_2 group inserted into it compared to the original reactant, GeH_4. As was mentioned before, this is in contrast with most compounds that form from SiF_2 cocondensations which have two or more SiF_2 groups in them. Perhaps we are dealing with an unusual type of SiF_2 reaction here. More likely, however, GeH_3SiF_2H is a decomposition product of compounds initially formed containing more SiF_2 groups. This possibility is substantiated by the fact that this germylfluorosilane would form (to a small extent) when GeH_4 gas was deposited on top of recently formed silicon difluoride polymer at 77°K, a reaction that is <u>not</u> a cocondensation reaction and that must take place between GeH_4 and SiF_2 telomers, since no SiF_2 monomer can be expected to survive the condensation process. Thus, a true simultaneous deposition of the two reactants was not necessary for some reaction to take place.

Interestingly, Timms et al.[17] have reported that $GeH_3Si_2H_5$ reacts rapidly with aqueous alkali evolving hydrogen but no monogermane, while I have found that GeH_3SiF_2H reacts rapidly with aqueous alkali evolving monogermane, almost quantitatively, but no hydrogen. While no detailed explanation can be given to this phenomenon, most likely the attack of base on the mixed hydride initiates at the Si-H bond, but not in the case of the germylfluorosilane.

Thermal cracking of GeH_3SiF_2H at 450°C and 4 torr appeared not to split off GeH_2, as in the cracking of Ge_2H_6, but greater amounts of the $GeSiF_3^+$ peak were seen in the mass spectrum of the cracking products. This suggests that the compound GeH_3SiF_3 is a decomposition product of GeH_3SiF_2H. SiF_2H_2 was also a product of the cracking.

D. Work on the GeF_2 Species

GeF_2 was the final group IV carbenoid used in an attempt to effect a cocondensation reaction. The method employed for its production, passing GeF_4 over Ge metal at 350-450°C (in a carbon furnace), has been used before to produce it.[80] Moderate yields of GeF_2 were produced in this way, and cocondensation reactions at a 77°K surface were attempted with C_2H_2 and PF_3. Though C_2H_2 did produce a small amount of some unstable material, neither reaction gave any new volatile compounds in high enough yield and stability to characterize. It seems that GeF_2 is a very unreactive carbenoid.

In working on the GeF_4-GeF_2 system, it was found that GeF_4 has an extreme affinity for water adsorbed on the inner surfaces of the vacuum line, and that it forms a stable, volatile adduct with NH_3.

E. The CS Radical and the Formation of C_3S_2

By using the windings of the furnace in the reaction vessel (depicted in Fig. 6) as a high voltage conductor, the cocondensation apparatus can be used to react radicals originating in an electrical discharge set up within the furnace. This method was applied to CS_2 gas, perhaps to form the reactive species, CS.

The procedure consisted of slowly passing CS_2 vapor (at a rate of 0.2 mmoles/min) down the center tube of the apparatus through the furnace and then to the 77°K surface below. A tesla coil, one of whose output

terminals was grounded, was turned on and placed about $\frac{1}{2}$ in. from one of the electrical terminals to the furnace windings. The other terminal of the furnace was not grounded. The constant sparking in the high voltage circuit was necessary to produce a discharge in the flowing CS_2. A wire wrapped around the outside of the glass tube leading to the furnace from the top was grounded, so that the blue discharge inside the glass tube extended up to this wire, but not beyond. At the end of the experiment, a brown-yellow coating was always noticed extending throughout the length of the furnace tube.

It was found that, to produce a new product from this cocondensation, the furnace had to first be heated. Since it is well insulated, it could maintain a temperature over 300°C for a half hour, and the entire procedure usually took no more time than this (the furnace could not be heated directly, because then it would be grounded). If this heating was done and the electrical discharge started in the flowing CS_2, a new product appeared in the pump out of the gases condensed on the liquid nitrogen surface.

Upon warming the products on the 77°K surface, no violent reactions nor light emissions were observed, in contrast to the results of Martin[118] when he warmed the condensate derived from the passage of CS_2 first through an electrical discharge and then onto a cold surface. The absence of light emissions in my experiment could simply be due to lower CS concentrations here. Instead of these violent reactions, a small amount of a reddish material was found in the pump out, less volatile than CS_2.

This material gave two main peaks in the infrared: 2085(s) and 1028 (doublet, m). The mass spectrum showed the following peaks, which were assigned as follows: 32(s)-S^+; 36(m)-C_3^+; 44(s)-CS^+; 56(s)-C_2S^+; 64(w)-S_2^+;

68(s)-C_3S^+; 76(s)-CS_2^+; and 100(s)-$C_3S_2^+$. The infrared spectrum is in complete agreement with the compound C_3S_2 as well.[119] The infrared bands noted above are its infrared active anti-symmetric C=S stretch and anti-symmetric C=C stretch respectively. C_3S_2 is a red, slightly volatile, moisture-sensitive liquid, that can be kept in air, but polymerizes rapidly at room temperature. It is the homolog of C_3O_2.

The usual preparation of C_3S_2 is carried out by submerging a high amperage carbon arc beneath cold CS_2, the C_3S_2 forming being immediately stabilized in CS_2 solution.[119] C_3S_2 has also been made by the passage of CS_2 vapors between the electrodes of a 30 amp carbon arc followed by condensation of the products.[23] However, no report of its formation under the relatively mild conditions used in this work has been published, suggesting that a cocondensation reaction might be responsible for its formation here.

Cocondensation reactions with benzene and deuterated acetylene were tried with the materials exiting from the furnace. No reaction product resulted. Actually, in the case of acetylene, some deutero-diacetylene was observed, which must have come from the action of the discharge on the acetylene itself. The fact that this could happen suggests that the electrical discharge was impinging on the materials condensed out on the cold surface, causing a reaction to take place in the solid, rather than the LLIT state of matter. However, a similar process did not produce the C_3S_2, since a cold furnace plus a discharge did not yield any C_3S_2.

The polymers left on the surface of the reaction vessel, after the pump out, contained some sulfur. Perhaps CS formed in the discharge, and inserted into CS_2 twice to form the heterocyclic C_3S ring compound, C_3S_4, which then decomposed to sulfur and C_3S_2 (the low concentrations of CS

present militate against this mechanism).

No further studies were performed on this system to elucidate the nature of the reactions occurring.

THE PHOSPHORUS-FLUORINE SYSTEM

F. The Low Temperature Cracking of P_2F_4

At the suggestion of Dr. Peter L. Timms, the thermolysis of the compound P_2F_4 was investigated as a possible source of radicals for cocondensation reactions.

P_2F_4 was only recently discovered,[20,21] though it had been sought for many years. It is an endothermic compound at ambient temperatures, decomposing to PF_3 and PF polymers, and therefore, at elevated temperatures, would have a large driving force to fission into unusual high temperature species. Specifically, by analogy with the N_2F_4-NF_2 equilibrium,

it would be expected that P_2F_4 would dissociate into PF_2 radicals under low pressure and high temperature. Indeed, Parry has given some epr[20] and chemical[81] evidence for the existence of PF_2 radicals in P_2F_4..

P_2F_4 shows unusual behavior whenever it is passed around the vacuum system from one trap to another. Although it is a white solid under normal conditions, it condenses out yellow at 77°K. This yellow solid turns to a white solid with about a 30° rise in temperature, which, on further warming, liquifies to pure P_2F_4. All that is needed to form the yellow color again is revaporization and recondensation of this P_2F_4. What is still more unusual, is that very low pressure condensation of P_2F_4 (below 10 millitorr) or very high pressure condensation (above 1/2 atm), onto a 77°K surface, will result in a white solid being formed, not a yellow one. Finally, the yellow color does not form when a foreign gas, such as PH_3 or PF_2I (neither of which react with P_2F_4 in any way), is mixed with the P_2F_4 before it is condensed.

P_2F_4 passed through the furnace in the reaction vessel (depicted in Fig. 6) at a rate of 0.5 mmoles/min and at a furnace temperature of 300-450°C, and the directly to the liquid nitrogen cooled surface below, gives a much more intensely yellow condensate than under normal vacuum line conditions. This color again turns white upon slight warming and the volatiles given off consist mostly of P_2F_4 (with a slight amount of PF_3 from decomposition). Passing the P_2F_4 through the furnace at 800-950°C under otherwise identical conditions gives entirely different results which will be gone into in the next chapter. Here we only need note that the condensate formed at the 77°K surface has a very light to transparent orange-yellow color, not deep opaque yellow.

This behavior can now be compared with N_2F_4. N_2F_4 forms a violet-colored solid when condensed at 77°K from the gas phase, due to the

presence of NF_2 radicals in equilibrium with N_2F_4 gas at room temperature. Passing N_2F_4 through a furnace at a moderate temperature will increase the amount of NF_2 in equilibrium, and hence increase this color formed in condensation.* If the pressure of N_2F_4 gas condensing is above 1/2 atmosphere, a colorless solid is obtained, rather than a violet one. This behavior is identical to that of the high pressure versus low pressure condensation of P_2F_4, and, in this case, has been explained in terms of a shifting of the equilibrium in N_2F_4 gas at high pressures to remove most of the NF_2 radicals present. If the yellow color for P_2F_4 were caused by PF_2 radicals, a similar explanation could be offered in its case.

However, N_2F_4 has no low pressure limit to the formation of its violet color upon condensation. Also, this color remains upon warming up the violet solid to the liquid state, so that N_2F_4 can only be obtained in a colorless form upon condensation from the high pressure gas. Thus, the NF_2 violet species is stabilized in the liquid phase, while the PF_2 yellow species is not even stable in the solid above 100°K.

The yellow color seen in the P_2F_4 condensation can not simply be due to a lone PF_2 species trapped in the solid because such a species would be expected to form in higher yields at lower pressures, but does not beyond a certain point. Also, PF_2 isolated in the matrix (see page 172) has been found to have no visible absorption spectrum. On the other hand, it seems likely that a PF_2 radical is partially responsible for this yellow color. Perhaps the explanation of this phenomenon lies in the existence of a complex, structured $PF_2 \cdot (P_2F_4)_n$ species in the solid state.

---

* However, at still higher temperatures, and under immediate condensation conditions, no new compounds are observed to form with N_2F_4, as is the case with P_2F_4. Instead, the N_2F_4 decomposes to N_2 and NF_3.

This species would be yellow, due to the delocalization of the odd electron in it, and would readily decompose by recombination of PF_2 radicals upon warmup of the solid.

At very low condensation pressures, little heat needs to be conducted away per unit time to effect solidification. Therefore, the surface activity in the LLIT state would be small and the rearrangement of condensing PF_2 and P_2F_4 molecules to form the yellow structure could not take place before total solidification occurred. This would not be the case at intermediate pressures, and at very high pressures the equilibrium concentration of PF_2 in the gas phase would be too small to form the yellow structure to any appreciable extent. Any molecules condensing with the P_2F_4 would tend to break apart this structure as well, and this would explain the effect of adding an inert gas noted above. Finally, the heat of the furnace produces more PF_2 which increases the yellow color formed upon condensation up to a point, beyond which there would be so little P_2F_4 coming from the furnace that the yellow would start to decrease again.

Due to this strange behavior, and the possible analogy with the N_2F_4 - NF_2 equilbirium, a search was made for the PF_2 radical.*

1. Mass Spectrometric Study of the P_2F_4 Cracking

A mass spectrometric study of the cracking of P_2F_4 was done in the hopes of identifying new species formed at high temperatures, in much the same way that Fehlner[82] was able to identify several interesting species in the cracking of P_2H_4.

---

* Some of the results of this search, along with some other facts about the P_2F_4 cracking, have been published in a preliminary paper: D. Solan and P. L. Timms, Chem. Comm. 23, 1540 (1968), reprinted in Appendix G.

The cracking was done using a 5 mm I.D., 30 cm long quartz tube with a movable 7 cm long furnace around it, attached via a direct inlet to the ionization region of a Bendix time-of-flight mass spectrometer. The exit of the quartz tube opened into a 30 mm I.D. tube that was 30 cm from the actual ionization region, so wall collisions were experienced by some of the molecules exiting from the furnace before being ionized, and molecular sampling was not being effected. It is well known that hotter gases will give a smaller peak intensity in a mass spectrometer, but this temperature effect would not be too important here because many of the molecules ionized first struck the cold walls of the 30 mm I.D. tube after the furnace before being ionized. The flow rates of P_2F_4 going through the furnace were very low (to accommodate the low pressures of the mass spectrometer) and it was estimated that the pressure inside the furnace was 0.01 torr. At this pressure there would be few molecule-molecule collisions and so no dimer-monomer equilibrium could possibly be maintained in the furnace. Also, the electron gun in the machine had a large spread of energies, so appearance potentials would be inaccurate. Finally, the instrument sensitivity for different ions at different pressures was not known, so no accurate estimate of the relative amounts of species exiting from the furnace could be made.

Despite all these difficulties, the time-of-flight machine did allow simultaneous monitoring of any two peaks desired. The furnace was first positioned nearest the mass spectrometer's ionization region and a constant flow of P_2F_4 gas was maintained through it while its temperature was raised. As the temperature rose from 25 °C to 800 °C, the mass spectrum of the

effluent gas, taken at 20 ev, showed only peaks normally present in the spectrum of P_2F_4, but their relative intensities changed. Above 350°C, the intensities of $P_2F_3^+$ and $P_2F_4^+$ were observed to decrease, and that of PF_2^+ to increase, with temperature, in a reciprocal manner. By 700°C, the ratios of the intensities, $PF_2^+/P_2F_3^+$ and $PF_2^+/P_2F_4^+$, had each increased ten-fold over their values in the spectrum of P_2F_4. This reciprocal relationship was reversible with lowering of the furnace temperature. When the furnace was moved back from the inlet to the mass spectrometer, so that the effluent gases from it experienced more wall collisions, a small decrease in the $PF_2^+/P_2F_4^+$ ratio was noted, as well as the appearance of two new peaks, corresponding to PF_3^+ and P_2^+.

Still more important, at 13 ev ionization energy, no spectrum was observed for the effluent gases with the furnace temperature below 350°C. Above 350°C, PF_2^+ appeared and increased in intensity with temperature, which shows that a new species is forming in the furnace that has a lower appearance potential for the formation of PF_2^+ than P_2F_4 has.

This mass spectrometric study proves that P_2F_4 dissociates into PF_2 radicals at high temperatures and low pressures, and that the PF_2 radicals formed have a low ionization potential and can withstand several wall collisions without decomposing. The only other way to explain these observations is to assume the existence of a higher molecular weight phosphorus-fluorine species (other than P_2F_3) that has no parent peak* and decomposes readily to PF_2^+ upon electron bombardment. This is unlikely, to say the least. This study also shows that at ambient temperature and very low pressure, little P_2F_4 exists in the form of PF_2 radicals (unlike the behavior of N_2F_4).

* PF_3 has a large PF_3^+ parent peak.

2. EPR Investigation of the Solid Formed from the Cracking of P_2F_4

At least four epr studies have been done in the past on a presumed PF_2 radical trapped in a solid matrix at low temperatures. Parry and coworkers[20,83] performed an epr experiment on solid P_2F_4 condensed from the gas phase and found a weak signal, which was not present when P_2F_4 was solidified from the liquid phase or when solid P_2F_4 was warmed slightly and recooled. In Canada, Wan et al.[84] radiolyzed ND_4PF_6 with gamma rays at 77°K. They found a triplet of doublets which they assigned, by comparison with the NF_2 epr spectrum, and by elimination of all other possibilities, to the PF_2 species. Since this same epr spectrum could not be reproduced on radiolysis of NH_4PF_6, their assignment was not conclusive. Recently, Fessenden and Schuler[85] continuously radiolyzed a mixture of 99% SF_6 plus 1% PF_3 at -135°C with 2.8 MeV electrons, to produce the identical epr spectrum of Wan. They thus assumed an isolated PF_2 was forming, perhaps by a reaction of an excited S-F species with PF_3. Still more recently Gendell et al.[86,87] slowly passed P_2F_4 (or PF_2H), mixed with a 200-600 fold excess of argon, over a hot wire (above 200°C), and trapped the species formed on a 21°K sapphire rod. A twelve line epr spectrum resulted that could be interpreted as being due to oriented PF_2 radicals rapidly rotating about one of their axes. The following preliminary assignment was made: $g_{\parallel} = 2.0067$; $g_{\perp} = 2.001$; $A_{\parallel}(F) = 217G$, $A_{\perp}(F) = 32G$; $A_{\parallel}(P) = 137G$, $A_{\perp}(P) = 17G$.* These authors also photolyzed both PF_2H

*Using the last four values, we obtain averaged hyperfine splitting constants of $a_P = 57G$ and $a_F = 94G$, fairly far away from the values Wan obtained (vide infra).

and P_2F_4 trapped in matrices of xenon, krypton and argon, to produce the same spectrum. It was found that the P_2F_4 matrix did not photolyze as readily as the PF_2H matrix to produce this "PF_2" spectrum. The photolyzing radiation used was from an unfiltered, medium pressure, AH-4 lamp, which could have been causing the photolysis through higher energy radiation than the 270 nm radiation used in this work for effecting the photolytic decomposition of P_2F_4.

In this work, P_2F_4 was passed through a furnace at 400-500°C and then quickly condensed at 77°K in a quartz epr tube to give a yellow solid. Since the lifetime of PF_2 in the gas phase seems to be relatively long, it was hoped that this method would increase the radical concentration in the solid. The epr tube was then sealed under vacuum with the yellow material inside always kept below 100°K, and transferred to the epr spectrometer.

The results showed a single, broad, medium intensity line at g = 2.010 with an approximate peak to peak line width of 55 gauss. Upon warming to 115°K and recooling, the spectrum was wiped out, as was the yellow color. No evidence of absorptions at much lower or higher fields was noticed, suggesting the absence of triplets. After the spectrum was taken, analysis of the contents of the tube showed mostly P_2F_4, with some PF_3.

If this were a spectrum of isolated PF_2, with the hyperfine interactions being wiped out in the solid, due to either dipole-dipole interactions between the electron obrital magnetic moment of one molecule and the electron paramagnetism of another, or to lattice electron exchange occurring between molecules in the solid, so that a broad single peak is observed in place of many fine ones, then Wan's spectrum should have certain similarities to this one. Wan found a g value of 2.0108 (which does correspond to my value), but averagedhyperfine splitting constants of a_P = 36.0 G

and a_F = 60.5 G. These values would mean that a broadened spectrum of the same species would have a minimum half width of 157 G, a value much larger than the 55 G observed. Thus, more weight is lent to the contention that this yellow color, which most likely does represent a radical existing in the solid P_2F_4, comes from a more complicated species than just isolated PF_2, (such as $PF_2 \cdot (P_2F_4)_n$ - see page 117).

G. The High Temperature Cracking of P_2F_4 and Cocondensation Reactions with Its Products -- the Formation of P_4F_6

As was mentioned previously, the high temperature cracking of P_2F_4 gives markedly different results than its low temperature cracking. P_2F_4 passed through a 800-950°C quartz furnace at approximately 2 torr pressure and immediately condensed out at 77°K, in the reaction vessel shown in Fig. 6, produces high yields of highly unstable compounds upon warmup, which leave phosphorus-rich deposits on the surfaces of the vacuum system where they are condensed. Traces of white phosphorus are present, and a small amount of an unstable, viscous liquid that can be trapped out at -60°C is also formed. This liquid is obtained in higher yields the higher the furnace temperature (though its yield never amounts to more than 10% of the P_2F_4 decomposed), and its yield correlates with the yield of the unstable compound. The yield of this liquid also increased when a 5:1 excess of xenon gas was mixed with the P_2F_4 before it was passed through the furnace. Mass spectroscopy and nmr spectroscopy conclusively proved that this liquid was P_4F_6, and it will be referred to by that name from now on.

Along with the unstable material and P_4F_6, PF_3 in large amounts is formed in the furnace. However, at no time was SiF_4 noted in the products, suggesting that there was no reaction in this case with the SiO_2

in the hot zone, and that the products observed were truly coming from high temperature phosphorus-fluorine species. Passing P_2F_4 through an 800 °C, 6 mm bore furnace and then down a short 6 mm bore tube, before condensation, produced no new volatile materials on warmup. This shows that the phosphorus-fluorine species reacting are quite unstable and must be transferred immediately to the cold surface to effect a reaction.

Since a small amount of white phosphorus (which would have existed in the form of P_2 in the furnace) was noted in the pump out after each pyrolysis of P_2F_4, an experiment was undertaken to see what effect phosphorus had on the reaction. A double furnace attachment was set up in the central tube of the reaction vessel depicted in Fig. 6, so that P_4 vapor (from white phosphorus*) could be vaporized in a stream of P_2F_4 and then the mixture passed through the high temperature furnace and to the 77 °K surface below. Though a large excess of P_4 was used, no difference in the P_4F_6 yield was noted. However, above 850 °C, a brown color did form at the cold surface. It was found that this same brown color formed when passing the gases exiting from the furnace some distance along the vacuum line, so this color did not come from a highly reactive species. From the etching of the quartz in the furnace, and from the presence of the brown color at the cold surface when P_4 was passed through the furnace by itself, it was ascertained that this color came from a phosphorus - SiO_2 reaction product, and had nothing to do with the P_2F_4.

---

* Red phosphorus was tried at first, since it does not spontaneously ignite in air and is safer than white phosphorus, but it was found to have a very low vapor pressure. The reason was that though its equilibrium pressure is high at the temperatures used, its rate of evaporation, due to the structural changes necessary for this evaporation, is extremely slow (see L. Brewer and J. S. Kane, J. Phys. Chem. 59, 105 (1955)).

The unstable substances being formed in the P_2F_4 cracking mean that radical reactions are occurring at the 77°K surface. Therefore, this system might be ideal for cocondensation reactions, and several were tried with it.

Cocondensation reactions with the effluent gases coming from the furnace in the low temperature (less than 500°C) cracking of P_2F_4 were attempted for PH_3, C_2H_2 and C_2F_4, and in no case was any sign of a reaction noted.

However, the higher temperatures, which produced the P_4F_6 upon condensation, also produced reactions in some of the cocondensations tried. Cocondensing P_2F_4 with the products coming out of the high temperature furnace increased the yield of P_4F_6, and mass spectroscopy of the products of the reaction also showed the presence of a mass peak at 288 amu, which would correspond to P_5F_7, but no such substance was ever isolable. Cocondensation reactions with B_2F_4 and C_2F_4 yielded no detectable products other than a small amount of P_4F_6. A cocondensation reaction with N_2F_4 was contemplated, but it was found that this compound reacts with P_2F_4 at room temperature in the gas phase forming unidentifiable products, and so the reaction was not carried out.

PH_3, C_2H_2 and GeH_4 do not react with P_2F_4 in the gaseous state at room temperature. Yet cocondensation reactions of these compounds with the products of the P_2F_4 cracking all seem to give new products other than P_4F_6, as evidenced, for one thing, by the different physical characteristics of the polymers remaining in the lower portion of the reaction vessel after pump out. All three compounds formed some PHF_2, identified by its volatility and infrared spectrum.[88] Both C_2H_2 and PH_3 formed products which gave a set of peaks from 100 - 102 amu in their mass

spectrum. The intensity alteration of these peaks with electron voltage suggested that they correspond to $P_2F_2H_2$. However, this compound was also too unstable to isolate. The PH_3 cocondensation gave the highest yields of both PHF_2 and of the unstable material that might have been $P_2F_2H_2$. With C_2H_2, some mass spectral evidence for C_2PF_5 was obtained, but such a compound was not isolated. No volatile germanium compounds seemed to form in the reaction with GeH_4.

H. The Reaction of PF_3 and PF_5 with Superheated Phosphorus

The double furnace attachment mentioned before was used again in an attempt to determine whether the high temperature species formed in the cracking of P_2F_4 could also form from the simple reduction of PF_3 or PF_5 with superheated phosphorus. Unfortunately, the reaction of P_4(or P_2) with SiO_2 interfered here as it did before.

Nevertheless, some interesting observations were noted. First of all, PF_5 plus P_4 passed together through the furnace at 900°C yielded PF_3 in the products, showing that some reduction was taking place. P_2F_4 was never observed in either reduction. A cocondensation reaction of the P_4-PF_3 high temperature species with P_2F_4 admitted from the side arm did form a very small amount of P_4F_6. Cocondensation with PH_3 produced no new products, such as PHF_2.

I. The Fluorine and Phosphorous NMR Spectra of P_4F_6

Fairly conclusive evidence for the identification of the unstable liquid, formed from the pyrolysis of P_2F_4 followed by the immediate condensation of the products of this pyrolysis, as being P_4F_6, came from the fluorine and phosphorus nmr's alone. Low temperature nmr was feasible since this substance could be kept in the liquid phase for many hours at temperatures below -20°C without decomposition. No broadening of the spectra was observed ruling out any high concentration of radicals such as PF_2 in equilibrium with P_4F_6 in the liquid phase.

A proton nmr was done on the compound and showed no signal from -14 ppm to 0 ppm (relative to TMS). The observed phosphorus and fluorine nmr spectra are shown in Fig. 10. No other peaks were noted. The phosphorus nmr, run at 40.48 MHz, was unfortunately complicated by overlapping machine sidebands (which were necessitated by the fact that the phosphorus spectra were run in an unlocked mode) that had a frequency of separation (2500 cps) that was very close to the separation of the outer two doublets of the main triplet (2448 cps), thus obscuring their exact form and making integrations and absolute chemical shift measurements impossible.

Both the fluorine and phosphorus spectra did not change to any noticeable extent with temperature (samples were taken from -20°C to the supercooled liquid at -95°C), and the fluorine spectrum, taken at 56.4 MHz, appeared to duplicate the shift, splittings and features of the one taken at 94.1 MHz, but with less resolution. The ratio of the areas of the low field doublet to the high field doublet in the fluorine nmr was measured to be 1.01, which is close enough to 1.00 within experimental error. A fluorine spectrum of P_4F_6 dissolved in CS_2 at room temperature

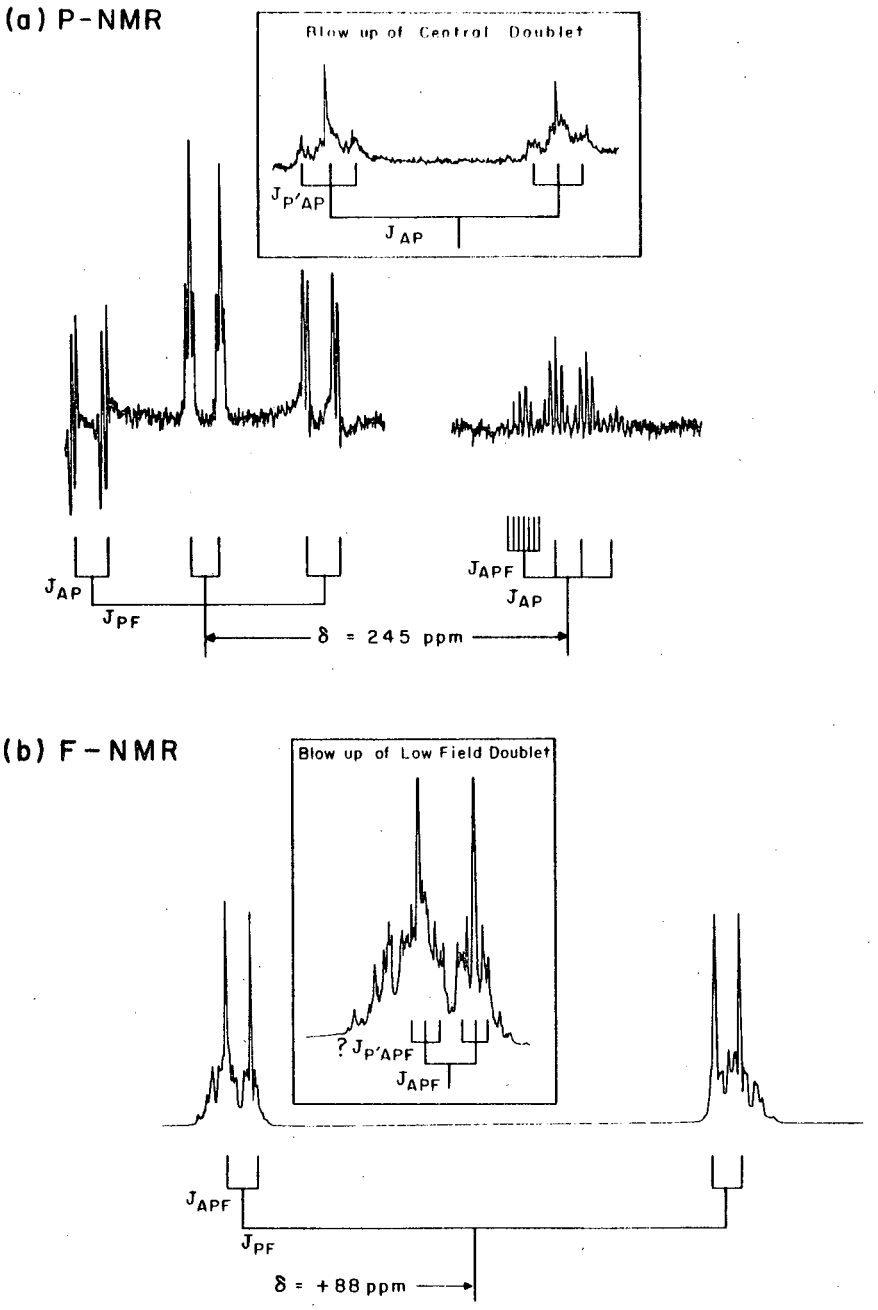

Fig. 10 The phosphorus and fluorine NMR spectra of P_4F_6 neat liquid.

(shown in Fig. 11) was also taken, and duplicated the spectrum shown in Fig. 10b, but with less of the "second order" lines present.

The phosphorus nmr spectrum of P_4F_6, assumed to have the structure $P(PF_2)_3$ as depicted in Fig. 12, should be a triplet of doublets of triplets of quintets plus a 1/3 smaller quartet of septets, and the fluorine nmr should be a doublet of doublets of triplets of quintets, if only first order interactions are considered. As can be seen from Fig. 10, both spectra do have these general first order forms, but also have many other lines super-imposed on the simple first order ones. Two possible explanations of this "second order" effect are that intermolecular association is complicating the spectra, or that more than one form of P_4F_6 exists, perhaps as different rotamers. But one would expect these effects to change with temperature, and no such change was noted. Also, one would expect the former effect to change with dilution in a solvent, which did not produce any drastic changes, and to change with external magnetic field and resonating frequency, since this would change the chemical shift differences, but, as noted above, this was not seen in the fluorine spectrum. Due to the steric hindrance in the $P(PF_2)_3$ structure, it is most likely that P_4F_6 exists as a single rotamer in the liquid phase.

There are two other causes of complex spectra that might be operating here. If a C_3 structure for P_4F_6 such as shown in Fig. 12 is assumed, then there would be two different sets of three chemically equivalent fluorine nuclei and the possibility would arise of a splitting between two adjacent fluorine nuclei being greater than a chemical shift difference between them. This would produce second order effects. The fact that the spectra did not change appreciably from 56.4 to 94.1 MHz resonating frequency sets a limit to the magnitude of spectral complexity caused by this effect.

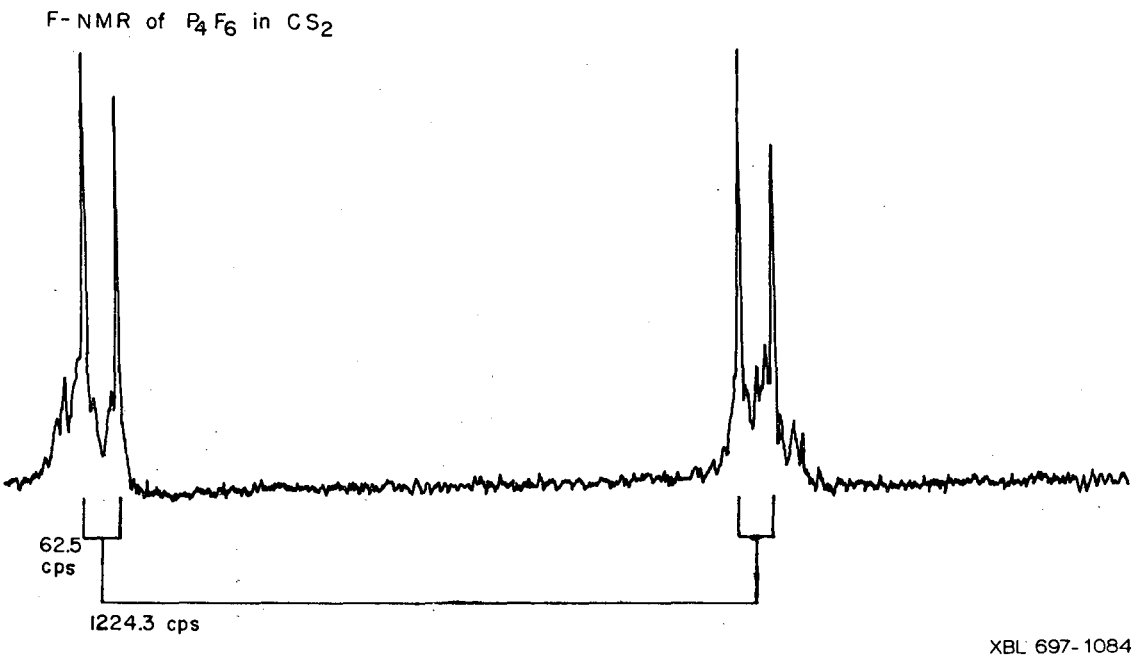

Fig. 11 The fluorine NMR of P_4F_6 in CS_2 solution.

The final possible cause, and the most likely one here, is magnetic non-equivalence[89] of the phosphorus and fluorine nuclei in a frozen configuration of the P_4F_6 molecule. This cause would be identical to the cause of the analogous "second order" effects in the nmr spectra of P_2F_4.[90] The magnetic non-equivalence is of such a nature, that even if the phosphorus and fluorine nuclei were chemically equivalent with the other nuclei of their kinds in the molecule, and even if the molecule were rotating freely about its P-P bonds and inverting rapidly (on an nmr time scale) about each of its phosphorus atoms, a complex spectrum would still result. Using common nomenclature, we may denote the central phosphorus by the letter "A," and with primes designating magnetic non-equivalence, we could call this an $APP'P''F_2F'_2F''_2$ spectrum.

Using this assumption, the fluorine and phosphorus spectra would not be as difficult to analyze as it first might seem. Due to the fact that there are only three sets of magnetically non-equivalent nuclei, the nmr spectral parameters determining the spectrum, other than the obvious couplings with the central phosphorus (A), can be reduced to three in number: the short range and long range P-F coupling constants, and the short range P-P coupling constant.* Here the short range F-F and long range P-P coupling does not affect the spectrum (assuming chemical equivalence), and the long range F-F coupling constant can reasonably be assumed to be negligible. The reason for the apparent first order form

---

* This is true because $J_{PF} = J_{P'F'} = J_{P''F''}$ and $J_{PF''} = J_{P'F''} = J_{PF'} = J_{P''F'} = J_{P'F} = J_{P''F}$ and $J_{PP'} = J_{PP''} = J_{P'P''}$.

of the spectra might then lie in the facts that $J_{PP'}$ is small* and perhaps that nucleus A, because of its large chemical shift difference, does couple first order with the other nuclei.

The large chemical shift difference noted for the two different phosphorus nuclei implies either a greater electron density on the central phosphorus atom, or a diamagnetic shielding of it being created by outside "ring currents" around the periphery of the molecule. The difference of over 200 ppm is not, however, as great as it might seem, since trivalent phosphorus compounds usually exhibit a large range of phosphorus chemical shifts. It is interesting to note here that the spectrum of the central phosphorus nucleus does not seem to be affected by complex nmr effects. The absolute chemical shift of this central phosphorus is about -60 ppm from $(CH_3O)_3P$, though this value was measured only very crudely. The fluorine chemical shift was measured using PF_2I as an internal reference.

Detailed calculations would be required to analyze these spectra in order to arrive at accurate J values. However, approximate (absolute) J values can be ascertained by simply measuring the distances between the highest peaks of the spectra recorded. Such values are listed in Table IV. Not even the sign of J is certain. Manatt et al.,[91] using various nmr double resonance techniques, have recently shown that the assumption of a positive directly bonded J_{PF} value in some compounds is incorrect, the absolute value being negative.

---

* In the fluorine spectrum, the fact that $J_{PP'}$ is small means that, in calculating the spin Hamiltonian matrix, the spin states with the three peripheral phosphorus's not all of the same spin will not add greatly to the complexity of the spectrum, while the two states with the phosphorus's all of the same spin will simply give an intense doublet, as is seen.

Table IV. Approximate NMR splittings in the P_4F_6 molecule [a,b]

	Fluorine spectrum	Phosphorus spectrum
J_{PF}	1226	1224
J_{AP}	-	324.5 and 322
J_{APF}	62	60
$J_{P'AP}$	-	36
$J_{P'APF}$	15(?)	-

[a] Splittings in cps.

[b] A is the central phosphorus.

J. The Compound P_4F_6

It is clear that the unstable liquid formed from the immediate condensation at 77°K of the products of the cracking of P_2F_4 at 800-950°C is P_4F_6, both from the above evidence and mass spectral evidence to be presented shortly. It seems that freshly prepared P_4F_6 is more unstable than P_4F_6 that has been transferred around the vacuum line several times, since more decomposition occurs in these transferrals with the freshly prepared material. This might signify that a small amount of a very unstable impurity (P_3F_5?) is present, or perhaps a linear P_4F_6 precursor to the branched variety seen in the nmr.

P_4F_6 is a viscous, oily, colorless liquid, at times yellow-orange owing to decomposition. It melts at -68°±2°C, though it supercools readily, and upon melting seems to always form a black precipitate in the liquid (this behavior is unexplained). The liquid has no appreciable vapor pressure throughout its range of stability. Though no values were measured, it was estimated that liquid P_4F_6 has a vapor pressure of 1 torr at 0°C. At temperatures below -10°C, the liquid phase is quite stable. With a slight rise in temperature, however, its decomposition is very rapid, forming orange-yellow polymers (which have been analyzed to have the formula $PF_{1.4}$) and PF_3 gas. In the vacuum line, P_4F_6 can be trapped out in a -60°C trap.

In handling P_4F_6 in the vacuum line, it was found that its decomposition could be reduced considerably by slowing its rate of vaporization during transferral to various portions of the line. This reduction was due not only to the lower temperatures at which the liquid could be kept during these transferrals, but also the gas phase stability of P_4F_6 at <u>low</u> pressures.

This stability was also demonstrated in its matrix infrared spectrum, where the P_4F_6 was evaporated at pressures below 0.01 millitorr, and where the PF_3 lines were very small in comparison to the P_4F_6 lines. Slight amounts of grease in the vacuum line greatly catalyze the decomposition of gaseous P_4F_6.

P_4F_6 fumes slightly in air, though does not catch fire as it oxidizes. It decomposes and dissolves completely in Na_2O_2 aqueous solution. P_4F_6 was reacted with a sample of B_8F_{12}, kindly supplied by Mr. Ralph Kirk, at -40°C. The reaction was over in a few seconds, and resulted in the complete decomposition of the P_4F_6 to phosphorus-fluorine polymers and PF_3 gas. Since most of the B_8F_{12} was recovered from the reaction, it is likely that it merely acted as a catalyst to the decomposition of P_4F_6. As would be expected, some $B_4F_6 \cdot PF_3$ was found in the products, as well as BF_3.

Interestingly, P_4F_6 readily dissolves in CS_2 (as does tetrahedral white phosphorus) to form a solution that is completely stable at ambient temperatures, even though the neat liquid decomposes rapidly at these temperatures. This solution shows no epr spectrum, and its fluorine nmr (see Fig. 11) is composed of a doublet of doublets with the exact same splittings found in pure liquid P_4F_6 at lower temperatures (no chemical shifts were measured here). This spectrum, as mentioned before, shows less fine structure than neat P_4F_6 does.

Since P_4F_6 in solution is stable at room temperature, it is likely that the absence of its decomposition in the liquid phase below -10°C is not due to a temperature barrier to the decomposition of a single P_4F_6 molecule by itself, but rather to a barrier to polymolecular condensation of two or more P_4F_6 molecules. The CS_2, then, would isolate

single P_4F_6 molecules from each other, preventing their polymerization, and thus their decomposition. This mechanism for decomposition would also be consistent with the low pressure stability of P_4F_6, and with the pyramidal arrangement of phosphorus atoms in it, leaving them open for attack by phosphorus atoms of other P_4F_6 molecules. Indeed, T. P. Fehlner[82,92] has suggested, after studying their mass spectra meticulously, that P_2H_4 and P_3H_5 do not decompose as monomers either. He believes that a second order wall reaction operates in their decomposition. A similar type of wall reaction might be occurring in the case of gaseous P_4F_6, since its decomposition products are always found to coat the walls of the vacuum system or to deposit out in any grease that is present.

T. P. Fehlner[92] has claimed the production of P_4H_6 by the decomposition of P_3H_5 passed through a long tube leading into a mass spectrometer. The $P_4H_6^+$ ion at m/e 130 was clearly observed. In an attempt to isolate P_4H_6 in a "hot-cold" reactor, he formed a white solid that was neither PH_3, P_2H_4, P_3H_5, nor "polymer." Every attempt at vaporization of this solid resulted in its decomposition.[93]

A mass spectrum of P_4F_6 was obtained at 50 ev, and is shown in Table V. The 238 m/e peak, which is the highest mass peak seen in the spectrum, increases relative to the others at lower electron voltages, though at no voltage is it observed to exceed the 69 (PF_2^+) peak. The fact that PF_2^+ was so intense in the spectrum, would mean that many $P_3F_4(P(PF_2)_2?)$ fragments were forming in the ionization section of the spectrometer, some of which would be expected to give the $P_3F_4^+$ ion. This peak, however, was exceedingly weak. Perhaps the $P_3F_4^+$ ion is metastable, decomposing to PF_3 and P_2F^+, and indeed, a very intense P_2F^+ peak is observed. However, because of the noise level in the time-of-flight machine, no weak,

Table V. Mass spectrum of P_4F_6

Mass number	Probable identity	Relative height
238	P_4F_6	15
170	$P_2O_2F_4$(?)	1
169	P_3F_4	0.5
154	P_2OF_4(?)	0.3
150	P_3F_3	2
138	P_2F_4	6
119	P_2F_3	2
100	P_2F_2	2
88	PF_3	3
81	P_2F	16
69	PF_2	100
62	P_2	12
50	PF	11
47	PO(?)	1
31	P	2
19	F	0.3

Spectra take at 50 ev. ionization energy on a Bendix Time-of-Flight Machine. Sample evaporated directly from the condensed phase into the mass spectrometer ionization region.

broad metastable peak corresponding to the decomposition of $P_3F_4^+$ to P_2F^+ and PF_3 could be seen. Also, the intense P_2^+ ion observed could have formed from the decomposition of a metastable $P_3F_3^+$ ion (which itself could come from the splitting off of PF_3 from $P_4F_6^+$) into P_2^+ and PF_3.

The $P(PF_2)_3$ structure shown by the nmr evidence would lead to either C_{3v} or C_3 symmetry, depending on whether the fluorines attached to the phosphorus's pointed back in the direction of the central phosphorus, or to one side, creating a "propeller-like" structure (which would have optically active d and l forms). In either case, the P_4 superstructure would be expected to be pyramidal, since the lone pair of electrons on the central phosphorus would make a planar structure extremely unlikely. Figure 12a shows a proposed picture of P_4F_6 in the C_3 configuration, and Fig. 12b shows the Newman diagram looking down one of the P-P bonds for this configuration. Notice that $\theta = 180°$ corresponds to the C_{3v} structure.

The electronegativity of fluorine combined with the available electron pair on each phosphorus would tend to put a partial negative charge on each of the fluorine atoms, which would then repel each other. These large F-F interactions around the periphery of the molecule would reduce θ from 180° (see Fig. 12) and promote C_3 symmetry. C_3 symmetry would also be favored by delocalization of the three lone pairs of electrons on each peripheral phosphorus by means of the empty d orbitals on adjacent peripheral phosphorus atoms, since this bond formation would be favored by θ less than 180°. Dative bonding into the vacant d orbitals of the central phosphorus by all of the peripheral phosphorus atoms is probably quite insignificant here, because the central phosphorus could not accommodate much overlap from each of the three peripheral phosphorus

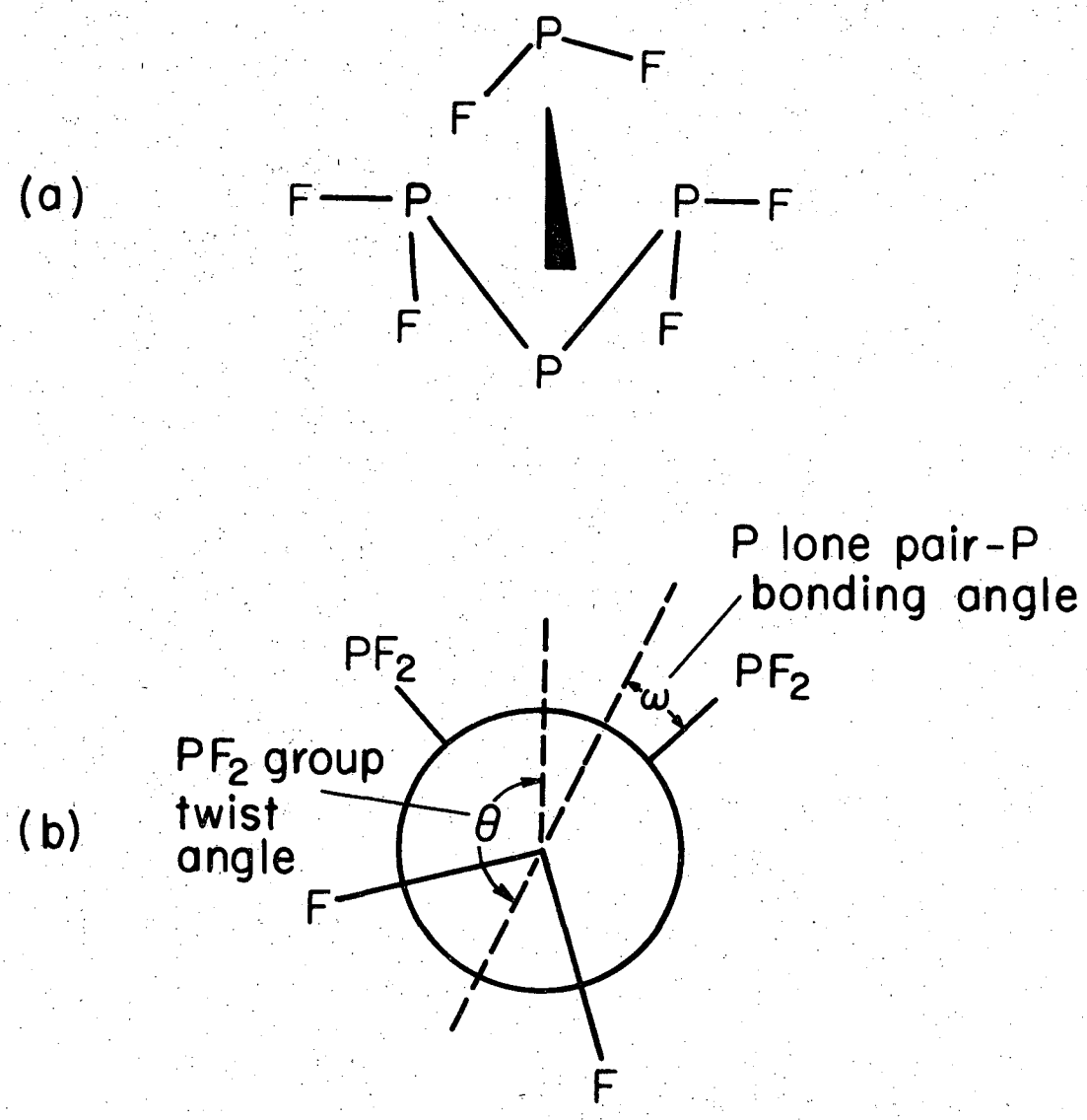

Fig. 12 The proposed C_3 structure of the P_4F_6 molecule

atoms. On the other hand, assuming the following values for the bond distances and bond angles of P_4F_6-- P-P = 2.12Å, P-F = 1.78Å, P-P-P = 106°, F-P-F = 94°, P-P-F = 100° -- a geometrical calculation of the F-F distance between fluroine atoms in neighboring PF_2 groups in the C_{3v} structure gives 4.76Å, a distance that would seem to preclude any strong F-F repulsive interactions.

Phosphorus has a remarkable tendency to form tetrahedrally arranged species, as evidenced by such molecules as P_4, P_4O_6, P_4O_{10}, and $P_4(N(CH_3))_6$, in all of which the three bonds emanating from each of the phosphorus atoms are connected, directly or through one intermediate atom, to each of the other three phosphorus atoms. Thus the peripheral phosphorus bonding hypothesized for P_4F_6 would make it a form of fluorinated P_4, as it were.

The question of how P_4F_6 is forming in this reaction will be deferred until a complete description of the matrix isolation evidence has been given.

K. The Matrix Infrared Spectrum of P_4F_6

Due to the gas phase instability of P_4F_6, its spectrum in an infrared gas cell with sodium chloride windows at ambient temperatures was complicated by extensive decomposition to yellow polymeric materials. The lines observed (in Kaysers) were: 1025(w,br), 977(m,br), 922(m), 893(w) - PF_3, 828(s), 508(w,br), 486(w,br) and 464(w,br). It is highly suspect whether all, or even any, of these lines correspond to gaseous P_4F_6. However, the absence of any lines above 1025 K rules out the presence of oxygen in the decomposition products and hence in the original compound, since the P=O stretch would appear at approximately 1400 K, and the phosphorus-oxygen bond is a strong bond that is not easily broken.

A solid infrared spectrum of P_4F_6 frozen out on an NaCl plate at 80°K showed one very broad, symmetrical peak at 807 K, with two very weak, broad peaks at 908 and 877 K.

Since P_4F_6 does not decompose in the low pressure gas, it was thought that the slow flow of P_4F_6 at very low pressures onto a matrix target (with the rare gas cocondensing on the target to effect isolation) would result in fairly pure P_4F_6 trapped and isolated in the matrix environment. Furthermore, this matrix would give an infrared spectrum free of the broadening and complicating effects of rotation that a molecule as large as P_4F_6 might be expected to produce in the gas, thus giving sharp (matrix-shifted) peaks corresponding to the normal modes of vibration for P_4F_6.

Solid P_4F_6, in a glass container at -120°C, was allowed to slowly evaporate through the furnace entrance jet of the matrix flange (with the furnace at room temperature) onto the target. It was assumed that a volatile impurity in the P_4F_6 was not interfering here. Xenon was added from the side jet as usual. It is estimated that M/R ratios of about 500 and 1000 were achieved in two separate experiments. Both spectra were the same in these two experiments suggesting that no (concentration-dependent) dimer was being trapped in the matrix.

The infrared absorption spectrum of P_4F_6 isolated in a xenon matrix (M/R ≈ 500) is shown in Fig. 13, and the lines are listed in Table VI. The spectrum showed seven fundamentals in the phosphorus-fluorine stretch region, and no clearly discernible peaks in the lower frequency portion of the spectrum to 300 K, though several questionable, very weak peaks observed are recorded in Table VI. It should be noted that little, if any, PF_3 was observed in this spectrum, suggesting that under the deposition

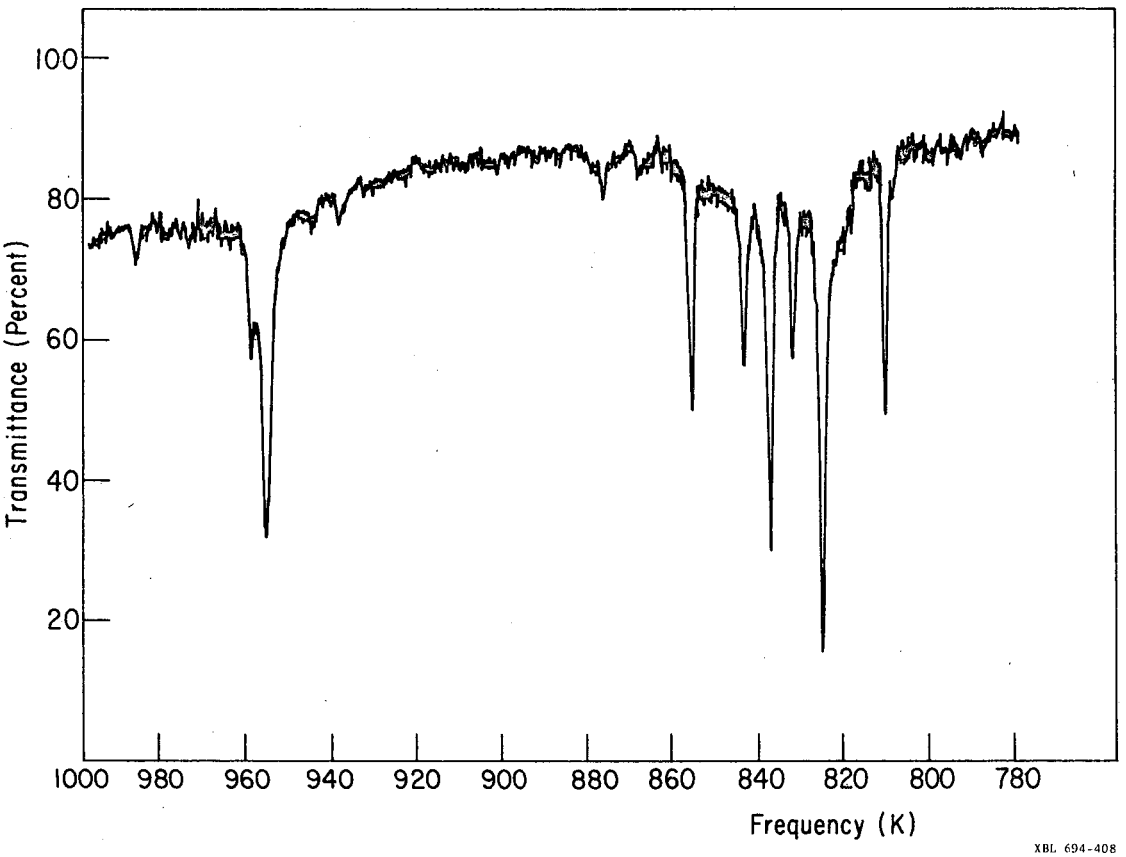

Fig. 13 The infrared absorption spectrum of P_4F_6 isolated in a xenon matrix

conditions maintained, little decomposition of the P_4F_6 was occurring. Photolysis of this matrix using a mercury high pressure AH-6 lamp showed no change after one hour of photolysis.

Table VI. P_4F_6 matrix infrared bands in xenon including their tentative assignment

Very Weak Bands

1118, 985, 944, 938 and 819. 876(w, PF_3?) seen also. Lower frequency lines: 519, 361 and 294.

Seven Fundamentals in P-F Stretch Region

A Species	
Symmetric PF_2 stretch, all in-phase	955(vs) and 959(m) (count as one mode)
Antisymmetric PF_2 stretch, all in-phase	824(vs)
E Species	
Antisymmetric PF_2 stretch, one out-of-phase	855(ms) and 843(m) - split by site symmetry
Symmetric PF_2 stretch, one out-of-phase	837(s), 831(m) and 810(ms) - split by site symmetry and a Fermi Resonance

All frequencies in Kaysers; assume C_3 symmetry, splitting of E species bands, and a Fermi Resonance.

It is assumed that only one type of isolated P_4F_6 exists in the matrix environment and that all the major peaks observed correspond to this isolated P_4F_6, not an impurity, nor an overtone or combination band, nor an aggregate peak.

To arrive at the above assignment, we begin with the assumption that P_4F_6 has either C_3 or C_{3v} symmetry. Of its 30 degrees of freedom, 24

would be vibrational modes. Its symmetry would then determine the number and kind of normal modes of these 24 that would appear in its infrared absorption spectrum. By using the method described on page 43 of this dissertation, we can obtain the irreducible representations for the molecular movements of P_4F_6 vibrations. For C_3, these come to 8 A and 8 E species of normal vibrations, and for C_{3v}, these come to 5 A_1, 3 A_2 (these are I.R.-inactive), and 8 E species of normal vibrations. Thus, altogether, 16 lines should be observed for C_3 P_4F_6 and 13 lines for C_{3v} P_4F_6(in general, the lower the symmetry of a molecule, the larger the number of fundamentals observed in the infrared spectrum). The E species modes are doubly degenerate in the gas phase, but because of the bulkiness of the P_4F_6 molecule, they might split in the matrix environment (even of xenon) into two separate lines (see page 44).

Since the spectra taken in the phosphorus-fluorine stretch region proved to give the only intense peaks, we must find which of the above symmetry species correspond to P-F stretches. These stretches, of course, would be accompanied by movements of the P_4 superstructure, but the latter would be expected to be of low amplitude and not change the stretching vibrations very much from normal P-F stretches.

To determine the species corresponding to the phosphorus-fluorine stretches, we represent the configuration of P_4F_6 in terms of its six phosphorus-fluorine bond distances, labeled one through six. This gives a partial six element column matrix representation. We now find the trace of the 6×6 matrix corresponding to each symmetry element of P_4F_6 that is to operate on these six element column matrices. The reducible representation thereby obtained has within it the representations of the phosphorus-fluorine stretches, which can then be simply obtained by reducing the

representation. The exact calculations for C_3 and C_{3v} are shown in Table VII. The final result is 2 A and 2 E species of normal vibrational P-F stretches for C_3 symmetry, and 1 A and 2 E species for C_{3v}.

Table VII. Stretching species for P_4F_6

(a)	C_3			(b)	C_{3v}		
reducible representation	E	C_3	C_3^2		E	$2C_3$	$3\sigma_v$
	6	0	0		6	0	0
reduced to:	2 A and 2 E species				1 A_1, 1 A_2, and 2 E species		
final result, infrared active:	2 A and 2 E species				1 A_1 and 2 E species		

From these and more detailed considerations, the tentative assignment listed in Table VI was obtained. Recourse has been made to matrix splittings of the E species modes and a Fermi Resonance for a C_3 P_4F_6 structure.

L. The Matrix Infrared Spectrum of PF_3

In order to more clearly understand the nature of the cracking of P_2F_4, matrix isolation studies on P_2F_4 and its cracking products were undertaken. Krypton and xenon were used as matrix gases (it was found that xenon gave better isolation) with M/R ratios from 50 to 200. Both infrared and ultraviolet absorption studies were done on these resulting matrices, as well as diffusion and photolysis experiments. In the infrared, several weak bands appeared that could not be accounted for (see p. 173). These bands, for the most part, will be ignored in what is to follow,

since the major bands that did appear gave consistent results. In the ultraviolet portion of the spectrum, such complications did not arise.

Since P_2F_4 is an endothermic compound, one of whose decomposition products, PF_3, is quite volatile, and since P_2F_4 was to be passed through a furnace which might further enhance this decomposition to PF_3, it was thought advisable to first obtain a matrix spectrum of PF_3 by itself before the P_2F_4 work was undertaken.

Despite the fact that PF_3 is one of the longest known phosphorus-fluorine compounds,* its chemistry is not known in great detail, with the possible exception of its action as a coordinating agent in transition metal complexes. For instance, up until 1964, an accurate value for the heat of formation of PF_3 was not known, though it does undergo reactions that are capable of accurate calorimetric study. This lack of knowledge about PF_3 has also shown up in the interpretation of its gas phase infrared spectrum. This spectrum was analyzed correctly by Wilson and Polo[94] to give the following fundamentals for PF_3 (ν_1 to ν_4 consecutively): 892, 487, 860 and 344 K. Due to the complex rotational structure of the bands of PF_3, and the poor resolution of infrared spectrometers built twenty years ago, two previous assignments for the fundamentals were wrong. Yost and Anderson[95] gave the four frequencies as 890, 531, 840 and 486 K, and Gutowsky and Liehr[96] gave them as 892, 487, 848 and 532 K.

Figure 14a shows the gas phase infrared spectrum of PF_3 in the P-F stretch region, and Figs. 14b and 14c show the same region of the spectrum of PF_3 in the matrix state in xenon, at M/R ratios of 200 and 2000 respectively. It is interesting to note the extreme simplifying effect

* PF_3 was mentioned in the literature as early as 1884 -- see H. Moissan, C. R. Acad. Sci., Paris 99, 655 (1884).

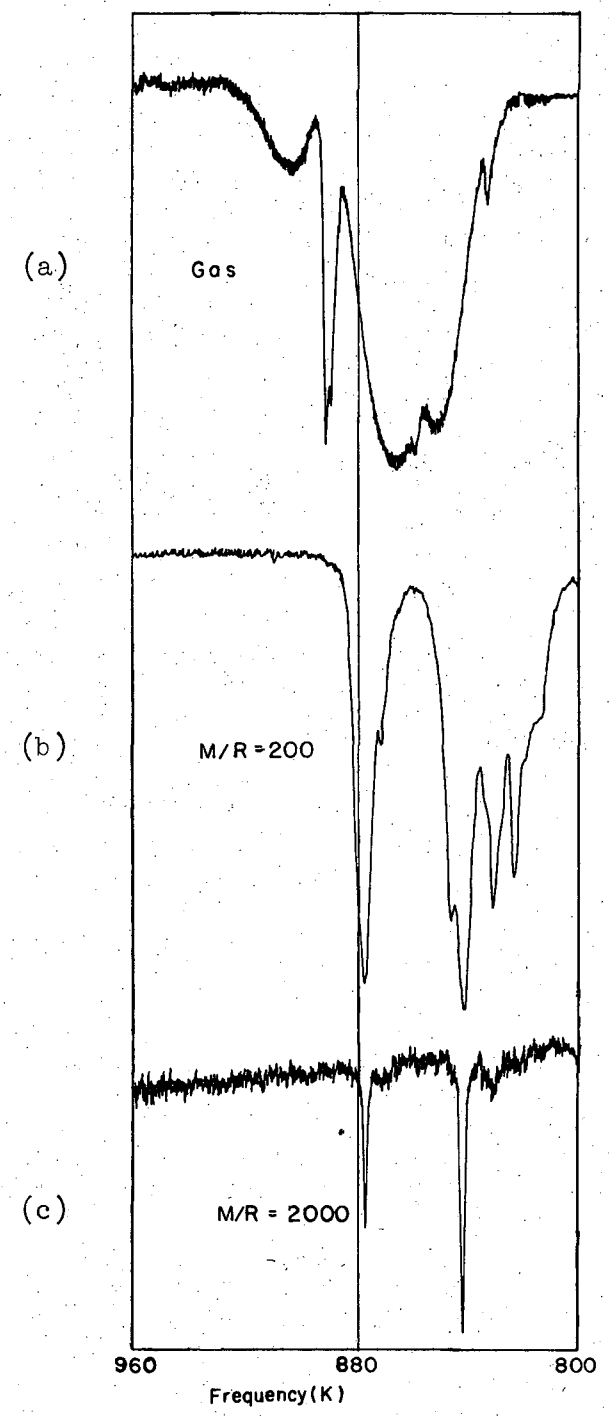

Fig. 14 The infrared spectrum of PF_3.

the very dilute matrix (M/R = 2000) introduces into this spectrum (in the lower frequency matrix spectrum, not shown, one sees the slightly shifted 487 and 344 K bands very clearly as well), making the assignment of fundamental frequencies trivial. The fundamental frequencies of PF_3 in the gas phase and in the matrix are listed in Table VIII along with the ν_3/ν_1 absorbance ratios and average half-widths of each band.

Table VIII. The Fundamental Frequencies of PF_3

	ν_1	ν_2	ν_3	ν_4	Average $\frac{1}{2}$ width	Absorbance ratio for ν_3/ν_1
Gas phase	891 (s)	487 (s)	860 (s)	344 (mw)	~30	?
Krypton M/R = 150	883	488	847	350	16	1.6
Xenon[a] M/R = 2000	878.2	-	843.0	-	1.5	1.85
Xenon M/R = 200	878.5	475	843.5	348	5.0	1.5

All frequencies in Kaysers

[a] Also seen were 831.6 and 871 K bands, both weak and broad.

As an aside, one may note that this table clearly shows the varying effects of the matrix environment on different modes of vibration. The red shifts are predominant for the higher frequency modes, xenon giving a larger shift than krypton, while the blue shift takes effect at the lower frequencies, krypton giving a larger one than xenon, just as would be predicted.

Table VIII does not give all the matrix bands observed for PF_3 (as can be seen in Fig. 14b). Even at M/R = 2000, one sees weak broad peaks in the PF_3 spectrum. These peaks, and others, become much larger at smaller M/R ratios. Table IX lists these "aggregate" peaks. Furthermore, a warmup of the xenon M/R = 2000 matrix above the xenon phase transition of 60.7°K (see chapter Q in this section), and subsequent cooling causes the two fundamentals to decrease in size drastically, with the formation of three weak, broad peaks at 870, 831 and 813 K, and with a net decrease in the total PF_3 integrated absorption of at least 50%.

Table IX. Aggregate bands of PF_3

Xenon	873(w)*	850(m)	833(m)*	825(m)	815(w)*
Krypton	874(w)	851(m)	836(m)	826(m)	816(w)

* similar bands also appear on warm up of isolated PF_3 in a xenon matrix.

Usually, an M/R ratio of 200 is quite sufficient to isolate an unreactive compound in a matrix environment, especially with high boiling xenon as the matrix gas. Yet here this dilution seems to be quite insufficient for isolation purposes. Obviously, PF_3 molecules have a strong attraction for one another in the condensed phase at low temperatures, and therefore have a tendency to dimerize or telomerize in the matrix, most likely as they are condensing out in the LLIT state of matter. This attraction of two PF_3 molecules for each other can be rationalized. First of all, PF_3 has a large dipole moment of 1.025 D to help this dimerization. Burg[97] has shown that PF_3 and $(CH_3)_3N$ form a weak compound that dissociates at -78°C, even though both are bases.

Apparently, the lone pair of electrons on the nitrogen dative bonds to the empty d orbitals of the phosphorus in PF_3. There is no reason why a similar bonding could not exist in pure PF_3. Carbon monoxide, a compound that behaves chemically like PF_3 in certain circumstances, was also found to have an anomalously high tendency towards dimerization in matrix isolation deposition.[29] Thus, the peaks listed in Table IX can be attributed to telomers of PF_3.

Since PF_3 will always be produced when PF_2 is produced (especially after the furnace becomes contaminated with P-F polymers), we should expect to see at least four increased PF_3 absorptions in the infrared when the furnace temperature is raised, and perhaps three more for PF_2 (unless any of these latter ones overlap the four bands of PF_3). Furthermore, some of the aggregate bands of PF_3 might be causing some of the weak peaks seen in these spectra that were not definitely identified.

In the ultraviolet, PF_3 has no absorption above 200 nm in either the gas or the matrix, as would be expected for such a stable molecule.

M. The Ultraviolet Absorption Spectrum of P_2F_4

Before we go into the observations on the matrix photolysis of P_2F_4, it would be wise to investigate the ultraviolet absorption of P_2F_4 which causes this photolysis to occur.

The ultraviolet absorption spectrum of gaseous P_2F_4 in the pressure range of 0.05 to 5.0 torr has three major bands above 200 nm, one of which is very strong and all of which are broad and partially overlapping (see Table X). In the hope that one of these bands might be due to PF_2, temperature-pressure variations were carried out on P_2F_4 gas in the ultraviolet cell to see if a marked dependence in the absorbances of any of these bands on such variations could be observed, as Colburn[22] noted

Table X. The ultraviolet absorption spectrum of P_2F_4 in the gas[a] and matrix phases

Gas Peak[b]	Half Width[b,c]	Extinction Coefficient[d]	Krypton[b] Matrix	Xenon[b] Matrix
299.6	39	780		
260.6	17	20,500	264.9 (red-shaded)	267.7 (symmetrical)
202.2	18	2600		

[a] Taken at 25°C and approximately 0.5 torr pressure.

[b] In nanometers (nm).

[c] At a peak absorbance of 2 units.

[d] In liters/mole cm; calculated by the formula $\epsilon = (A \times V)/(l \times n)$, where ϵ is the extinction coefficient, A is the absorbance, l is the length of the cell, and n/V is the molar density of the gas.

for the 260.2 nm absorption of NF_2 in equilibrium with N_2F_4. Consistent results of variation with temperature or pressure were not obtained for any of these bands. Part of this inconsistency was due to the decomposition of P_2F_4 under ultraviolet photolysis and elevated temperatures, and to the limited accuracy of the Mcleod gauge used to measure the low pressures involved, but most likely, it was mainly due to the lack of any such dependence in the absorbances. The absence of any appreciable amounts of PF_2 in equilibrium with gaseous P_2F_4 at these temperatures and pressures is also borne out by the mass spectral studies mentioned earlier, in which no PF_2^+ peak was observed at all at 13 ev ionizing voltage when the furnace through which the P_2F_4 was passed was kept at room temperature. However, the relative absorbances of the infrared peaks assigned to PF_2 and P_2F_4, in the matrix isolation spectra of P_2F_4 passed through the furnace at room temperature, did amount to 1:15, so presumably some PF_2 does form from P_2F_4 at very low pressures at room temperature. Since PF_2 was shown to lack any noticeable ultraviolet absorptions at high concentrations in the matrix, it is not surprising that no such absorption shows up in the gas at low concentrations.*

Figure 15 shows the 260 nm absorption of P_2F_4 in two different matrices and in the gas phase. One can see the noticeable red shift

---

* In highly concentrated matrices of PF_2, it was sometimes noted that after photolysis of the PF in the matrix, a series of extremely weak bands in the 330 nm region could be made out. These bands were never strong enough to have their frequencies measured well, and could have been due to some residual PF in the matrix as well as to grating defects rather than to a PF_2 absorption.

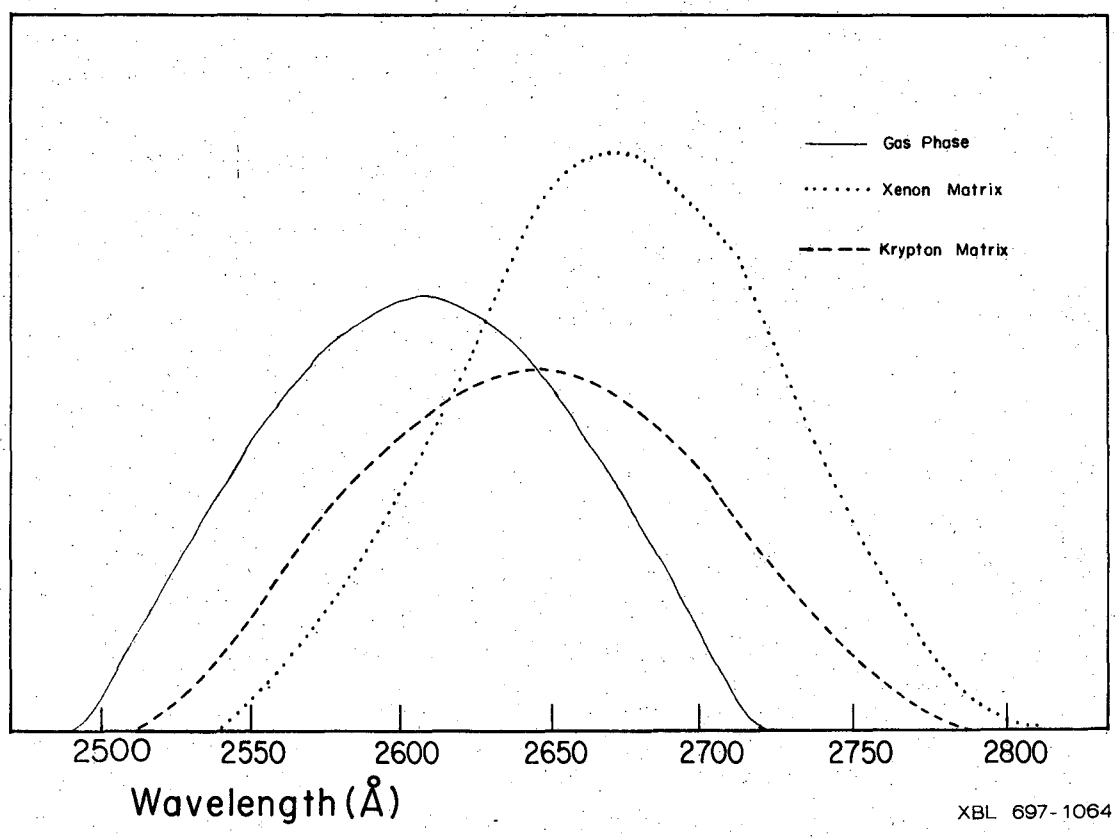

Fig. 15 The 260 nm absorption band of P_2F_4.

combined with the broadening effect that the matrix induces in this absorption, and how these effects differ in krypton and xenon.

The infrared evidence for P_2F_4 points to a frozen trans structure having C_{2h} symmetry. This suggests that a partial double bond exists between the two phosphorus atoms in the ground state, hindering rotation, which could come from a delocalization of the lone pairs of electrons on each of these atoms (two "resonance" structures would be possible here) into the vacant 3d orbitals of the other atom, and the geometry of the d orbitals would explain the resulting trans structure, as opposed to a cis structure.[98] A double bond between the two phosphorus atoms in P_2F_4 would also be consistent with theoretical arguments concerning P-P bond strength in P_2F_4 versus P_2Cl_4,[99] and indeed, the P-P stretching frequency of P_2F_4 (541 K[20]) is larger than the P-P stretching frequency of P_2Cl_4 (410 K[100]).

This explanation, however, has some difficulties. Double bond formation (utilizing π bonding p orbitals) is much more likely for atoms of the first row of the periodic table than for atoms of the second row, and since N_2F_4 is presumed to have C_2 symmetry with hindered rotation about its central bond,[101] and therefore to have a single central bond, it is hard to see why P_2F_4 should have a double bond. Furthermore, P_2H_4 is also presumed to have C_2 symmetry with hindered rotation about its central bond.[102] The best answer is that each of the phosphorus atoms d orbitals are lowered in energy in P_2F_4, so as to make them capable of participating in an overlap with the lone pairs of electrons on the other phosphorus. Low-lying d orbitals do not exist for nitrogen and presumably arenot low-lying enough in energy in P_2H_4.

The question remains of why are the 3d orbitals of phosphorus low-lying in P_2F_4? In hydrogen-like atoms, d and p orbitals have the same energy (to a high approximation). In multi-electron systems, on the other hand, d orbitals are higher in energy than p orbitals because (given a Slater-type approximation) they are too diffuse and do not penetrate the closed shell far enough. This results in an electron in such an orbital not being able to get very close to the positive core to reduce its energy nor being able to overlap well with another orbital of another atom. But it has been shown through Hartree-Fock calculations that d orbitals in multi-electron atoms can be far more compact than the corresponding Slater-type approximation when electronegative groups are attached to the atom under consideration.[103] In particular, for SF_6, whose central atom is next to phosphorus in the periodic table, the electronegative fluorines are presumed to cause a great enough charge drain from the central atom to contract the radial d wave functions so as to produce the stable hexavalent coordination of sulfur in this compound[104] (the same argument probably applies to PF_5).*

Thus it appears that the P-P bond in P_2F_4 is indeed partially double due to d orbital participation. The high intensity of the gas phase P_2F_4 absorption at 260.6 nm (a lower limit of 0.09 was calculated for its f value neglecting deviations from the linear curve of growth -- see

---

* Another analogy is with Si_2F_4. This species almost always forms first in SiF_2 cocondensation reactions and then subsequently inserts in bonds of the stable cocondensing reactant. Its stability could also be due to d orbital participation. If this were so, one might expect to see a very strong ultraviolet absorption for it trapped in a matrix, as is the case for P_2F_4. No such absorption has been reported yet.

Appendix A) can then be explained as being due to a transition from a bonding, delocalized molecular orbital to the corresponding anti-bonding orbital of the P-P bond. The intensity of this discrete charge transfer band would come from the large shift in the electronic distribution upon excitation. This possibility is shown in the figure below.

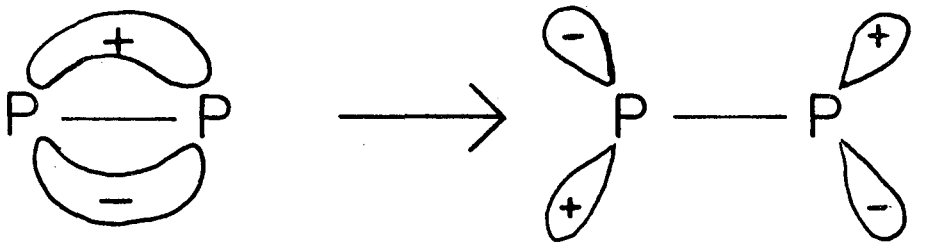

π_u bonding M.O. ground state

π_g anti-bonding M.O. excited state

Fig. 16 The 260.6 nm electronic transition of P_2F_4

This absorption would be analogous to the intense Schumann-Runge bands of O_2, which occur at about 170 nm (and which are responsible for the inability of ultraviolet spectrophotometers to give readings in air below 185 nm). As a result of this excitation, the P-P bond would become single, freely rotating and weaker, thus increasing the reactivity of this excited state, as is observed in photolysis experiments (vide infra).

P_2F_4 isolated in a matrix was observed to have only one absorption band in the ultraviolet, corresponding to the most intense band in the gas (see Table X). The 299.6 nm gas phase band was not seen and neither was the 202.2 nm band (in the latter case, this was due to the cutoff in the efficiency of the grating in reflecting short wave radiation in this region as well as to the inefficiency of the SWR plates used, to respond to such radiation).

In both xenon and krypton matrices, the 260.6 nm band showed small red shifts. This would corroborate the above hypothesis as to the origin of this band, for not only would the increase of polarizability in such a transition be small (due to the large polarizability in the delocalized ground state), but also the excited state would have an electron far from the center of the molecule (in an anti-bonding orbital) so that electron-electron repulsion forces would raise the energy of the excited state in the matrix (as it does in the case of atomic transitions) and thus the energy of the transition as a whole, thereby reducing the red shift.

N. The Matrix Photolysis of P_2F_4

Photolysis experiments were performed in the matrix as mentioned previously. Since an undetected absorption band might have been causing the photolysis, it was experimentally verified, through the use of filters, that the light causing the photolysis of P_2F_4 in the matrix environment was that light strongly absorbed by P_2F_4 from 260 to 285 nm. And since the high pressure mercury arc cuts off all ultraviolet radiation in the 253.6 to 260 nm region through resonance self-absorption, it was mostly the portion of the P_2F_4 absorption band shaded to the red that was absorbing the photolyzing radiation.

When P_2F_4 is photolyzed in the matrix, no new bands in the ultraviolet absorption spectrum are observed to appear as the 270 nm absorption disappears, even when large amounts of P_2F_4 are photolyzed away. In the infrared, all the major absorptions attributed to P_2F_4 (see Table XII on page 169) are observed to decrease. In their place a great many other absorptions appear. Thus, new materials are forming that have an infrared

but no visible-ultraviolet spectrum. Four of these infrared absorptions correspond exactly to the four absorptions due to PF_3 fundamentals, and increase proportionately as photolysis continues. At least ten other major absorptions are observed to increase during photolysis. Their frequencies, along with weaker bands that appear, are tabulated in Table XI. Figure 17 shows a sample spectrum of P_2F_4 and PF_2 (and some PF_3), from the high temperature furnace, trapped in a xenon matrix at M/R = 200 before and after photolysis. These spectra were only taken in the phosphorus-fluorine stretch region of the infrared.

Photolysis of P_2F_4 in the matrix gave quite erratic results as far as its rate was concerned (though the products formed were always the same) -- sometimes a few minutes of photolysis would completely destroy 10 micromoles, and at other times one hour would be required, and, at still other times, an hour of photolysis would not be sufficient, and a certain amount of residual P_2F_4 remained. More perplexing was the fact that photolysis from behind the matrix (the irradiating light going through the target first and then striking the matrix where it was initially deposited) at times was totally ineffective in removing any appreciable amounts of P_2F_4, no matter how long the photolysis continued, in matrices that were easily photolyzed from the front. Various hypotheses were offered to explain these phenomena (such as selective absorption of certain radiations by the target material), but when experimentally tested, all failed to give satisfactory results save one.

The clue to this anomalous behavior came from the products of the photolysis themselves. PF_3 was definitely one of the products, since the four infrared absorption lines attributed to it all increased proportionately upon photolysis. At least four other distinct bands in the

Table XI . Infrared bands that appear and increase from the matrix photolysis of P_2F_4 [a]

(P_3F_5 Bands)

Phosphorus-Fluorine Stretch Region Dual Grating (4000-650 K)		Low Frequency Region CsBr Prism (700-300 K)	
Xenon	Krypton	Xenon	Krypton
956.5(mw)	960(m)	475(ms)-PF_3	487(ms)-PF_3
915.5(s)	918.5(s)	400(m)	
891.5(m)	894(m)	394(m)	
889.5(w)		368(m)	
878.5(s)-PF_3 (and P_3F_5?)	881(s)-PF_3 (and P_3F_5?)	347(m)-PF_3	350(m)-PF_3
843(vs) - PF_3	846.5(vs)-PF_3	325(mw)	
743(w)	749(m)	300(s)	

Very weak bands increasing: Xenon: 969, 890, 748, 557, 381, 333, 322 and 314.
Krypton: 836, 578.

[a] All frequencies in Kaysers.

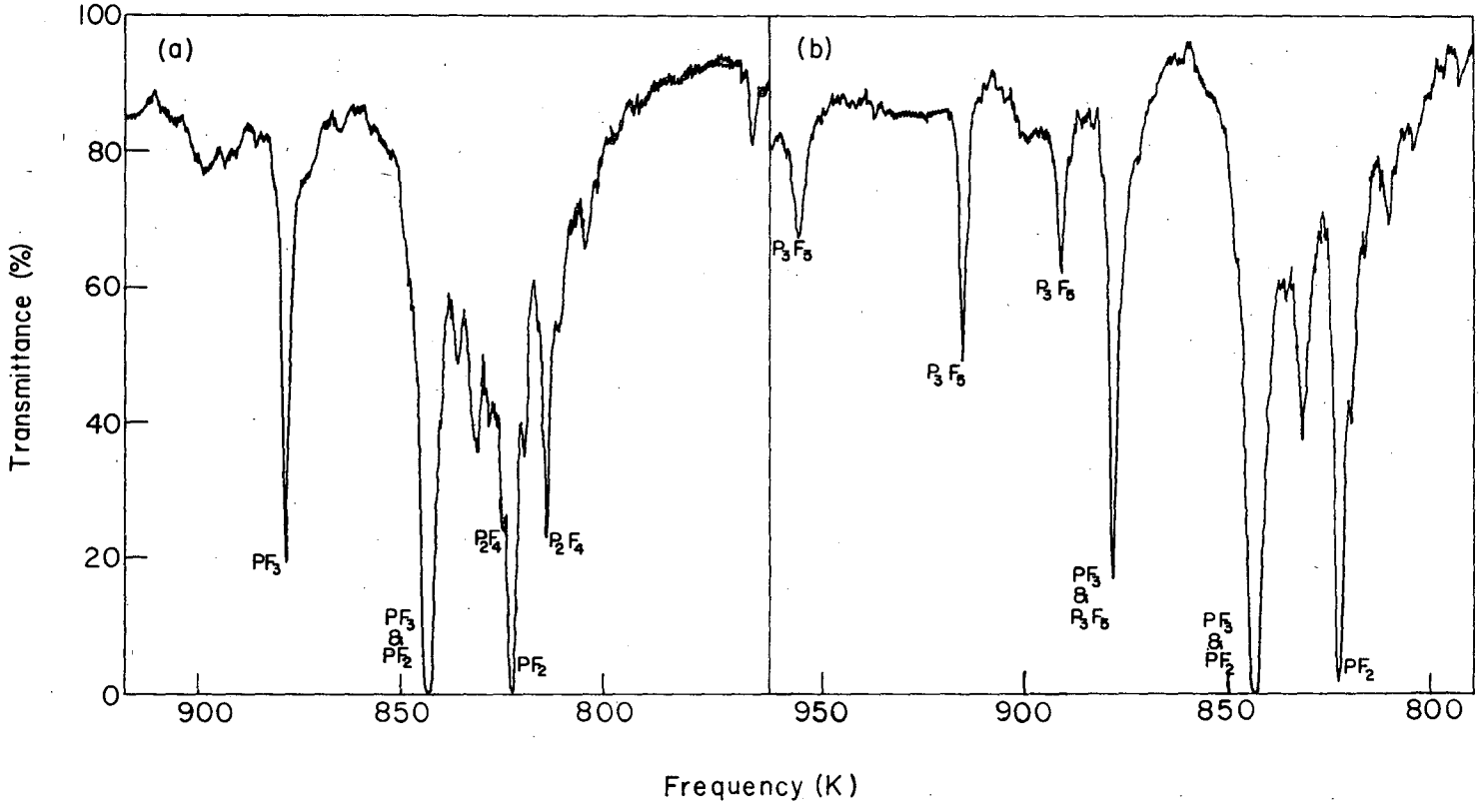

XBL 696-731

Fig. 17 The infrared spectra of matrices containing P_2F_4 and PF_2 before and after photolysis. (a) before photolysis; (b) after photolysis.

P-F stretch region (750-1000 K) arose that were due to the other product(s) forming. This number of bands is too great to be produced by diatomic PF, which would be the obvious stoichiometric guess. In any event, it was believed that PF had already been trapped in the matrix in the pyrolysis of P_2F_4 (see page 180), giving a series of bands in the 3300 Å region of the U.V. spectrum, which the P_2F_4 photolysis products did not have. Assuming nothing lost to the gas phase nor polymeric products forming during photolysis, the only other products that could form from the photolysis of a single P_2F_4 molecule are atomic P and F. This is a virtual impossibility considering the infrared spectral evidence and the high reactivity of these species. It was concluded, therefore, that more than one P_2F_4 molecule is required for production of each molecule of photolysis product.

In the P_2F_4 ultraviolet spectrum, the 260.6 nm band most likely is a discrete band spectrum transition, not a continuum nor a predissociation. In the matrix environment, which would tend to increase the steepness of the potential energy curve for P_2F_4, it is probable that this absorption by itself does not result in any splitting of the bonds of P_2F_4. Therefore, the photolysis might be ascribed to a reaction of an excited P_2F_4 molecule(s) with, most likely, one other P_2F_4 molecule.

To test out this hypothesis, photolysis of P_2F_4 was done at various concentrations in the matrix. At high concentrations (M/R = 30), photolysis was complete in a matter of minutes. The lower the concentration of P_2F_4 the slower the photolysis rate. An experiment was also performed with pure solid P_2F_4 deposited on top of a concentrated P_2F_4 matrix. Photolysis for two hours gave no noticeable reduction in the (blurred out) P_2F_4 infrared bands. This last result is explicable since

the solid layer of P_2F_4 would be expected to absorb all the radiation capable of photolyzing matrix isolated P_2F_4, and so if it did not photolyze away, neither would the P_2F_4 underneath it. Another experiment was performed with a large predeposition of pure rare gas on the matrix to build up a thick M atom back layer next to the target before any P_2F_4 was added at all. Photolysis from the back in this matrix did destroy the P_2F_4, as it does from the front. Upon warmup of a photolyzed matrix, the bands arising from photolysis (other than PF_3) disappear (without new bands taking their place), yet no reformation of P_2F_4 occurs.

Though the four fundamentals of PF_3 all appeared upon photolysis of P_2F_4 and increased proportionately, none of its aggregate bands appeared at all. This would suggest that the PF_3 forming was in a well-isolated environment.

It is suggested that the reaction of two P_2F_4 molecules is occurring upon photolysis, and that this reaction could fully explain the above results. When the matrix becomes too dilute in P_2F_4, no photolysis reactions can occur. When it becomes too concentrated, the cage effect predominates, and the photolysis products, if formed, immediately react to reform the reactants (two P_2F_4 molecules). However, irreversibility of the photolysis reaction upon warmup suggests that a simple monomolecular fission is unlikely, since the latter would be expected to result in the reformation of P_2F_4 on warmup. A site in the matrix that had two contiguous P_2F_4 molecules, would probably not also have a PF_3 molecule nearby, so the reaction of two P_2F_4 molecules to produce a single PF_3 molecule would form it in a well-isolated environment, and the consequent abrupt cooling would prevent diffusion and dimerization of PF_3 to form aggregates.

Reactions of two matrix-isolated molecules upon photolysis are common in matrix work. For instance, Pimental and Haller[39] have shown that photolysis of a matrix containing N_2O and C_2H_2 results in the formation of O atoms that then react with the acetylene to form H_2CCO. Such photolytic reactions occur because the bond rupture necessary to form the radicals from the parent is accompanied by excess energy in these radicals which causes them to diffuse through the solid a short distance. But in the present work, it is proposed that we have a reaction of a mere excited state of a molecule, not a dissociated one, a kind of "excitation photolysis." Since one of the "advantages" of matrix phase photolysis is that it is supposed to stop secondary photolytic processes coming from, among other things, chemical reactions of excited states, this behavior noted is quite unusual.

An explanation of this behavior is that what is really occurring in the matrix photolysis of P_2F_4 is a reaction of two excited P_2F_4 molecules. P_2F_4, as noted before, has a very high intensity absorption from 260 to 280 nm in the matrix. It was calculated that because of this high absorption, 90% of all incident light on a M/R = 50 matrix would be absorbed in just three wavelengths of thickness of the matrix. Thus the possibility exists that two contiguous P_2F_4 molecules would each absorb a photon approximately within the lifetime of their excited states, and it is the reaction of these two excited species that produces PF_3 and the other product(s). Such a mechanism would be very dependent on relaxation rates in the matrix, since it would involve a sort of "hot layer" of continually excited molecules in the matrix. In back photolysis, this layer of continual excitation would exist close to the cold target, so that the target could take enough energy away from one excited P_2F_4

molecule before a nearby one could be excited to react with it. Photolysis from the front, on the other hand, would produce this hot layer insulated from the cold target by a large amount of inert gas plus matrix. Localized heating could occur to effect diffusion and therefore a reaction. The same principle applies to the observations on back photolysis of a matrix with a large predeposition of pure inert gas.

If a double excitation reaction is really the cause of the P_2F_4 photolysis, then the rate of disappearance of P_2F_4 upon photolysis should depend on the intensity of the light squared (as well as the concentration of P_2F_4 squared). This dependence could vary over a considerable range with slightly different intensities of light or concentrations of P_2F_4, and would explain the large variability noted for the photolysis rate.

As was mentioned previously, the excited state of P_2F_4 would be expected to have a weaker P-P bond than the ground state, and so would be expected to be more reactive than this ground state, especially with respect to either fission of, or insertion into, its P-P bond.

Such a mechanism would also explain the photolysis of PF (PF is produced whenever PF_2 is produced, as shown in Chapter R of this section). PF isolated in a matrix (along with P_2F_4) will <u>not</u> photolyze away when the radiation it absorbs is incident on it. However, 270 nm radiation will readily photolyze it away, even from the back. In one experiment on a dilute krypton matrix containing a relatively large amount of PF (obtained by premixing the P_2F_4 with krypton before passing it through the furnace -- see page 185), as well as P_2F_4, PF_3 and PF_2, after a photolysis from the <u>back</u>, the three high frequency peaks to be assigned to P_3F_5 all formed to a clearly discernible extent as the PF disappeared. These peaks are the strong ones appearing in the photolysis of P_2F_4, yet

presumably no P_2F_4 photolyzed here at all. It seems, therefore, that the ultraviolet radiation is exciting P_2F_4 molecules, making them mobile and reactive enough to react with PF and scavenge it away in the matrix.* Most likely, PF cannot insert into the partial double bond between the phosphorus atoms of P_2F_4 in its ground state, but can and does insert, as a carbenoid, into the weakened P-P bond in the excited state to form P_3F_5. This is also corroborated by warmup experiments on PF matrices, which show PF to be an unreactive species.

If we ignore the fact that here we have a mobile P_2F_4 molecule, not a mobile PF molecule, we could claim from this piece of evidence that a transient, mobile PF species is also the reactant in the pure P_2F_4 photolysis, reacting there with an excited P_2F_4. However, it is difficult to explain why one excited P_2F_4 should remain excited while another one dissociates.

In a parallel photolysis experiment on P_2F_4 gas in the photolysis cell mentioned on page 71, with the cold finger of this cell maintained at -65°C, an unstable compound was formed that condensed out on the cold finger. But its stability was too low and its yield too small for any analysis to be undertaken. Perhaps this compound was P_3F_5, as it is also believed to form in matrix photolysis of P_2F_4 as well as in the cocondensation reaction at 77°K of the products of the P_2F_4 pyrolysis.

There are many pieces of evidence, besides that mentioned above, which would suggest that P_3F_5 is the other product in the P_2F_4 photolysis. First of all, many P_3R_5 compounds have been prepared in the past [such as $P_3(CF_3)_5$[105]], and their instability has been attributed to their tendency

---

* The possibility of a PF absorption overlapping the P_2F_4 absorption and causing its photolysis is excluded because the gas phase absorption spectrum of PF should not have any strong bands in this region -- see page 180.

to polymerize, not to a weak P-P-P structure. Therefore, isolation in the matrix could stabilize such compounds relative to the condensed phase. P_3F_5 would probably not have any ultraviolet spectrum, as is observed. It would have C_s symmetry and its infrared P-F stretches would be five in number (3A' and 2A" species) and all be infrared active. Though only four peaks were seen in the infrared that could possibly be ascribed to P-F stretches, the fifth band could be accidentally degenerate with another P_3F_5 band, could be too weak to be observed, or could be overlapping a PF_3 peak. The best explanation I can offer is this last one, specifically, that the fifth P_3F_5 band is overlapping the ν_1 PF_3 band in the matrix. As will be mentioned in the next section, careful measurements on the increases of the absorbances of the ν_1 and ν_3 bands of PF_3 during photolysis showed that the ratio of these increases ($\Delta\nu_3/\Delta\nu_1$) was lower than that which is normal for pure PF_3 in the matrix (this ratio was measured to be 1.0 in krypton and 1.1, 1.1 and 1.2 in three experiments in xenon). This could be explained by assuming a P_3F_5 band growing in with the ν_1 band of PF_3. Since P_3F_5 has low symmetry, it would be expected to have many bands in the lower frequency portion of the infrared (13 altogether), and as much as ten were observed in the xenon matrix. Upon warmup, P_3F_5 would be expected to polymerize, and the infrared bands of the product do disappear upon warmup without any new bands taking their place. And of course, stoichiometrically P_3F_5 is quite plausible.

There is one problem however, and that is why there is no P_3F_5 observed on initial deposition of P_2F_4 that has gone through the furnace. (Actually, an extremely small 918 K peak was observed in one PF_2 deposition when the P_2F_4 was premixed with krypton.) The best answer I can give is that two factors may come into play here. One, there is a large

excess of inert gas condensing on the target making it unlikely that a PF molecule will collide with a P_2F_4 molecule in the LLIT state before being frozen out. Two, perhaps PF can only insert in activated P_2F_4 that might exist from a reaction of two PF_2 species in the LLIT state. But there, with large amounts of inert gas condensing all around it, the quenching rates are so fast that this newly formed excited P_2F_4 is quickly quenched before it collides with a PF molecule so that no insertion does take place (such would not be the case in normal cocondensation reactions where no inert gas is present, and where condensation temperatures are much higher).

Another stoichiometric and chemical possibility in this photolysis is the formation of two PF_3 molecules and one P_2F_2 molecule. Since N_2F_2 and P_2H_2 are well known species, the existence of P_2F_2 cannot be precluded on simple chemical grounds. However, in such a reaction, one might expect some of the aggregate bands of PF_3 to appear, since two molecules of them would be forming close to each other, but only the four bands of PF_3 characteristic of the isolated molecule appeared. The activation energetics of such a reaction would seem highly unfavorable, since it would require the breaking of <u>two</u> P-P bonds. Trans P_2F_2 would be expected to be the stable isomer, and its C_{2h} symmetry would only allow <u>one</u> infrared active P-F stretch, but at least three are seen. Recourse to asymmetric sites would have to be had in order to explain its actual spectrum in the P-F stretch region. In any event, the large number of other bands in the low frequency portion of the infrared spectrum could not be explained. Finally, P_2F_2, with a double bond between the phosphorus's, would be expected to have an ultraviolet absorption spectrum, but none was observed.

0. Pyrolyzed P_2F_4 in the Matrix Environment -- the Matrix Infrared Spectrum of PF_2

Parry and coworkers[20] have analyzed the infrared and Raman spectra of P_2F_4 in the gas and liquid states respectively, and, since they found mutual exclusion to hold, assigned most of its predicted fundamental modes on the basis of a rigid trans structure having C_{2h} symmetry. As was previously mentioned, such a structure would be in agreement with the strong ultraviolet absorption band observed in this work (see page 155). If their assignment is correct, P_2F_4 in the matrix would have only two infrared active fundamentals in the P-F stretch region, corresponding to the gas phase values of 842.9 and 830.8 K, which are the PF_2 antisymmetric, out-of-phase pair of stretches, and the PF_2 symmetric, out-of-phase pair of stretches (ν_5 and ν_{10}) respectively; and two infrared active fundamentals in the low frequency region, corresponding to the gas phase values of 365 and 361 K, which are the PF_2 symmetric, out-of-phase deformation, and the PF_2 antisymmetric twisting (ν_{11} and ν_6) respectively. Due to its center of symmetry, these are the only vibrational modes of P_2F_4 above 200 K that are predicted to be infrared active. However, because of the near impossibility of removing all PF_2I from P_2F_4, strong PF_2I bands at 412.2 and 378.7 interfere with the spectrum of P_2F_4 in the gas phase, and presumably do so in the matrix as well.

The matrix infrared spectrum of P_2F_4 isolated in krypton and xenon is listed in Table XII (see also Fig. 17). Frequencies that can be attributed to PF_2 or PF_3 have been omitted from this table. The assignments of Parry are verified completely. Furthermore, one sees that the matrix shifts from the gas phase bands for the lower frequency modes differ from one another, especially in krypton, the deformation having a much greater

blue shift than the twisting. This difference is explicable in terms of the geometry of the site the molecule finds itself in.

Table XII. The fundamental frequencies of P_2F_4

	ν_5	ν_{10}	ν_{11}	ν_6
Gas Phase	842.9(vvs)*	830.8(vvs)*	365(m)	361(m)
Krypton	828(s)	817(s)	383(w)	363(m)
Xenon	825-828(s)	813(s)	367(vw)	355(mw)

Also, 407 (Kr, vw) and 398(Xe, vw) observed, perhaps a PF_2I impurity band.

* R and P branches averaged.

Besides the bands shown in Table XII, four very weak bands corresponding exactly with the four fundamentals of PF_3 are observed, owing to the slight decomposition of P_2F_4 to PF_3. ν_3 seems to be inordinately larger than ν_1 in this PF_3 spectrum. Another very weak band between the two P_2F_4 fundamentals stands out in the phosphorus-fluorine stretch region.

When P_2F_4 is passed through the furnace at a temperature of 750°C (at the same rate as the room temperature deposition, about 20 micromoles/hour) before deposition in the matrix, its two fundamentals in the P-F stretch region decrease in intensity as expected. Also, the two PF_3 fundamentals increase greatly in intensity in this region (because of decomposition of the P_2F_4), with the absorbance ratio of ν_3/ν_1 becoming still larger than before, and much larger than in pure PF_3 (see Table XIII). Lastly, that very weak band mentioned before increases greatly in intensity. We will refer to this deposition from now on as the PF_2

deposition. Other weak bands do appear in this PF_2 deposition, but only one of them has been assigned (to the stretch in PF, as will be discussed below)- see the footnote for Table XIV.

If the photolysis of P_2F_4 in these matrices continues long enough, the two large P_2F_4 absorptions in the P-F stretch region as well as the P_2F_4 absorptions in the lower frequency range can be completely wiped out. No other peaks are observed to disappear. In their place arise the four fundamentals of PF_3, and the peaks assigned to P_3F_5. In experiments on a pure P_2F_4 deposition, and on a PF_2 deposition, measurements of the intensity changes of the 878.5 and 843.5 bands of PF_3 upon photolysis were carried out. If these two bands were caused by only one compound, PF_3, the ratio of their absorbances should remain the same as they increase irrespective of the concentration of PF_3 in the matrix. But in fact it was noted that the ratio of their absorbances differed in the pure P_2F_4 matrix and in the PF_2 matrix, and the ratios in both these matrices differed from the ratio in pure PF_3 (as stated above). The ratios differed before and after photolysis as well, approaching the PF_3 ratio as photolysis continues, and did not increase during photolysis in proportion to their original value. Sample results are shown for two such experiments in xenon in Table XIII.

Notice that in this experiment we are making use of the fact explained on page 52, that infrared peak heights in the matrix can be considered direct indications of the amounts of materials present, due to the broadening of rotational lines. The agreement between the ratio of the increases of the absorbances upon photolysis and the ratio of the absorbances in pure PF_3 is only fair (and has been explained as due to an overlapping with a P_3F_5 band -- see page 166), but an overlapping at the 843.5 K peak

Table XIII. Behavior of PF_3 band intensities on photolysis of P_2F_4 and PF_2 xenon matrices

	P_2F_4 thru cold furnace				P_2F_4 thru hot furnace		
	% Trans.	Absorbance	Ratio	Ratio	% Trans.	Absorbance	Ratio
Before Photolysis							
843.5	26	0.585	2.12	1.5	0.3	2.523	3.62
878.5	53	0.276			20	0.698	
After Photolysis							
843.5	10	1.000	1.52	1.5	0.25	2.60	3.38
878.5	22	0.658			17	0.770	
Ratio of Increase of Absorbances After Photolysis			1.09	(1.5)			1.10

is substantiated quite strongly by the evidence. It is therefore believed that one of the PF_2 fundamentals overlaps the ν_3 fundamental of PF_3, and that PF_2 does not photolyze away while P_2F_4 does (during photolysis, the PF_2 peak that does not overlap any other peak remains the same, showing that the entire change in the intensity of the 843.5 line comes from PF_3 forming). The presumed overlapping of a PF_3 and PF_2 fundamental is required in both krypton and xenon to explain the observed spectra, so that the relative matrix shifts for PF_2 and PF_3 must remain the same in two different matrices.

The lower frequency region of the infrared is more difficult to interpret because at the M/R ratios employed in these experiments, aggregate or multiple site peaks occur in this region. After eliminating those bands due to P_2F_4 and PF_3, another band, appearing in the PF_2 deposition, seems to be the PF_2 band, due to its intensity, position and lack of change upon photolysis. The PF_2 bands observed are listed in Table XIV. The justification for the assignments of ν_1 and ν_3 will follow in the next chapter. The "gas phase" values for PF_2 are its matrix values adjusted to the most probable gas values by adding average extrapolated xenon and krypton matrix shifts for PF_3 and P_2F_4 to those matrix values for PF_2.

PF_2 was shown to have no observable peaks in the ultraviolet. A diffusion experiment carried out on a PF_2 deposition showed the PF_3, P_2F_4 and PF_2 peaks all decreasing proportionately in the infrared as the temperature of the matrix was raised, even though one would expect PF_2 to disappear faster than the others, and form P_2F_4 as its product. However, the P_2F_4 absorption was observed to increase in the ultraviolet upon warmup, and so perhaps its decrease in the infrared came from its absorption there being broadened as the temperature was raised.

Table XIV. The fundamental frequencies of PF_2*

	ν_1	ν_2	ν_3
krypton	847(s)	329(w)	826.5(vs)
xenon	843	-	822
"gas phase"	850	325	830

Also, 509 (Kr, vw) seen.

*Other weak bands observed in the PF_2 deposition, not attributable to PF, PF_2, PF_3, P_2F_4 nor P_2F_5, included, in krypton, 836.5, 831, 824 and 809 K, and, in xenon, 835, 830, 818.5 and 803 K.

P. A Force Constant Analysis of PF_2

Thus, we now have the three normal frequencies of the bent, triatomic, symmetrical molecule PF_2. These frequencies correspond to the v"=0 to v"=1 transition in the ground state of PF_2, and not the harmonic frequency for this state that could be derived by a detailed analysis of the ultraviolet emission spectrum of PF_2. As was stated previously (page 44), the vibrational contribution to the absolute entropy of PF_2 can be determined from these frequencies. From this determination, combined with other thermodynamic estimates for PF_2, the stability of PF_2 as an equilibrium gas phase species can be predicted (as will be done in Chapter T of this Section). By assuming various equations for the expression of the potential energy of the PF_2 molecule, these three frequencies can also lead us to estimates of the bond force constants of the PF_2 molecule, as will be discussed here.

Expressing the potential energy in terms of simple central forces was not attempted, since this method is highly unreliable.[44] However, a simple valence bond force calculation was done, for two different

assignments of the normal modes of PF_2, the results of which are shown in the second and third columns of Table XV. The stretching and bending constants were derived from Eqs. (8) and (9) on page 40 of this dissertation, the first two equations in the simple valence bond expression. Also in Table XV is shown the consistency of this valence bond approach as judged by the prediction of the value of $\lambda_1\lambda_2$ from the third equation of this approach, (10) on page 40, as compared with the actual value of this product derived from ν_1 and ν_2. It is seen that by assuming that the symmetric stretch, ν_1, is smaller than the antisymmetric stretch, ν_3, for PF_2, which is the case for most C_{2v} bent triatomics, we obtain unbelievably good agreement with the simple valence bond force assumption -- such good agreement that it would seem this $\nu_1 < \nu_3$ assumption is wrong!.

In going to a more complicated valence force assumption for the potential energy, as expressed in Eqs. (11), (12), and (13) on page 41, we again obtain evidence against this $\nu_1 < \nu_3$ assignment. In this case, the interaction between the two P-F stretches term, k_{12}, is equal to zero (column five of Table XV). This is highly unlikely. But fairly reasonable results are obtained in both of the above approximations for the assignment $\nu_1 > \nu_3$, that is, assuming that the symmetric stretch is 850 K and the antisymmetric stretch is 830 K for PF_2.

This assignment, actually, would be consistent with that for other difluorides of elements near phosphorus in the periodic table, such as CF_2, NF_2 and OF_2, all of whose assignments are known conclusively. The relative intensities of ν_1 and ν_3 (the 850 band is observed to be at a smaller intensity than the 830 band) would also agree with this assignment, since the dipole moment does not change as much in the symmetrical stretch (ν_1) as it does in the antisymmetrical stretch (ν_3). Since it is well

Table XV. PF_2 force constants from the "gas phase" normal frequencies

Force Constants	Simple Valence Forces		Complex Valence Forces		Most Complex Valence Forces
	$\nu_1 = 850$ $\nu_3 = 830$	$\nu_1 = 830$ $\nu_3 = 850$	$\nu_1 = 850$ $\nu_3 = 830$	$\nu_1 = 830$ $\nu_3 = 850$	$\nu_1 = 850$ $\nu_3 = 830$
k_1	4.596	4.820	4.830	4.820	4.971
k_{12}	-	-	0.2342	-0.0001	0.3753
k_α/l^2	0.640	0.4245	0.4238	0.4246	0.4112(min.)
$k_{l\alpha}/l$	-	-	-	-	0.1619
For Simple Only					
$\lambda_1\lambda_2$ (actual)	2648.3	2525.2			
$\lambda_1\lambda_2$ (calc.)[a]	3630.0	2524.8			

Assume $2\alpha = 96°$

l = P-F bond length; $\nu_2 = 325$ K for all calculations; and force constants in units of millidynes/Å .

[a] Calculated by means of Eq. (10) on page 40.

known that the electronegativity and compactness of fluorines can cause them to repel one another in the same compound (as has been hypothesized for P_4F_6 -- see page 138 -- and PF_5[96]), it might be expected that this effect would make itself felt more in the symmetric stretch than the antisymmetric stretch, since in the former the two fluorines experience more steric hindrance, and so raise the frequency of the symmetric stretch.

The most general expression of the potential energy of the PF_2 molecule results in four independent quadratic force constants (see Eqs. (15), (16) and (17) on page 41). Since only three frequencies have been given (and no isotopic studies were possible), a fourth condition must be imposed before we can solve for the four constants uniquely. This fourth condition, according to Linnet and Heath,[47] is that the value of the bending constant, $k_{\alpha/1}{}^2$, be at a minimum. Using this condition, plus the three equations mentioned above, plus the frequency assignment $\nu_1 > \nu_3$, the results shown in the last column of Table XV were derived (see Appendix C for a sample calculation). These results are reasonable, as can be seen by comparison with other difluoride values listed in Table XVI. Table XVI also gives other information comparing the difluorides, and includes values for PF_3 that were calculated by me from known frequencies.

Table XVI shows a relatively large value for the angle-bend interaction constant, $k_{1\alpha/1}{}^2$, for PF_2. This means that the P-F stretching force constant changes quite a bit with a change in the F-P-F angle. Since the stretching force constant is dependent, to a certain degree, on the hybridization of the phosphorus atoms' orbitals, the large variation in the force constant implies that this hybridization changes a great deal with angular bend. Given a simple $s^{a^2} p^{k^2}$ hybridization for the bond of a central phosphorus atom to fluorine, it can be shown that one of the hybrid orbitals is,

Table XVI. Normal frequencies, angles and quadratic force constants for some fluorine-containing molecules

	CF_2 [a]	NF_2 [b]	OF_2 [b]	SiF_2 [c]	PF_2	PF_3 [d]
ν_1	1222	1070	929	855	850	891
ν_2	672	573	461	345	325	487
ν_3	1102	931	826	872	830	860 (and ν_4 = 344)
k_1	6.76	5.1	4.6	5.019	4.971	4.992
k_{12}	2.21	1.5	1.5	0.310	0.4	0.27(k_1')
$k_{\alpha/1^2}$	1.30	1.15	1.0	0.440	0.4	0.64
$k_{1\alpha/1}$	0.92	0.4	1.0	0.123	0.16	(0.14-$k'_{\alpha/1^2}$)
Estimated or Observed Angle	105°	104°	103°	101°	96°	98°12'

All frequencies in Kaysers and correspond to the (1,0) vibrational transition of the ground state; all force constants in millidynes/Å; and angles correspond to the Y-X-Y angle in XY_2 or XY_3.

[a] B. A. Thrush and J. J. Zwolenik, Trans. Faraday Soc. 59, 582 (1963); D. E. Milligan, D. E. Mann, M. E. Jacox and R. A. Mitsch, J. Chem. Phys. 41, 1199 (1964); reference 74; and force constants were calculated by this author.

[b] M. D. Harmony and R. J. Myers, J. Chem. Phys. 37, 636 (1962).

[c] V. M. Khanna, R. Hauge, R. F. Curl, Jr. and J. L. Margrave, J. Chem. Phys. 47, 5031 (1967).

[d] The author's calculations, based on the work of F. Lechner, Wien. Ber. 141, 633 (1932) and reference 46. The value for the F-P-F angle came from O. L. Hersch, Ph.D. dissertation, University of Michigan (1963).

$$|\phi_1\rangle = \frac{1}{\sqrt{a^2+k^2}}(a|S\rangle + k|p_x\rangle) \qquad (28)$$

and that the angle between such hybrids is θ, where $a^2 = -k^2 \cos\theta$. Differentiating a^2 with respect to θ, and considering k to be a constant, we find that the maximum change in hybridization with change in angle occurs when the angle θ is 90°. Since, presumably, we have a large change in hybridization with angle for PF_2, its angle is probably close to 90° (my estimate was 96°). However, this reasoning seems to fail completely for OF_2 (whose values have not been accurately determined).

The comparison of PF_3 with PF_2 is instructive in several ways. The larger value for the bending constant of PF_3 is explicable in terms of the greater steric hindrance of three fluorines versus two fluorines. The two compounds, however, have almost identical stretching force constants. Since Morse's Law[106] tells us that the stretching force constant for the bond between two particular atoms in any ground state molecule is proportional to l^{-6}, where l is the distance between the two atoms in the molecule in question, the P-F bond lengths in PF_2 and PF_3 must be nearly equal (in PF_3 it has been measured to be 1.537Å, and my estimate for PF_2 was 1.55Å).

Q. The Xenon Phase Transition

An interesting effect was noted in the warmup of xenon matrices of PF_2 and P_2F_4, and those of PF_3 alone, especially in those matrices deposited for a long time and which consequently contained much xenon. At 60.7°K, a sharp increase in the slope of the temperature versus time curve was noted. If the warmup was continued long enough, the slope would again level off. This behavior was noted for a PF_3 matrix that was very dilute

and for a concentrated PF_2 matrix, thus strongly suggesting that the recombination of phosphorus-fluorine radicals had nothing to do with the increase in the slope of the warmup curve. Also, the abrupt change in the warming rate at 60.7°K was accompanied by an almost instantaneous jump in the pressure, the gauge going from 2×10^{-3} microns to over 1×10^{-2} microns in a second or less. This behavior is quite common in exothermic solid phase transitions, and is due either to a momentary heat rise, or to a phase change causing entrapped air and other permanent gases to be released from the interstitial sites in which they were trapped in the metastable solid. Furthermore, the amount of heat needed to warm up the entire target holder of the cryotip could never come from the small amounts of P-F compounds used, and so must be coming from the inert gas itself. Therefore, it is believed that the observed heat effect arose from a metastable to stable xenon phase transition.*

Exactly what kind of phase transition this corresponds to is very questionable. Pure xenon itself has a ccp structure, at <u>all</u> temperatures. Xenon, that contains a dissolved impurity, usually takes on an hcp structure, at <u>all</u> temperatures. Thus, neither type of solid xenon after deposition would be expected to undergo any phase transition upon warming. A possibility here, suggested by Professor Leo Brewer, is that the phosphorus-fluorine compounds used are either extremely insoluble in xenon at low temperatures, or do not "dissolve" in it under matrix deposition conditions, and so allow the xenon to form the ccp structure, characteristic of xenon in its pure state, upon deposition (even though they would be interfering with the regular lattice). Upon warmup however, their solubility increases to the point where they cause a ccp → hcp transition to an homogeneous, slightly impure, solid xenon.

---

* Exothermic processes that occur on addition of heat are necessarily irreversible.

R. The PF Diatomic Molecule

Douglas and Frackowiak[107] discovered the PF diatomic molecule spectroscopically in the gas phase in 1962. A flowing mixture of helium plus a trace of PF_3 was passed through a glass tube within a microwave discharge, the emission spectrum of the discharge being photographed at very high resolution. Bands appeared from 500 to 220 nm, with the most intense emissions occurring around 330 nm, where, unfortunately, the band heads were diffuse and a great deal of overlapping occurred. They were able to positively identify six separate electronic levels of PF from this work, four in a singlet system and two in a triplet system. No singlet-triplet transitions were observed, either in the cavity or in the afterglow.

The PF radical has twelve electrons. If d orbitals and partial ionic character (which probably would not interfere with the following order of energy levels) are ignored, and we assume a molecular orbital model, for its ground state configuration we would have the following molecular orbitals filled: $2s\sigma$, $2s\sigma^*$, $2p\sigma$, $2p\pi_x$, and $2p\pi_y$. These account for ten electrons. The last two electrons in the ground state would fill the degenerate anti-bonding $2p\pi_x^*$ and $2p\pi_y^*$ orbitals. According to multiplet theory, these two electrons in these two degenerate orbitals can occur in a $^3\Sigma^-$ state (the lowest-lying) or in a singlet state, $^1\Sigma^+$, where the two electrons would each occupy one of the π orbitals, or in a doubly degenerate singlet state, $^1\Delta$, where the two electrons would be both in one of the π orbitals. In the excited configuration, $2p\pi_x$, $2p\sigma^*$, there would exist a low-lying $^3\pi$ state and an excited $^1\pi$ state. All these five states were claimed to have been observed by Douglas. Also, he observed a very high energy $g^1\pi$

state, that might have been a Rydberg state, not specifiable by simple molecular orbital models.

Since the matrix environment quenches all molecules to their ground electronic states, the single transition that would be observed here is the triplet system, $B^3\pi_{0,1,2} \leftarrow X^3\Sigma^-$ (assuming singlet-triplet prohibition in the matrix). This will be the only transition referred to for the rest of this chapter.

The constants for the two states are as follows: $^3\Sigma^-$ has an ω_e of 846.75 K and the $^3\pi$ state has an approximate ω_e (actually a $\Delta G\ (v + \frac{1}{2})$ value) of 436 K. The ground $^3\Sigma$ state has no noticeable triplet splitting, but the $^3\pi$ state has a very large splitting of 142 K. This means that the difference between the π_0 and π_2 levels for each vibrational state is 284 K, a number that is close to the spacing between the vibrational states themselves (436 K). In the matrix, where the states are broadened in energy considerably, the absorption spectrum would probably give a smeared out, poorly resolved set of bands, as opposed to a regular, sharp progression of bands.

Douglas measured the rotational structures of the 0-1, 0-4, 0-5, 1-0 and 1-1 transitions fairly completely, but only reported two band heads: the 0-1 band at 28,500 K and the 1-0 band at 29,790 K (to the $^3\pi_0$ substate), and did not report the relative intensities of any of these bands. Since the ground state has a 1.59Å internuclear distance, while the triplet π has a 1.75Å internuclear distance, the Franck-Condon factors in absorption from the v"=0 level of the ground state would be expected to be greatest for fairly highly excited v' levels of the excited π state, so that the transitions around 4-0 would be expected to have the highest intensity. Such a transition would have a gas phase value of

about 31,050 K. Due to the matrix red shift for molecules, as well as the change in the potential well for the excited electronic vibrational levels, this maximum intensity peak would shift to about 30,000 K in xenon.

When P_2F_4 is passed by itself through the hot furnace onto the matrix in the PF_2 deposition, a pseudo band system is observed in the ultraviolet, with a maximum in the region of 29,800 K in a xenon matrix. This system does not form when the furnace is at room temperature and increases in intensity as the furnace temperature is raised in deposition. It does not correspond to any bands of PF_3, P_2F_4, PF_2I, nor P_2.[108] Neither can it be PF_2, for it photolyzes away quite rapidly, even upon back photolysis, while the infrared bands ascribed to PF_2 remain upon photolysis. The fact that the high intensity mercury arc can photolyze it away in seconds shows that it corresponds to a very small amount of material trapped in the matrix with a large extinction coefficient (and thus would explain why no large infrared bands were observed corresponding to this 29,800 K band).

The actual spectrum observed consisted of a series of about seven absorptions, that were not evenly spaced nor of equal intensity, impressed upon a much more intense continuum-like background. The frequencies and intensities of these absorptions in two different matrices are listed in Table XVII. From the smearing out of these absorptions, their position and intensity, and their mode of formation, it is quite clear that they belong to the PF diatomic molecule, trapped in the matrix at small concentrations. Also, the changes in frequency from one band to the other (Delta Frequency) vary in units of three. If we assume that the 30,248 to 29,223 bands in xenon correspond to the 31,173 to 30,089 bands in krypton, we obtain relative matrix shifts between xenon and krypton that decrease with decrease in frequency of the absorption, just as would be expected.

Table XVII. PF matrix ultraviolet absorption bands

Intensity	Wavelength (Å)[a]	Frequency (K)[b]	Delta Frequency
PF in Krypton			
vw	3423	29206	
			328
vw	3385	29534	
			299
m	3351	29833	
			256
vs	3322.5	30089	
			281
vs	3291.7	30370	
			273
ms	3262.4	30643	
			241
mw	3237	30884	
			289
vw	3207	31173	
PF in Xenon			
vw ?	3488	28662	
			561
mw	3421	29223	
			274
ms	3389.2	29497	
			267
vs	3358.6	29764	
			221
s	3334	29985	
			263
w	3305	30248	

Transitions are from the $X^3\Sigma^-$ state to the $B^3\pi_{0,1,2}$ states.

[a] Wavelength in air.

[b] Frequency corrected to vacuum by dividing by 1.000287 (approximate refractive index of air).

The experimental results on photolysis of PF in the matrix have been discussed on page 164. Suffice it to say here that PF does not photolyze away by absorption of the radiation it absorbs in this 30,000 K region, but rather by P_2F_4 in the matrix absorbing 270 nm radiation, which presumably weakens the P-P bond in it making it susceptible for PF insertion to form P_3F_5.

From Douglas's report we can calculate the expected v"=0 to v"=1 vibrational transition in the ground triplet state, using the formula $G(1) - G(0) = \omega_e - 2\omega_e X_e$. This comes to 837.8 K. Given a reasonable xenon matrix red shift of about 8 K, we would expect to observe a small infrared absorption at about 830 K in the matrix. Indeed, a very small 831 K peak has been observed in a xenon matrix in the PF_2 deposition that disappeared upon back photolysis of the matrix (while all other peaks remained the same) at the same time that the ultraviolet absorption spectrum for PF was seen to disappear.

Warmup experiments on PF matrices were done. PF did not disappear in a krypton matrix until the matrix was maintained at 55°K for four minutes. This would suggest that PF is quite an unreactive carbenoid.

Fluorescence experiments were tried taking great care to exclude all exciting radiation but that which corresponded to the most intense absorption of PF. The emission spectrum was observed from 330 to 400 nm, but no fluorescing radiation was ever detected other than light scattered from the mercury high pressure arc. No fluroescence studies on gas phase PF have ever been reported either.

A very intriguing result was obtained when P_2F_4 was premixed with a 200-fold excess of xenon and the mixture passed through the furnace at 550°C. In this case almost no P_2F_4 bands were observed in the matrix infrared

at all. Instead, PF_2 and PF_3 bands were observed, along with one other strong band at 831 K. If this band were due to PF, it would be forming here at much greater concentrations than it does when P_2F_4 is passed through the furnace by itself. Furthermore, passing a mixture of krypton and P_2F_4 ($Kr:P_2F_4$ = 17:1) through a 600°C furnace onto the matrix increased the intensity of the PF ultraviolet absorption greatly, as well as making it much more difficult to back-photolyze away with the mercury arc.

The formation of PF under these conditions would closely correspond to the conditions Douglas used to obtain his PF gas phase species, since he also used a large excess of inert gas (helium)to stabilize the PF formed in the microwave discharge. PF could possibly be stabilized in a large excess of inert gas through three distinct processes: one, it could be quenched by the inert gas from an excited state, that is very reactive and/or unstable, very quickly after it forms from P_2F_4 fission; two, it could be "isolated" from other species such as PF_3 with which it could react; and three, the P_2F_4 would suffer many more collisions with hot rare gas atoms in these experiments, because of the high pressure, than it would with the hot walls in the experiment without rare gas passing through the furnace, and so could be raised to an appropriate temperature for heterolytic fission (550°C) without going so high (around 800°C) to cause further decomposition.

If PF is indeed forming under these conditions in large quantities, a photolysis of its matrix would not destroy all the PF since the amount of P_2F_4 in the matrix would be lessthan the amount of PF, and this seemed to be the case for the krypton experiment. Removing all the P_2F_4 by photolysis might show up PF bands that were hidden by the P_2F_4 absorption. Also, singlet-triplet transitions or fluorescence might be observed, under these conditions of high concentrations of PF.

S. General Interpretation -- the Radicals in the Furnace and the Reactions at the Cold Surface

Quite a bit of the evidence I have obtained points to the existence of radicals in the pyrolysis of P_2F_4, especially at high temperatures. It seems these radicals reach the cold surface in the reaction vessel and react there as they condense.

Some evidence comes from cocondensation results. It is highly unlikely that the unstable compounds formed could ever have existed in the hot zone itself. So they must have formed beyond the hot zone at the cold 77°K surface, either upon condensation or upon pump off. Furthermore, if the condensation of the products of the furnace was not done immediately beyond the furnace, no unstable products were formed. This shows that the high temperature species responsible for the reactions decompose or recombine readily at lower temperatures in the gas phase. Finally, cocondensation reactions were definitely observed for PH_3 and GeH_4. In these reactions, the pressure was so low and the geometry of the cocondensate sprayer was of such a nature that gas phase reactions could be ruled out. Thus the reactions took place on the cold surface, and only low-valent, reactive species would react at these low temperatures.

Passing phosphorus plus phosphorus trifluoride through a very hot furnace probably also produces a high temperature species. The evidence for this comes from the cocondensation reaction of the product of this high temperature reaction and P_2F_4 (sprayed from the cocondensate arm), which did produce a small amount of P_4F_6. Unfortunately, the understanding of this reaction is hindered greatly by the reaction of superheated phosphorus and SiO_2.

Matrix isolation spectroscopy on the products formed in the P_2F_4 pyrolysis gave more direct and conclusive evidence for the existence of radicals in this pyrolysis. Pressures were so low in the furnace in this case, however (using Dushman's equations they were calculated to be several millitorr), that only the qualitative features observed here, concerning the kinds of species detected, could be extrapolated to the much higher pressure P_2F_4 pyrolysis in cocondensation reactions.

The JANAF tables of thermodynamic properties[109] list the following gaseous phosphorus-fluorine species: P, P_2, P_4, F, F_2, PF, PF_2, PF_3, and PF_5. They do not mention P_2F_4. I have added one other possible species to this list: P_2F_2. From the existing chemical evidence and mass and ultraviolet spectra on the phosphorus-fluorine system and related systems, it can be predicted that no other species would be important here. The question arises which of these species forms and reacts under the conditions of the experiments described in this dissertation.

The evidence for PF_3 forming is conclusive, along with some of the original P_2F_4, which might not be exiting from the furnace as such in the higher pressure cracking, but which nevertheless is always recovered to some extent in the pump out.

The evidence for PF_2 forming is also conclusive, coming from chemical analogy with N_2F_4 and NF_2, mass spectroscopy, epr spectroscopy and matrix isolation spectroscopy. However, it is unlikely that low concentrations of PF_2 can effect a cocondensation reaction on the cold surface by themselves. Matrix isolation studies show that moderate furnace temperatures (about 500°C) do produce a considerable amount of PF_2 from P_2F_4, yet cocondensation of the radicals coming from such a furnace with PH_3 produces no reaction, nor does a moderate furnace temperature produce much P_4F_6

without cocondensate, as the high temperature cracking does. Also, PF_2 seems to have a very high stability in the matrix phase and remains in the matrix up to very high temperatures. Finally, on the basis of bond energy considerations, PF_2 would not be expected to be capable of abstracting fluorine from another P-F species, and, in general, would just react with other doublets in a recombination reaction. This fact is not deducible from the ineffectiveness of PF_2 to abstract fluorine in the cases of C_2F_4 and B_2F_4, since the C-F and B-F bonds are much stronger than the P-F bond. Although it is unlikely that PF_2 is the sole reactant in these cocondensation reactions, it might have something to do with the reactions observed.

The evidence for PF forming is almost as conclusive as that for PF_2, and it appears that PF is one of the main reactants at the cold surface. Stoichiometrically, one would expect its formation both because PF_3 is observed coming out of the furnace, and because, at room temperature, P_2F_4 decomposes to PF_3 and PF polymers. The most intense portion of the gas phase ultraviolet spectrum of PF, observed in emission, corresponds very nicely with the absorption spectrum of pyrolyzed P_2F_4 seen in the matrix. Finally, a small infrared matrix absorption is noted at just the frequency one would expect for the PF stretch, and correlates with the ultraviolet absorption mentioned above. This infrared absorption increases greatly when P_2F_4 plus a large excess of inert gas are passed through the furnace together, a condition that might be expected to stabilize PF in the gas phase. N_2F_4 is different from P_2F_4 in that it does not heterolytically fission to NF radicals at high temperatures, and this difference could be due to its weaker N-N bond.

There are some analogies between this system and the BF radical work of Timms.[2] In Timms' BF cocondensation work, a higher yield of B_3F_5

and B_8F_{12} was noted when B_2F_4 was cocondensed with the BF radical, just as I noted a larger yield of P_4F_6 (and perhaps P_3F_5) when P_2F_4 was cocondensed with the species exiting from the furnace. B_3F_5 was formed first in this reaction, and was then converted to B_8F_{12} upon standing for several hours at -50°C. Here it is possible that P_3F_5 could be forming along with the P_4F_6. Finally, B_8F_{12} is believed to be the dimer of $B(BF_2)_3$ from x-ray analysis of $B_4F_6 \cdot PF_3$,[110] and so is structurally related to P_4F_6.

Since a very small amount of white phosphorus was always noted in the pump out after each reaction, another species that might be reacting in the cocondensation reactions is P_2. However, when this idea was tested by adding a large excess of P_4 vapor to P_2F_4 just above the furnace entrance, no change in the yield of products was noted. Probably, neither P_4 nor P_2 are reactants in the furnace nor at the cold surface.

The question arises of how P_4F_6 is being formed in the solid during or after condensation. P_2F_2 can be ruled out as a reactant since it was never observed, and since P_2 has just been ruled out as a possible reactant, the only two radical reactants left that could possibly be precursors to P_4F_6 formation are PF_2 and PF. It is likely that both these radicals participate in the formation of P_4F_6.

The yields of P_4F_6 increase with increasing furnace temperature, and from matrix isolation we know that these higher furnace temperatures do produce more PF. P_2F_4 plus a five-fold excess of xenon passed together through the furnace of the reaction vessel did increase the yields of P_4F_6, and these conditions are believed to stabilize PF. The fact that the $P + PF_3$ high temperature reaction produced a small amount of P_4F_6 upon cocondensation with unheated P_2F_4, and the fact that this high temperature

reaction is known not to produce any PF_2 whatsoever (from the absence of P_2F_4 in the pump out), would again add weight to the contention that a PF species is the reactant at the cold surface (and that, in this case, it is forming by reduction of PF_3 with P_2 in the furnace). Finally, in the matrix phase photolysis of PF in a P_2F_4 matrix, PF inserts into a weakened P-P bond in P_2F_4 to form P_3F_5, a reaction that could be a preliminary to P_4F_6 formation in a cocondensation reaction.

One simple set of reactions to explain both P_3F_5 and P_4F_6 formation in the cocondensation reaction follows:

$$PF_2 + PF_2 \rightarrow P_2F_4^* \quad \text{(where "*" means excited)}$$
$$PF + P_2F_4^* \rightarrow P_3F_5$$
$$PF + P_3F_5 \rightarrow P_4F_6$$

In this set of reactions, the PF_2 radicals merely act as sources of energy to excite the resultant P_2F_4 molecule making it amenable to an insertion reaction by the carbenoid, PF. Thus, PF only inserts into an excited molecule like $P_2F_4^*$, or a highly reactive one like P_3F_5, and is otherwise unreactive. This scheme is also plausible on the grounds that PF insertion might take some time, because it is a triplet insertion, during which a second PF could insert into the P_3F_5 forming.

Another set of reactions would involve the active chemical participation of the PF_2 species:

$$P_2F_4 + PF_2 \rightarrow PF_3 + P_2F_3 \text{ or } PF + PF_2 \rightarrow P_2F_3$$
$$PF_2 + P_2F_3 \rightarrow P_3F_5$$
$$P_2F_3 + P_2F_3 \rightarrow P_4F_6$$

Since no evidence for the P_2F_3 radical was obtained from the matrix

isolation studies, this latter set of reactions is less likely. Notice that the first schema of reactions would most probably take place in the LLIT state of matter, while this is not necessary for the second schema.

There is quite a bit of evidence to suggest that the very unstable material that forms with the P_4F_6 in the cracking and immediate low temperature condensation of P_2F_4, is P_3F_5 (besides the analogy with Timms' work as mentioned above). The yield of this material correlates well with the yield of P_4F_6, so that the former could form from the same general reactions (as those above) that produced P_4F_6. The photolysis results also agree with the existence of P_3F_5. The unstable material formed decomposes completely in three or four transferrals around the vacuum system, but only upon condensation, not in the gas phase (as does P_4F_6). Callen and Fehlner[111] state that the characteristic instability of compounds such as P_2H_2, P_2H_4 and P_3H_5 is not due to weak phosphorus-phosphorus bonds in the chain, but to the extremely facile condensation reactions which they undergo, reactions that would be promoted in the condensed phase (see page 167). The decomposition of this unknown material is indeed promoted in the condensed phase. The polymers formed from the decomposition of this unstable material have been shown by analysis to have little fluorine present. These same authors state that the above-mentioned compounds decompose to form phosphorus-rich polymers, such as P_9H_2. So perhaps just two new compounds are forming in this cocondensation reaction, P_3F_5 and P_4F_6.

P_3F_5 formed from the photolysis of P_2F_4 in the matrix does not decompose upon warmup in the matrix to form P_4F_6. Therefore, it is unlikely that the P_3F_5 formed from any of the radical reactions mentioned above acts as a simple precursor to P_4F_6 upon warmup of the cocondensate in the reaction vessel after the deposition is completed. Of course, the actual set of reactions taking place upon warmup of the cocondensate

could be much more complicated than the radical reactions outlined above.

T. Thermodynamic Calculations on the Phosphorus-Fluorine System

Thermodynamic calculations on the high temperature phosphorus-fluorine system were performed to see how the expected equilibrium concentrations compare with the actual species observed reacting in cocondensation reactions and isolated and identified through matrix isolation spectroscopy.

In order to do this, four main sources of thermodynamic data were looked into: the JANAF values, a Russian compilation,[112] an Argonne National Laboratory report,[113] and my own estimates. The JANAF, Russian and Argonne data themselves come from estimates, and such experimental observations as heats of reaction, heat capacities from absolute zero, vapor pressures, spectroscopic determinations of energy levels and dissociation limits, electron or x-ray diffraction, kinetic data and others. It was found that the values given in the JANAF tables were superior to those given in the Russian tables for the phosphorus-fluorine species mentioned above. The JANAF data were also accepted for PF and P, though in these two instances there was disagreement with the Argonne values. My own estimates were based on extrapolations from the known data of other substances that might be related to the unknown species in question, as well as comparisons with the Argonne values for PF_2 and P_2F_4. Known bond energies, heats of formation, bond distances and angles, and fundamental frequencies for NF_2, NH_2, NF_3, NH_3, PF_3, PH_3, N_2F_2, N_2H_2, P_2H_2, N_2F_4, P_2H_4 and others were used to estimate the data for PF_2, P_2F_2 and P_2F_4.

The goal in any thermodynamic calculation to obtain equilibrium concentrations is to find, at a particular temperature, the free energy

of formation, from the elements in their standard states, of the compounds in question ($\Delta F^\circ_{f_T}$). From these values, by simple addition and subtraction, we obtain the free energy of reaction, ΔF°_T, for all the equilibrium reactions at that temperature. Using $\Delta F^\circ_T = -RT\ln K_p$ [Eq. (19) on page 46], where K_p is the equilibrium constant for the reaction expressed as a product of pressures (in atmospheres) of the species involved, we can derive the equilibrium constant for each reaction and hence the concentrations of the various species involved.

A computer program, ECOM ("entropy calculation" -- see Appendix D for the program listing), was written to use the equations on page 47 to obtain two numbers: the third law absolute entropy and the enthalpy content difference from 298.1°K, for any gaseous substance. The third law entropy of a gas is approximately the sum of its translational, rotational and vibrational components. This program computes the translational entropy from the molecular weight of the substance (MW); the rotational entropy from the product of the principal moments of inertia of the molecule (D) that is calculated beforehand from the bond lengths and angles of the molecule, and from a combination rotational symmetry factor plus electronic degeneracy of the ground state factor (S) that increases as the rotational symmetry increases and decreases as the electronic degeneracy increases; and the vibrational entropy from the normal frequencies of the molecule in question (W(J)). The units of the variables fed in are as follows: T in °K, D in units of 10^{-117} g^3cm^6, MW in amu, and the W(J) in Kaysers. The program prints out some of the separate contributions to the entropy and the enthalpy content difference as well as the total values.

To obtain the actual enthalpy of formation at T, one first estimates its value at 298.1°K. Then, using the change in the enthalpy content from

298° to T for the elements in their standard states (obtained from the JANAF tables), and for the compound in question (obtained from ECOM), one can calculate its enthalpy (or heat) of formation at T. The entropy of formation at T can be simple calculated by subtracting the absolute entropies of the elements in their standard states (obtained from the JANAF tables) from the absolute entropy of the compound that is composed of them (obtained from ECOM). Then using $\Delta F_f^\circ = \Delta H_f^\circ - T\Delta S_f^\circ$ (Eq. 18), we can derive the free energy of formation of the compound at the temperature T (see Appendix E), and from this value, as noted before, we obtain the equilibrium concentrations of all species involved.

Table XVIII lists some estimated and derived thermodynamic variables for PF_2, P_2F_2, P_2F_4 and PF_3. P_2F_2 and P_2F_4 are not listed at all in the JANAF tables, and the values for PF_2 are different from the JANAF values (the JANAF frequencies are approximated, while those listed here are those observed).

The enthalpy of formation of PF_3 was taken from more recent calorimetric determinations, which have thrown the JANAF data for this compound into serious doubt. Duus and Mykytiuk[114] experimentally found the heat of reaction at 298°K for, $PCl_3(g) + 3/2\ CaF_2(s) \rightarrow PF_3(g) + 3/2\ CaCl_2(s)$ to be -2.36 kcal/mole PCl_3. They did not check, using x-ray diffraction, whether the "CaF_2" formed in this reaction contained any CaFCl or not. From this value, using the thermodynamic data found in the Handbook of Chemistry and Physics, they calculated a ΔH_f° for PF_3 of -221.9 kcal/mole (corrected for the red, V modification of phosphorus as the standard state). Using their heat of reaction, but more accurate values for CaF_2 and $CaCl_2$ from the JANAF tables,[109] and for PCl_3 from NBS Technical Note 270-3,[115] I calculated the ΔH_f° of PF_3 to be -219.3 kcal/mole at 298°K, quite far

Table XVIII. Thermodynamic variables for PF_2, P_2F_2, P_2F_4 and PF_3 [a]

	PF_2 [c]			P_2F_2 [c]			P_2F_4 [c]			PF_3 [d]		
	298.1°	1100°	1200°	298.1°	1100°	1200°	298.1°	1100°	1200°	298.1°	1100°	1200°
absolute entropy (cal)	62.83	79.06	80.24	68.71	91.27	92.94	79.65	115.65	118.33	65.15	87.58	89.25
enthalpy[b] content at T°K (kcal)	0	10.20	11.55	0	14.25	16.17	0	22.79	25.87	0	14.20	16.11
entropy of formation (cal)	-8.95	-11.76	-11.75	-9.36	-31.07	-30.95	-28.14	-65.99	-65.65	-12.98	-32.98	-32.75
enthalpy of formation (kcal)	-114* (JANAF = -105)	-135.3	-135.3	-100*	-142.0	-141.9	-257*	-297.3	-296.9	-224 (JANAF = -212)	-244.7	-244.6
free energy of formation (kcal)	-111.33	-122.4	-121.2	-97.2	-107.9	-104.8	-248.6	-224.7	-218.1	-220.1	-208.5	-205.3
normal frequencies (Kaysers)	850, 325 and 830 (JANAF = 775, 376 & 890)			845*, 1025*, 450*, 810*, 320* & 155*			843, 831, 825, 803, 541, 453, 377, 365, 361, 214, 200* & 120*			892, 487, 860 (2) and 344 (2)		
symmetries, angles, and distances	C_{2v}, planar, F-P-F = 96°*, P-F = 1.55Å*			C_{2h}, planar, P=P-F = 125°*, P-F = 1.53Å*, P=P = 1.96 Å*			C_{2h}, trans, F-P-F = 104°*, P-P-F = 100°*, P-F = 1.54Å*, P-P = 2.08Å*			C_{3v}, pyramidal, F-P-F = 98°12', P-F = 1.537Å		
D value. (10^{-117} g^3cm^6)	291.33 (JANAF = 191)			4068.7			159, 425.3			1838.37		

(a) For phosphorus, crystalline red phosphorus is the standard state up to 704°K, and beyond, P_2 ideal gas at one atmosphere is the standard state. F_2 ideal gas at one atmosphere is the standard state for fluorine at all temperatures. All numbers calculated by adding machine and ECOM.

(b) From 298.1°K, at which the enthalpy content is optionally assigned to be zero.

(c) My estimated values. * = indicates estimated value by extrapolation of values of known similar variables for other related materials.

(d) JANAF values.

away from the JANAF value of -212 kcal/mole. Still more recently, E. H. Van Deventer, E. Rudzitis and W. N. Hubbard burned PF_3 in fluorine using the method of fluorine bomb calorimetry. They obtained a ΔH_f° for PF_3 of -224.6 kcal/mole (corrected to the red, V modification of phosphorus as the standard state).[116] Since their work in the past, using fluorine bomb calorimetry, has been very successful (they measured the enthalpy of formation of PF_5 to be -380.8 ± 0.3 kcal/mole,[117] while the JANAF tables list an earlier determination as -381.4 ± 0.4 kcal/mole), the value I have used here for PF_3 is close to theirs, -224 kcal/mole.

None of the species in the cracking of P_2F_4 was expected to have low-lying excited electronic states that would influence the thermodynamic data at temperatures around 1200°K. The doublet ground state of PF_2 and the triplet ground state of PF were taken into account in the calculation of their entropy. The standard state for phosphorus was taken as the crystalline, red, V form below 704°K, and P_2 ideal gas at one atmosphere fugacity from 704°K to 6000°K. This change in standard state for phosphorus accounts for the sharp break in energies of formation of the phosphorus-containing species between 298°K and 1100°K.

Using the data in Table XVIII, along with JANAF data, some equilibrium concentration calculations were done with respect to a select few of all the possible reactions among the P-F species listed on page 187 (a sample of these calculations is shown in Appendix E). Table XIX lists the results of three sets of such calculations assuming an equilibrium between P_2F_4 and PF_2 only, P_2F_4, PF_3 and PF only, or PF_2, PF_3 and PF only, respectively, along with the equilibrium constants used to obtain these results. We can see from this table that the data predict that the relative driving forces for the two types of P_2F_4 fission should be about equal, and that both of them are quite large at elevated temperatures.

Table XIX. Equilibrium concentrations of phosphorus-fluorine species at 1100°K and 1200°K with respect to three selected reactions[a]

	$P_2F_4 \rightleftharpoons 2\ PF_2$			$P_2F_4 \rightleftharpoons PF + PF_3$			$2\ PF_2 \rightleftharpoons PF + PF_3$		
	298.1°K	1100°K	1200°K	298.1°K	1100°K	1200°K	298.1°K	1100°K	1200°K
K_p	8.69×10^{-20}	9864	26680	4.45×10^{-6}	35516	73010	5.12×10^{13}	3.6007	2.7362
Gaseous Substance[b]									
P_2F_4	2.0	5.34×10^{-7}	1.97×10^{-7}	1.835	3.7×10^{-8}	1.8×10^{-8}	-	-	-
PF_2	1.15×10^{-8}	2.0	2.0	-	-	-	1.4×10^{-7}	0.417	0.4642
PF	-	-	-	0.0787	1.0	1.0	1.0	0.791	0.768
PF_3	-	-	-	0.0787	1.0	1.0	1.0	0.791	0.768

[a] Assuming a total pressure of about 2.00 torr and a fluorine/phosphorus ratio of about 2.00.

[b] Values listed here are the concentrations of these species in partial pressures of torr. These numbers would only take on physical significance if all other reactions possible at the temperatures in question were kinetically hindered. This assumption is quite untenable at 298°K for the PF species, which would polymerize readily at these temperatures.

The values in Table XIX do not yield the equilibrium concentrations of P-F species relative to the elements. To obtain these, a computer program was developed called PFIT (standing for "phosphorus-fluorine iteration"), which is listed in Appendix D. It was used to calculate equilibrium concentrations of PF_3, PF_2, PF, F, P, P_2, P_4 and P_2F_2 at high temperatures in the gas phase. The program will not give any values for a non-equilibrium situation, nor can it take into account any reaction of the species mentioned with the containing walls. It assumes that no solids or liquids are entering into the equilibrium, and that molecular F_2, P_2F_4 and PF_5 are not present to any appreciable extent so that they can be ignored.*

The units of the variables used in the program are as follows: ΔF values in kcal/mole, concentrations in partial pressures of torr, temperatures in degrees Kelvin and logarithms to the base 10. The following equilibrium reactions are taken for the gaseous phosphorus-fluorine system:

$$8\ PF_3 + P_4 \leftrightharpoons 12\ PF_2 \qquad P_2 \leftrightharpoons 2\ P$$

$$2\ PF_2 \leftrightharpoons PF_3 + PF \qquad PF \leftrightharpoons P + F$$

$$P_4 \leftrightharpoons 2P_2 \qquad 2\ PF \leftrightharpoons P_2F_2$$

---

* Fluorine, in any form, will not form until very high temperatures, at which it would be dissociated into F atoms; it is presumed that all the P_2F_4 put into the furnace, will be dissociated at equilibrium; and no PF_5 was every observed in the products after P_2F_4 was passed through the furnace.

(Notice that there are other sets of reactions equivalent to these six, but they conveniently stoichiometrically relate every species to every other species, and were the ones used in the calculations of the program.)

The input to the program consists of: initial concentrations (guesses) of PF_3 (CPF3) and P_4 (CP4), for the purpose of providing values for the program's first iteration to work on; the molar fluorine/phosphorus ratio (FPRAT); the total pressure of all the species together (TOTP); the temperature of the system (T); the log K_p values for each of the species in question (LK(J)), which are obtained from the JANAF tables or my own estimates, and which are printed out by the program along with the free energies of formation (DFF(J)) they correspond to (obtained from $\Delta F^\circ_T = -2.303\ RT\log K_p$); and finally, the uncertainties in the $\log K_p$ values (U(J)) for each of the species, if a print out of three different sets of equilibrium concentrations is desired corresponding to the addition or subtraction of these uncertainties from the $\log K_p$ values. (If only one set of concentrations is required, this card is left blank.)

Briefly, the program operates in the following manner. Given the stoichiometric relationships for interconversion of the various species into one another, given the equilibrium constants, K_p, for each of these reactants, and given the initial concentrations of just two of the reactants, PF_3 and P_4, the program completes one iteration by calculating the equilibrium concentrations of all the species involved in the equilibrium. It then checks to see if the results compare within a specified limit to the desired P/F ratio and total pressure. If not, it changes the concentrations of PF_3 and P_4 accordingly and performs another iteration, constantly going on like this, checking also to see if its iterations

are converging towards a limit and correcting the concentrations if they are not. Several print outs occur after a given number of iterations, and if the correct values have not been arrived at after 150 iterations, the final values are printed whether they are within the limits designated or not. The results are shown in Table XX.

This table shows that, given the most probable values for the free energies of formation, mostly PF_3 and P_2 or P_4 will exist at 1100°-1200°K. However, within the range of the uncertainties involved, PF_2 could be a very important equilibrium species at these temperatures, or at slightly higher temperatures, though no PF_2 formed when P_2 and PF_3 were passed through the furnace together. Even if PF_2 is at low concentrations at equilibrium under these conditions, it probably will not have a great thermodynamic driving force for its decomposition, so that a slight kinetic barrier to this decomposition could insure a very large concentration of PF_2 from the homolytic fission of the P-P bond in P_2F_4.

On the other hand, this table clearly shows that, under conditions of equilibrium at 1200°K or lower, the highest possible concentration of PF, given our lack of knowledge, is less than one tenth of one percent. (Notice that the PF and PF_2 concentrations rise with temperature, and it was noted that a higher yield of P_4F_6 resulted when the furnace temperature was raised.) Yet PF production is believed to be one of the main requirements for the observed cocondensation reactions to take place. This would suggest, therefore, that the production of PF was being carried out in this cracking in a non-equilibrium situation with respect to elemental phosphorus and PF_3.

Many other facts are consistent with the hypothesis that the source of PF here is a heterolytic fission of the P-P bond in P_2F_4. First of

Table XX. Equilibrium concentrations of phosphorus-fluorine species at 1100° and 1200°K

Gaseous substance	Free Energy of Formation [a] (kcal/mole) 298.1°K [c]	1100°K [d]	1200°K [d]	Equilibrium Concentrations [b] (torr) 298.1°K [e]	1100°K [f]	1200°K [f]
PF_3	-220.1 ± 1	-208.5	-205.3	1.796	1.683 1.679 1.364	1.639 1.635 1.14
PF_2	-111.3 ± 18	-122.4 ± 12	-121.2 ± 12	0	0.368 0.0017 10^{-5}	0.592 0.0049 10^{-5}
PF	-21.18 ± 3	-39.13 ± 3	-39.47 ± 3	0	10^{-5} 10^{-5} 10^{-6}	0.000151 10^{-5} 10^{-5}
F	+14.78	+3.01	+1.50	0	10^{-12}	10^{-11}
P	+69.80	+43.69	+42.29	10^{-46}	10^{-8}	10^{-7}
P_2	+30.39 ± 0.5	0.00 ± 0.5	0.00 ± 0.5	10^{-15}	0.261	0.353
P_4	+17.33 ± 0.5	-14.47±0.5	-10.96 ± 0.5	0.2132	0.0674	0.0163
P_2F_2	-97.2 ± 18	-107.9 ± 13	-104.8 ± 13	0	10^{-5} 10^{-8} 10^{-11}	10^{-5} 10^{-7} 10^{-10}

Table XX (Continued)

[a] Relative to standard states of F_2 ideal gas, and crystalline red phosphorus V below 704°K, and P_2 ideal gas above 704°K. Values obtained from the JANAF tables and my own estimations.

[b] Assume a total pressure of about 2.00 torr and a fluorine/phosphorus ratio of about 2.00. Concentrations are in partial pressures, and calculated by the PFIT program.

[c] These are the actual full uncertainties appended to the free energy values.

[d] Notice that in some cases, the uncertainties used were smaller than the actual full uncertainties. These uncertainties were used to calculate the limits of the concentrations shown in the 1100°K and 1200°K columns to the right.

[e] The values listed here do not consider solid forms of phosphorus and phosphorus-fluorine polymers, as well as F_2 gas and perhaps P_2F_4, that all might contribute to the equilibria at this temperature.

[f] The middle value given for a particular compound is simply the concentration calculated from the best value for the free energy of formation. The upper limit of the concentration is obtained by taking the lower value of ΔF for the compound in question plus the higher values for the ΔF's of all the other compounds, and deriving a set of concentrations for these ΔF's, and conversely for the lower limit of the concentration.

all, the yield of PF is observed to rise, as evidenced by P_4F_6 formation and the increase in intensity of the matrix infrared and ultraviolet absorption of PF, when a large excess of inert gas is passed through the furnace with the P_2F_4. If PF were thermodynamically unstable under the conditions of its formation, then an inert gas could stabilize it by the processes mentioned on page 185. According to the results listed in Table XX, elemental phosphorus species should be very important at equilibrium at the temperatures worked with, yet no such species were ever noted in any great quantity as evidenced by the very small amount of P_4 resulting after warmup. Finally, adding P_4 vapor to the P_2F_4 just before it enters the furnace does not seem to have any effect on the products formed, yet one would expect, if equilibrium existed, that this large excess of P_4 (or P_2) would shift the equilibrium over to a completely different set of concentrations, which would, in turn, affect the final cocondensation results. So it seems that most of the PF formed is produced from the direct heterolytic fission of P_2F_4.

Though P_2F_2 would be highly unlikely to form under equilibrium with respect to the elements, it can be readily calculated, using the data for P_2F_2 and PF in Table XX, that P_2F_2 would be thermodynamically favored at 1100°K and 2 torr total pressure in equilibrium with respect to PF. However, no matrix spectroscopic evidence was noted for its formation in the furnace or from the dimerization of PF in the matrix upon warmup.

U. Possible Future Work on the P_2F_4 Cracking

Without a doubt, a great deal more experimental work could be done on the phosphorus-fluorine system, utilizing the cracking of P_2F_4.

Of course, the chemistry of P_4F_6 can be investigated further, especially the nature of its solution in carbon disulphide. Its matrix infrared spectrum also needs further verification and analysis.

The matrix containing PF and PF_2 could be looked into further, especially with regards to the fluorescence spectrum of the excited triplet state of PF, and the possible weak absorption transition of ground state PF to an excited singlet state, thereby obtaining the exact triplet-singlet energy difference for the low-lying triplet and singlet states, which would lend insight to the validity of molecular orbital calculations. The ultraviolet absorption spectrum of PF_2 definitely needs further investigation, perhaps by looking into the shorter wavelength portion of the spectrum.

There exist a great many synthetic possibilities with the concentrated PF matrix (formed from the cracking of P_2F_4 premixed with a large excess of inert gas). A third, normally unreactive species could be cocondensed on the matrix along with the PF and inert gas, and the chemical reactions upon warmup followed using infrared or ultraviolet absorption spectroscopy.

The photolysis of P_2F_4 is still a mystery, in that the explanation of a mobile, excited state of P_2F_4 diffusing through the matrix upon photolysis is very unusual, and might not be the entire exposition of the cause of the phenomena observed. For instance, exactly <u>which</u> excited state of P_2F_4 is reacting? Possibly a photolysis of a dilute P_2F_4 matrix with shorter wavelength radiation could give more readily

understandable results. Also, the possibility of fluorescence occurring in the P_2F_4 photolysis from an excited triplet state of P_2F_4 has not been looked into.

ACKNOWLEDGEMENTS

Having a superficial acquaintance with basic principles is one thing, but knowing how to apply them to specific problems you come up against, thereby translating them into practice, is another. The author received much help from several of the professors in the Chemistry Department at the University of California at Berkeley in going from the former to the latter. I would especially like to extend my appreciation to the following individuals who gave of their time to discuss areas of my research that they had expert knowledge in: Professor R. J. Myers, Professor G. C. Pimentel and Professor K. Raymond.

The two research directors I have had, Dr. Peter L. Timms and more recently, Professor Leo Brewer, have done their jobs in that respect eminently well, and this dissertation would not have been possible without their patient guidance. I owe a special debt of gratitude to Professor Brewer for taking several hours every week to organize and run a seminar for his graduate students. Lawrence Bragg once said that the best way to learn a topic is to promise to give a lecture on it, and I have found this method quite valuable in utilizing these seminars to teach myself as well as my fellow researchers. And of course, the help I received from the other members of Professor Brewer's group (especially Mr. Joel Tellinghuisen), both in and out of seminars, stimulated both my research and thinking on chemical matters.

This work was financed partially by the Army Research Office at Durham and partially by the United States Atomic Energy Commission. The support of a fellowship from the National Science Foundation is acknowledged.

A P P E N D I C E S

APPENDIX A

Sample Calculation - The Oscillator Strength (or f Value) of an Absorption Transition

Light of radiance I°_{ω} falls on a cell in which is a gas that undergoes an $n \leftarrow m$ transition throughout a range of frequencies, ω, and light of radiance I_{ω} comes out of the cell, where I°_{ω} can be considered a constant for all ω's (and so we shall hereafter call it I°), but I_{ω} is a function of ω. If we let I stand for the radiance of a small enough increment of frequency of the light going through the cell, we may write:

$$I_{\omega} = I^{\circ} e^{-k(\omega)l(n/V)} \tag{29}$$

where, $k(\omega)$ = extinction coefficient as a function of ω; l = length of the cell; and n/V = molar density of gas present in the cell.

The ultraviolet spectrophotometer used yields a value for absorbance equal to $A(\omega) = \log(I^{\circ}/I_{\omega})$, so that $A(\omega) = \frac{k(\omega)l(n/V)}{2.303}$, and combining this with (29), we have,

$$I_{\omega} = I^{\circ} e^{-2.303A(\omega)} \tag{30}$$

We now let $I^{nm}_{abs} = \int (I^{\circ} - I_{\omega})d\omega$, which is equal to the total radiance of the light absorbed by the transition in question. Thus, combining this with (30), we have,

$$I^{nm}_{abs} = \int I^{\circ}(1 - e^{-2.303A(\omega)})d\omega \tag{31}$$

But, we also know from Einstein's relationships [45] that,

$$I^{nm}_{abs} = I^{\circ} N_m B_{mn} h\omega_{nm} l \tag{32}$$

where, N_m = number of (m) molecules per cm^3 = $(n/V)L(1/1000)$, where

L = Avogadro's number; B_{mn} = Einstein transition probability of absorption; h = Planck's constant; ω_{nm} = frequency absorbed; and l = length of the cell (in cm), as before. This equation is only exact for a single rotational transition. Since different rotational-vibrational transitions will have different N_m and B_{mn} values, the application of this equation to a spread of frequencies can only be simply done by assuming the vibrational-rotational sum rules work, that is, that the sum of the B_{mn} values for all the rotational transitions of each vibrational transition are the same, and so are additive. Using this simplification, we can accept Eq. (32) as valid for what follows.

We also have,

$$f^{nm} = \frac{m_e h c^2 \omega_{nm}}{\pi q_e^2} B_{mn} \qquad (33)$$

where, f^{nm} = oscillator strength for the $n \leftarrow m$ transition, m_e = mass of the electron; c = speed of light in vacuo; and q_e = charge on the electron.

So, from (32) and (33), we have,

$$f^{nm} = \frac{m_e c^2 1000}{\pi q_e^2 (n/V) L l} I^{nm}_{abs}/I^{\circ} \qquad (34)$$

Substituting, $m_e = 9.109\times10^{-28}$; $c = 3\times10^{10}$; $\pi = 3.1416$; $q_e = 4.806\times10^{-10}$; $L = 6.0225\times10^{23}$; $l = 9.53$ cm (for the cell used); and $n/V = P/RT$, where P = 0.1085 torr and T = 300°K (these values pertain to the 260.6 nm gas phase absorption of P_2F_4 shown in Fig. 15), and including Eq. (31), we have,

$$f^{nm} = 3.392\times10^{-5} \times \int (1-e^{-2.303A(\omega)})d\omega \qquad (35)$$

From the actual curve plotted out by the ultraviolet spectrophotometer, we can derive the above integral. What is done is an approximation of

the absorbance integral by an isosceles triangle, a figure whose outline can be readily graphed and integrated as a linear function of ω. Specifically, using the curve for the 260.6 nm absorption of P_2F_4 in the gaseous state (at a total absorbance far above the linear curve of growth -- near 1.1 -- and so this calculation will not yield a true f value) shown in Fig. 15, we can derive the following equation for $A(\omega)$:

$$A(\omega) = 21.866 - 0.00053658\omega \text{ for } \omega \text{ between } 40,750 \text{ and } 38,700 \qquad (36)$$

This will give half the contribution to f, which can then be doubled to yield the actual f value. Using an exact calculation, we have,

$$f^{nm} = 3.392\times10^{-5} \times 2.00 \times \int_{38700}^{40750} [1-e^{-2.303(21.866-5.3658\times10^{-4}\omega)}]d\omega \qquad (37)$$

and f^{nm} comes out to be 0.0887.

APPENDIX B

1. Dushman's Equations of Flow for Fluids

The flow of fluids down uniform tubes can be qualitatively predicted from the tenets of kinetic molecular theory. The formulas are derived in Saul Dushman's book[60] and are here reproduced in limited form.

The equations for fluid flow down a cylindrical tube make use of the following variables:

P = average pressure along length of tube

P_2 and P_1 = entrance and exit pressures respectively

T = temperature

a and l = radius and length of the tube respectively

dV/dt and dn/dt = rate of flow of gas in units of volume or moles, respectively, per unit time

F_t and F_v = molecular and viscous flow conductance respectively = $(P(dV/dt))/(P_2-P_1)$

σ = collision cross section of the molecules of the gas

M = molecular weight of the molecules of the gas

v_a = average velocity of the molecules of the gas = $\sqrt{(8RT)/(\pi M)}$

L = Avogadro's number = 6.025×10^{23} molecules/mole

R = the gas constant = 8.317×10^7 dyne cm/mole °K and = 62,400 torr cc/mole °K

η = the viscosity of the fluid = $\dfrac{3RT}{2.355\sqrt{2}\, L\pi\sigma^2 v_a}$

For molecular flow, where collisions with the wall are much more frequent than collisions with other molecules, as exists in ideal gases or in any gas at low enough pressure, we have the following formula for conductance:

$$F_t = \pi a^2 (2a/3l) v_a = \frac{4\sqrt{2}\, a^3}{3 \times l} \sqrt{\frac{\pi RT}{M}} \qquad (38)$$

For viscous flow, where collisions with other molecules are much more frequent than collisions with the wall, as in the case of liquids or high pressure gases, we have the following formula for conductance:

$$F_v = \frac{\pi \times a^4 \times P}{8 \times \eta \times l} = 0.1472\ a \sqrt{2}\ (PL/RT)\ \pi\ \sigma^2\ F_t \qquad (39)$$

2. Sample Calculation -- Pressure in the Furnace in the Reaction Vessel Shown in Figure 6

In order to calculate the pressure inside the furnace in the reaction vessel from the known flow rate of gases through the furnace, and from the preceding equations (using them in reverse to calculate the pressure from a given dn/dt value), we will have to make certain assumptions regarding flow conditions. We will assume that the furnace nozzle has a 2 mm bore and is 1 mm in length, and that this nozzle offers all the restriction to the flow of the gases through the furnace. We will also assume that $P_1 = 0$, P_2 = unknown, T = 900°C and the flowing gases have an average molecular weight of 66. Using these values substituted in Eq. (38), we obtain a value for F_t of 1.283 liters/sec at all pressures. At a flow rate of 0.6 mmoles/min, or 10^{-5} moles/sec, we would have a pressure in the furnace of 0.57 torr. For viscous flow, assuming a collision cross section of $6.5 \cdot 10^{-8}$ cm, for the same flow under the same conditions, the furnace pressure, calculated from Eq. (39), can be shown to be 0.50 torr, surprisingly almost the same as molecular flow.

APPENDIX C

Sample Calculation -- PF_2 Force Constants Assuming Most Generalized Potential Energy Formula

From Linnett and Heath[47] (see Fig. 3):

$$\lambda_3 = (1/m_Y + 2\sin^2\alpha/m_X)(k_1 - k_{12}) \tag{40}$$

$$\lambda_1 + \lambda_2 = (1/m_Y + 2\cos^2\alpha/m_X)(k_1 + k_{12}) + 2(1/m_Y + 2\sin^2\alpha/m_X)(k_\alpha/l^2)$$

$$-(k_{l\alpha}/l)(8\sin\alpha\cos\alpha/m_X) \tag{41}$$

$$\lambda_1\lambda_2 = \frac{2(1 + 2m_Y/m_X)}{m_Y^2}\left[(k_1 + k_{12})(k_\alpha/l^2) - 2(k_{l\alpha}/l)^2\right] \tag{42}$$

where, $\lambda_n = 4\pi^2c^2\nu_n^2$ and ν_n = wave number of normal mode in Kaysers (see page 41).

For $\nu_1 = 850$, $\nu_2 = 325$ and $\nu_3 = 830$, and assuming a mass conversion factor (amu to gms) has been placed onto the right and left hand sides of Eqs. (40) through (42), we have,

$$\lambda_1 = 4\times3.14159\times2.9979^2\times10^{20}\times1.66028\times10^{-24}\ (\text{gm/amu})\times850^2 = 0.42562\times10^5$$

and likewise, $\lambda_2 = 0.06222\times10^5$ and $\lambda_3 = 0.40582\times10^5$.

Here, $m_X = 30.9738$, $m_Y = 18.9984$ and $2\alpha = 96°$.

From Eq. (42) we have,

$$k_1 + k_{12} = \frac{2.1463 + 2(k_{l\alpha}/l)^2}{(k_\alpha/l^2)} \tag{43}$$

From Eq. (41) we have,

$$k_1 + k_{12} = 5.98236 + 1.57499(k_{l\alpha}/l) - 2.165526(k_\alpha/l^2) \tag{44}$$

Equating Eqs. (43) and (44), we have,

$$2.1463 + 2(k_{1\alpha}/1)^2 = 5.98236(k_\alpha/1^2) + 1.57499(k_{1\alpha}/1)(k_\alpha/1^2) - 2.165526\,(k_\alpha/1^2)^2 \qquad (45)$$

Now taking a derivative with respect to $(k_{1\alpha}/1)$, we let $\dfrac{d(k_\alpha/1^2)}{d(k_{1\alpha}/1)} = 0$ for a minimum in $(k_\alpha/1^2)$, and we obtain,

$$(k_{1\alpha}/1) = 0.393747\,(k_\alpha/1^2) \qquad (46)$$

Substituting Eq. (46) into (45) we have,

$$1.85545(k_\alpha/1^2)^2 - 5.98236(k_\alpha/1^2) + 2.146364 = 0 \qquad (47)$$

Solving Eq. (47), we have $k_\alpha/1^2 = 2.81297$ and 0.411233. Taking only the last value as physically meaningful, we find:

$$k_\alpha/1^2 = 0.411233,$$

$$k_{1\alpha}/1 = 0.16192,$$

$$k_{12} = 0.37532,$$

and,

$$k_1 = 4.97153,$$

all in units of millidynes/Å.

APPENDIX D

1. The ECOM Computer Program

```
CCOMPUTATION OF ENTROPY FROM MW,D,S,W DATA
      DIMENSION W(8),SV(8),DVH(8)
      REAL MW
505   IF(EOF,2)17,1
1     READ(2,2)T,MW,D,S,AC
      READ(2,3)(W(J),J=1,8)
2     FORMAT(4F10.3,A40)
3     FORMAT(8F10.1)
      STR=(1.987/2.0)*(3.0*ALOG(MW)+5.0*ALOG(T))-2.315
      SROT=1.987*(0.5*ALOG(D) + 1.5*ALOG(T)-ALOG(S))-0.033
      DO 4 J=1,8
      U=1.4387*W(J)/T$ U2=1.4387*W(J)/298.15
      IF(U)8,7,8
7     SV(J)=0.0$DVH(J)=0.0
      GO TO 4
8     SV(J)=1.987*(U/(EXP(U)-1.0)-ALOG(1.0-EXP(-U)))
      DVH(J) =1.987*((T*U*EXP(-U)/(1.-EXP(-U)))-(298.15*
     CU2 * EXP(-U2)/(1.-EXP(-U2))))/1000.0
4     CONTINUE
      PRINT 5,STR,SROT,AC
5     FORMAT(//*TRANSLATIONAL ENTROPY = *F13.7,5X*ROTATIONAL ENTROPY = *
     CF13.7,A26)
      PRINT 6,(SV(J),J=1,8)
6     FORMAT(*SEPARATE SV$S = *8F10.5)
      VHD=0.0$TSV=0.0
      DO 14 J=1,8
      VHD = VHD + DVH(J)
      TSV = TSV + SV(J)
14    CONTINUE
      TOTS=TSV+STR+SROT
      PRINT 9,TSV,TOTS,T,MW,D,S
9     FORMAT(*TOTAL VIB. ENTROPY = *F10.6,4X*TOTAL ENTROPY = *
     CF11.7,2XF6.1* DEGREES*F9.4* = MOLECULAR WEIGHT   D =* F11.4,F5.1*
     C= S*)
      PRINT 10,(W(J) ,J=1,8)
10    FORMAT(* OMEGAS = * 7X8F10.2)
      DIFH = VHD + 4.0*1.987*(T-298.15)/1000.0
      PRINT 15,VHD,DIFH
15    FORMAT(*ENTHALPY DIFFERENCE FROM H AT 298.15.   VIB. CONTRIBUTION
     C=* F9.5,8X*TOTAL INCREMENT =*F10.5)
      GO TO 505
17    RETURN
      END
```

2. The PFIT Computer Program

```
CITERATION METHOD ON P -F SYSTEM
      DIMENSION DFF(8),U(8)
      REAL LK(8),K
10    FORMAT(5F12.5)
2     BOOK=0.0
      IF(EOF,2)6,78
78    READ(2,10) CPF3,CP4,FPRAT,TOTP,T
11    FORMAT(8F10.5)
7     READ(2,11) (LK(J),J=1,8)
      READ(2,11)(U(J),J=1,8)
      DO 4 J=1,8
      IF(U(J))8,4,8
4     CONTINUE
      GO TO 9
8     BOOK = 2.0
12    FORMAT(//29HFLUORINE/PHOSPHORUS RATIO =  F6.3,6X14HTEMPERATURE =
     CF8.2,6X17HTOTAL PRESSURE = ,F7.3,X4HTORR/ 30H+INITIAL CONCENTRATIO
     CNS ARE - )
9     PRINT 12,FPRAT,T,TOTP
13    FORMAT(31X6HPF3 = ,E13.4,12H TORR, P4 = ,E13.4,5H TORR)
      PRINT 13,CPF3,CP4
14    FORMAT(/  34HASSUMED FREE ENERGIES OF FORMATION,/1H-9X3HPF39X3HPF2
     C11X2HPF12X1HF12X1HP11X2HP211X2HP410X4HP2F2)
505   DO 15 J=1,8
      DFF(J)= -4.575*T*LK(J)
15    CONTINUE
      PRINT 14
16    FORMAT(5HLOGK ,8(F12.5X))
17    FORMAT(6X8(F12.3X)//)
      PRINT 16,(LK(J),J=1,8)
      PRINT 17,(DFF(J),J=1,8)
      A=0$B=0$C=0
1     K=10.**(12*LK(2)-LK(7)-8*LK(1))
      CPF2=(K*CPF3**8*CP4*760.**3)**(1./12)
      K=10.**(LK(3)+LK(1)-2*LK(2))
      CPF=(K*CPF2**2)/CPF3
      K=10.**(2*LK(6)-LK(7))
      CP2=(K*CP4*760)**.5
      K=10.**(2*LK(5)-LK(6))
      CP=(K*CP2*760)**.5
      K=10.**(LK(5)+LK(4)-LK(3))
      CF=(K*CPF*760)/CP
      K = 10.**(LK(8)-2.*LK(3))
      CP2F2 = (K*CPF**2)/760.
      DIFRAT=(3*CPF3+2*CPF2+CPF+CF+2*CP2F2)/(CPF3+CPF2+CPF+CP+
     C2*CP2+4*CP4+2*CP2F2) - FPRAT
      COMP=CPF3+CPF2+CPF+CF+CP+CP2+CP4+CP2F2-TOTP
      IF(DIFRAT+.04)20,20,21
20    CPF3=CPF3-(CPF3*DIFRAT/(5-C))
      GO TO 22
21    IF(DIFRAT-.04)23,24,24
24    CP4=CP4+(CP4*DIFRAT/(6-C))
22    CP4=CP4-CP4*COMP/7
      IF(CP4) 33,33,34
33    CP4=.1*(C+1)**2/(B**3+1.)
34    CPF3=CPF3-CPF3*COMP/6
      IF(CPF3) 35,35,31
35    CPF3 = (C+1)**2/(B**3+1.)
31    B=B+1
      IF(B-30)1,32,32
32    C=C+1
      B=0.0
      IF(C-5)26,25,25
23    IF(COMP**2-.0011)25,22,22
25    A=1
26    PRRAT = DIFRAT + FPRAT
      PRPRS = COMP + TOTP
27    FORMAT(12HF/P RATIO = F9.6,3X11HPRESSURE = F9.6,5H TORR/7X3HPF3
     C13X3HPF213X2HPF14X1HF15X1HP15X2HP214X2HP414X4HP2F2)
      PRINT 27,PRRAT,PRPRS
28    FORMAT(8(E15.4X)/)
      PRINT 28,CPF3,CPF2,CPF,CF,CP,CP2,CP4,CP2F2
      IF(A-1)1,42,1
42    IF(BOOK)2,2,43
43    BOOK = BOOK - 1.0
      IF(BOOK)2,52,51
51    DO 53 J=1,8
      LK(J)=LK(J)+U(J)
53    CONTINUE
      GO TO 505
52    DO 54 J=1,8
      LK(J) = LK(J)-2.0*U(J)
54    CONTINUE
      GO TO 505
6     RETURN
      END
```

APPENDIX E

1. Sample Calculation -- Determination of ΔF°_T for PF_2 at 1200°K from the Output of ECOM and JANAF Data

ECOM gives S°_T and ΔH°_{T-298} for the compound and the JANAF tables give S°_T and ΔH°_{298} for the elements.

For PF_2 at 1200°K, we have, $\frac{1}{2} P_2 + F_2 \rightarrow PF_2$

ENTROPY

$$\Delta S^\circ_f (PF_2) = S^\circ(PF_2) - S^\circ(F_2) - \tfrac{1}{2}S^\circ(P_2)$$

$63.811 \div 2 = -31.905$

-60.084

-91.989

$+80.242$

-11.747

so, $\Delta S^\circ_f (PF_2) = -11.747$ cal/deg mole at 1200°K

ENTHALPY

Estimated $\Delta H^\circ_{f_{298}}$ for PF_2 is -114 kcal/mole, $P(r) + F_2 \rightarrow PF_2$ ΔH = -114 kcal/mole

$$\Delta(\Delta H^\circ) \text{ from } 298^\circ \text{ to } 1200^\circ = \Delta H^\circ(PF_2) - \Delta H^\circ(P(r)) - \Delta H^\circ(F_2)$$

-7.690

-6.021

-13.711

$-114.$

$+11.552$

-2.16

-2.159

$\Delta H_{f_{1200}} = -116.16$

We must now shift to the standard states:

$1/2\ P_2 \rightarrow P(r)$	$\Delta H_r = -19.17$
$P(r) + F_2 \rightarrow PF_2$	$\Delta H_r = -116.16$
$1/2\ P_2 + F_2 \rightarrow PF_2$	$\Delta H = -135.33$

$$\Delta H^\circ_{f_{1200}} = -135.33 \text{ kcal/mole}$$

FREE ENERGY

$$\Delta F^\circ_{f_{1200}} = \Delta H^\circ_{f_{1200}} - T\,\Delta S^\circ_{f_{1200}}$$

$$\begin{array}{r} -135.33 \\ +\ 14.1 \\ \hline -121.2 \end{array}$$

$$\Delta F^\circ_{f_{1200}} = -121.2 \text{ kcal/mole}$$

2. Sample Calculation - Equilibrium Concentrations of Species in the $2PF_2 \leftrightharpoons PF + PF_3$ Reaction at 1100°K

For, $P_2F_4(g) \leftrightharpoons PF(g) + PF_3(g)$ at 1200°K we have,

$$\Delta F^\circ_{f_{1200}}\ (P_2F_4) = -218.1 \text{ kcal/mole}$$

$$\Delta F^\circ_{f_{1200}}\ (PF_3) = -205.3 \text{ kcal/mole}$$

$$\Delta F^\circ_{f_{1200}}\ (PF) = -39.5 \text{ kcal/mole}$$

so $$\Delta F_{Rx_{1200}} = -26.7 \text{ kcal/mole}$$

where the word "mole" stands for one mole of the compound in question,

or one mole of reactants going to one mole of products.

From $\Delta F_{Rx} = -RT\ln K_p$ Eq. (19), we have,

$$K_p = 10^{\left(\frac{26.7 \times 1000}{4.575 \times 1200}\right)}$$

where, $R\ln 10 = 4.575$ cal/deg mole.

K_p for this reaction comes out to 73,011, so that mostly PF and PF_3 exist at equilibrium at 1200°K. With a total pressure of two torr, we can assume that the concentrations of PF and PF_3 would each be 1.00 torr partial pressure, making the concentration of P_2F_4 equal to:

$$\frac{[PF][PF_3]}{K_p} = 1/(73{,}011 \times 760) = 1.82 \times 10^{-8} \text{ torr.}$$

APPENDIX F

[Reprinted from Inorganic Chemistry, 7, 2157 (1968).]

CONTRIBUTION FROM THE DEPARTMENT OF CHEMISTRY, UNIVERSITY OF CALIFORNIA, BERKELEY, CALIFORNIA

The Reaction of Silicon Difluoride with Germane

BY D. SOLAN AND P. L. TIMMS[1]

Received August 28, 1967

Gaseous silicon difluoride, prepared at high temperatures from silicon and silicon tetrafluoride, has been shown to react with many volatile compounds upon cocondensation at low temperatures.[2-4]

These reactions of silicon difluoride provide a convenient way of preparing types of compounds containing one or, more commonly, two or three $-SiF_2-$ groups, which are difficult to synthesize by other methods.[4] A reaction between germane and silicon difluoride thus suggested itself as a method of making compounds which would be analogs of the known silicon–germanium hydrides[5,6] but with $-SiH_2-$ groups replaced by $-SiF_2-$ groups. An attempt to make fully fluorinated germanium–silicon compounds from silicon difluoride and germanium tetrafluoride had led to the explosive formation of silicon tetrafluoride and germanium fluoride polymers instead of the desired products.[7]

Results

Condensation of a low-pressure gaseous mixture containing silicon difluoride, silicon tetrafluoride, and germane in a roughly 4:2:3 mole ratio, at −196°, gave an orange-yellow solid. When this solid was warmed under vacuum, unreacted silicon tetrafluoride and germane were pumped off first, followed by a mixture of reaction products. The solid became colorless as it warmed up, and at about 0° it melted and foamed vigorously. The residue at room temperature was an air-sensitive, viscous liquid, containing mainly silicon and fluorine with a little germanium and hydrogen. At least 80% of the silicon difluoride which had been condensed was retained in this residue, and the remainder was combined in the volatile products.

Reaction also occurred if a mixture of silicon difluoride and tetrafluoride in a 2:1 mole ratio was first condensed at −196°, and then germane was condensed on top of it. The behavior of the combined condensate on warming was similar to that observed when the components were cocondensed. However, the yield of volatile reaction products was lower than with cocondensation.

(1) Department of Inorganic Chemistry, University of Bristol, Bristol, England.

(2) D. C. Pease, U. S. Patent 3,026,173 (March 20, 1962), assigned to the Du Pont Co., Wilmington, Del.

(3) P. L. Timms, R. A. Kent, T. C. Ehlert, and J. L. Margrave, *J. Am. Chem. Soc.*, **87**, 2824 (1965).

(4) P. L. Timms, T. C. Ehlert, J. L. Margrave, F. E. Brinckman, T. C. Farrar, and T. D. Coyle, *ibid.*, 3819 (1965).

(5) A. G. MacDiarmid and E. J. Spanier, *Inorg. Chem.*, **2**, 215 (1963).

(6) P. L. Timms, C. C. Simpson, and C. S. G. Phillips, *J. Chem. Soc.*, 279, 1467 (1964).

(7) P. L. Timms and J. L. Margrave, unpublished work, Rice University.

TABLE I

MASS SPECTRA OF THE GERMYLFLUOROSILANES AT 50 eV

m/e	Assignment	Intensity (relative to $Ge-GeH_2$ = 100)		
		GeH_3SiF_2H	$GeH_3Si_2F_4H$	$GeH_3Si_2F_6H$
47	SiF^+	40	83	12
66	SiF_2^+	20	7.5	...
67	SiF_2H^+	5	7.5	1.5
70–78[a]	$Ge-GeH_2^+$	100	100	100
85	SiF_3^+	20[b]	15	13
99–106[a]	$GeSiH-GeSiH_2^+$	...	5	68
113	SiF_3^+	...	...	3
114	$Si_2F_3H^+$	...	1.5	2
117–125[a]	$GeSiF-GeSiFH_2^+$	9	10	76
133	$Si_2F_4H^+$	...	1	...
136–145[a]	$GeSiF_2-GeSiF_2H_3^+$	33	22	66
145–153[a]	$GeSi_2F-GeSi_2FH_2^+$	...	...	63
155–163[a]	$GeSiF_3-GeSiF_3H_2^+$	3[b]	...	...
151	$Si_2F_5^+$	...	2[b]	...
183–192[a]	$GeSi_2F_3-GeSi_2F_3H_3^+$	...	7.5	53
203–211[a]	$GeSi_2F_4H-GeSi_2F_4H_3^+$	...	8	79
250–257[a]	$GeSi_3F_5H-GeSi_3F_5H_2^+$	...	...	48
269–277[a]	$GeSi_3F_6H-GeSi_3F_6H_3^+$	...	...	50

[a] The intensities are based on the sum of the heights of all of the peaks within the given mass range. [b] Peaks believed due to impurities in the germylfluorosilanes.

For either of the above reaction conditions, the products pumped off during warm-up proved to be a very complex mixture of compounds. The mixture could not be separated completely even using an efficient low-pressure distillation column. Attempts to use gas chromatography to separate the mixture, which had been very successful for the silicon–germanium hydrides,[6] caused complete decomposition of the products.

Five main fractions were collected, the compositions of which, judged by their mass spectra, were not appreciably changed by further distillation on the column. Two of the fractions were shown by their mass and infrared spectra to be nearly pure samples of the known perfluorosilanes Si_2F_6 and Si_3F_8.[3] The other three fractions were quite widely separated from one another in volatility. The amounts obtained of each decreased sharply from the most to the least volatile.

The mass spectra of the three fractions (Table I) showed that each contained the elements germanium, silicon, fluorine, and hydrogen. For all three, the most abundant group of ions was at m/e 70–78 corresponding to $^{70}Ge^+$–$^{76}GeH_2^+$. With the fractions considered in decreasing order of volatility, the most intense peaks at high m/e corresponded to $GeSiF_2H_3^+$, $GeSi_2F_4H_3^+$, and $GeSi_3F_6H_3^+$, respectively. The loss of at least one hydrogen atom on electron impact is known to occur frequently with the higher germanes and silanes.[8] Thus these ions suggested that the parent species were the saturated compounds containing one more hydrogen atom of molecular formula $GeSiF_2H_4$, $GeSi_2F_4H_4$, and $GeSi_3F_6H_4$, respectively.

The ions SiF_3^+ and $GeSiF_3H_2^+$ seen in the mass spectrum of the $GeSiF_2H_4$ fraction indicated a compound $GeSiF_3H_3$ as a possible impurity. Similarly, the small amount of the $Si_2F_5^+$ ion seen in the spectrum of the $GeSi_2F_4H_4$ fraction suggested that a compound containing an $-Si_2F_5$ group was present, but no more positive identification was possible.

Vapor density measurements on the $GeSiF_2H_4$ and $GeSi_2F_4H_4$ fractions gave values close to those expected for these formulas. Small amounts of impurities like $GeSiF_3H_3$, slightly richer in fluorine, would not have much effect on these measurements. Instability and low volatility prevented a vapor density determination on the $GeSi_3F_6H_4$ fraction.

The infrared spectra of the vapors of the three fractions each showed a strong absorption in the ranges 2190–2215, 2076–2150, and 774–778 cm^{-1}. These were assigned, respectively, by analogy with the silanes and germanes, to Si–H and Ge–H stretching frequencies and a GeH_3 symmetrical deformation frequency.[9] The group of strong absorptions in the 800–980-cm^{-1} range in all of the spectra could be assigned to Si–F stretching frequencies.[3]

On the basis of the infrared and mass spectra results, the structure of the main components of each fraction was indicated to be of the type $GeH_3Si_nF_{2n}H$. The position of the hydrogen atom attached to silicon in $GeH_3Si_2F_4H$ and $GeH_3Si_3F_6H$ was left uncertain by these results. Final confirmation of the structures of the components of the two most volatile fractions was obtained from their nmr spectra, but $GeH_3Si_3F_6H$ proved too unstable in the liquid phase to obtain reproducible nmr spectra.

The proton nmr spectra (Table II) showed resonances with chemical shifts similar to those of known fluorosilanes[10] and germanes.[11] The observed splittings corresponded to expected first-order interactions in the structures GeH_3SiF_2H and $GeH_3SiF_2SiF_2H$. In the spectrum of the GeH_3SiF_2H fraction, the ratio of the area of the Ge–H to Si–H resonances was 3.3:1.0. The ^{19}F nmr spectrum of the sample showed, in addi-

(8) F. E. Saalfeld and H. J. Svec, *Inorg. Chem.*, **2**, 50 (1963).

(9) W. L. Jolly, *J. Am. Chem. Soc.*, **85**, 3083 (1963).

(10) E. A. V. Ebsworth, "Volatile Silicon Compounds," Pergamon Press, 1963.

(11) J. E. Drake and W. L. Jolly, *Proc. Chem. Soc.*, 379 (1961).

TABLE II

NMR SPECTRA OF THE GERMYLFLUOROSILANES

Compound	Assignment	Chemical shift, ppm	J_{F-Si-H}, Hz	$J_{F-Si-Ge-H}$, Hz	$J_{H-Si-Ge-H}$, Hz	$J_{F-Si-Si-H}$, Hz	Remarks
		A. ^1H Spectra, $Si(CH_3)_4$ Reference					
GeH_3SiF_2H	Si–H	−4.96	53		3		Triplet of quartets
	Ge–H	−2.72		9	3		Triplet of doublets
$GeH_3SiF_2SiF_2H$	Si–H	−4.74	55			5	Triplet of triplets
	Ge–H	−3.00		7.5			Triplet
		B. ^{19}F Spectra, external CCl_3F Reference					
GeH_3SiF_2H	Si–F	+126.6	54.5	8			Doublet of quartets
		$J_{^{29}Si-F}$ = 344 Hz					Doublet of doublets of quartets
GeH_3SiF_3?	Si–F	+106		8			Quartet
		$J_{^{29}Si-F}$ = 343 Hz					Doublet of quartets

tion to the doublet of quartets expected for GeH_3SiF_2H, another quartet at lower field. The area of this was approximately one-tenth the area of the doublet of quartets. Similar coupling constants were found for these two sets of resonances with both the F–Si–Ge–H and the F–^{29}Si interactions. These results were consistent with the presence of the molecule GeH_3SiF_3 together with GeH_3SiF_2H. This had already been indicated in the mass spectrum of the fraction, and the two compounds would be expected to be of very similar volatility and thus difficult to separate.

The main components of the three fractions can be called germylfluorosilanes. Only the fraction containing GeH_3SiF_2H and GeH_3SiF_3, which was gaseous, was stable at room temperature. The other two fractions, particularly the $GeH_3Si_3F_6H$ fraction, decomposed readily above 0°. The fractions were pyrophoric and extremely sensitive to moisture. They all evolved germane on treatment with 10% KOH solution.

Discussion

There is much evidence that the normal pattern of reaction of silicon difluoride with another compound at −196° is as follows.[12,13] Two or more molecules of silicon difluoride come together upon condensation on the cold surface to form a short-lived diradical species. This can either interact immediately with other molecules cocondensed with the silicon difluoride to give products containing two or more silicon atoms or form a less reactive silicon difluoride polymer.

The reaction of silicon difluoride and germane does not fit this pattern. Reaction occurred both when the two compounds were cocondensed and when they were condensed one after the other. The major product containing germanium and silicon was GeH_3SiF_2H and not the disilicon compound. This suggests that germane attacked the silicon chain in a $(SiF_2)_n$ polymer, breaking off units containing one, two, or more silicon atoms. The diminishing stability of the germylfluorosilanes with increasing numbers of $-SiF_2-$ groups illustrates the large effect a germyl group has on an $-SiF_2-$ chain. The fraction containing $GeH_3Si_3F_6H$ gave polymers and lower germylfluorosilanes on decomposition.

Apart from their unexpected low stability, the spectroscopic and other physical properties of the germylfluorosilanes indicate they have some characteristics of both the silicon–germanium hydrides[6] and the perfluorosilanes.[3]

Experimental Section

Silicon difluoride was prepared as previously described[2] at the rate of about 0.8 mmol/min, at a pressure not exceeding 200 μ. It contained unreacted silicon tetrafluoride, the SiF_2:SiF_4 ratio being about 2:1. Germane was made by hydrolysis of magnesium germanide and was carefully distilled before use. It was added to the low-pressure silicon difluoride stream at the rate of about 0.6 mmol/min. The gas mixture was condensed on being pumped through a trap at −196°.

A few millimoles of volatile reaction products were pumped off on warming the above condensate. These were fractionated on a 3 ft long distillation column. The column was of an unpublished design used in the laboratories of R. Schaeffer at Indiana University, in which the volatiles moved under vacuum up the annular space between two vertical, concentric, glass tubes. Cold nitrogen gas, passing into the inner tube from the top, was warmed in passage down the column establishing an axial temperature gradient. The fractions collected off the column were handled in a grease-free vacuum line employing Viton O-ring stopcocks and joints.

Vapor Densities.—The vapor densities of the GeH_3SiF_2H and $GeH_3SiF_2SiF_2H$ fractions were measured on 10-mg samples in a calibrated constant-volume system, using a mercury manometer to determine pressure. The molecular weights were found to be 144 ± 4 (correct for GeH_3SiF_2H, 140; for GeH_3SiF_2H + 10% GeH_3SiF_3, 142) and 208 ± 6 (correct for $GeH_3SiF_2SiF_2H$, 209), respectively.

Mass Spectra.—Samples were evaporated directly from a condensed phase into the ion-source region of a Bendix Model 1400 time-of-flight mass spectrometer equipped with an all-glass input system. This method was well suited to getting reliable spectra for the less stable germylfluorosilanes.

Infrared Spectra.—All spectra were taken in the vapor phase at 5–20 mm in 6-cm glass cells with KBr or NaCl windows using an Infracord spectrometer. Quite rapid decomposition of $GeH_3Si_3F_6H$ was noticed. The observed frequencies (cm^{-1}) for the three germylfluorosilane fractions were as follows (intensities in parentheses): GeH_3SiF_2H: 2198 (s), 2090 (s), 980 (m), 960 (s), 885 (s), 870 (s), 774 (vs); $GeH_3Si_2F_4H$: 2190 (s), 2076 (s), 981 (m), 957 (s), 932 (vs), 884 (m), 844 (s), 807 (s), 778 (vs), 546 (m); $GeH_3Si_3F_6H$: 2215 (m), 2105 (m), 968 (vs), 945 (s), 870 (s), 850 (vs), 826 (m), 809 (m), 779 (s).

Nmr Spectra.—Proton nmr spectra were run on a Varian A-60 spectrometer using neat liquid samples containing about 2% tetramethylsilane, contained in 3-mm bore, thick-walled tubes.

(12) J. M. Bassler, P. L. Timms, and J. L. Margrave, *Inorg. Chem.*, **5**, 729 (1966).

(13) H. P. Hopkins, J. C. Thompson, and J. L. Margrave, *J. Am. Chem. Soc.*, **90**, 901 (1968).

Spectra were run at −30° for GeH_3SiF_2H and at 0° for $GeH_3Si_2F_4H$. The ^{19}F spectrum of GeH_3SiF_2H was obtained on a Varian HR-100 spectrometer at 94.1 Mc.

Physical Properties.—The melting points of the GeH_3SiF_2H and $GeH_3Si_2F_4H$ fractions were measured by the Stock ring method at −77 and −4°, respectively. Vapor pressure measurements on the GeH_3SiF_2H fraction over the temperature range −70 to −10° and on the $GeH_3Si_2F_4H$ fraction over the temperature range −40 to −4° gave log p *vs.* $1/T$ plots which could be fitted approximately to the equations $\log p_{mm} = 6.93 - (1162/T)$ and $\log p_{mm} = 10.10 - (2365/T)$. From the vapor pressure equation of the liquid GeH_3SiF_2H fraction, the boiling point of the compound is estimated to be 13°.

The Reaction with KOH.—A sample of the GeH_3SiF_2H fraction, corresponding to 0.30 mmol, was condensed on top of 5 ml of 10% KOH solution frozen in an ampoule. The ampoule was sealed, warmed to room temperature to allow reaction to occur, and then reopened on the vacuum line. The gas pumped out contained 0.28 mmol of germane, 94% of the theoretical yield.

Acknowledgments.—This work was supported by the Army Research Office, Durham, N. C. We also wish to thank the Germanium Information Center for a gift of germanium metal and the National Science Foundation for a fellowship to D. S.

Reprinted from

APPENDIX G

Chemical Communications

NUMBER 23/1968 4 DECEMBER

The Thermal Dissociation of Diphosphoros Tetrafluoride and the Formation of Tetraphosphorus Hexafluoride

By D. Solan and P. L. Timms*†

(*Department of Chemistry, University of California, Berkeley, California, U.S.A.*)

The Chemical Society

Burlington House London W1V 0BN

The Thermal Dissociation of Diphosphoros Tetrafluoride and the Formation of Tetraphosphorus Hexafluoride

By D. SOLAN and P. L. TIMMS*†

(*Department of Chemistry, University of California, Berkeley, California, U.S.A.*)

IT is well known that dinitrogen tetrafluoride, N_2F_4, dissociates readily into $\cdot NF_2$ radicals.[1] By analogy, the compound P_2F_4, described by Parry[2] and Colburn,[3] might be expected to dissociate thermally into $\cdot PF_2$ radicals, but only tentative evidence for this has been previously published.[2,4]

In an attempt to demonstrate the formation of $\cdot PF_2$, the thermal decomposition of P_2F_4 has been studied by mass spectrometry. Gaseous P_2F_4, at a maximum pressure of about 2 mtorr, was passed through a 5-mm. bore quartz tube, which could be heated. The gas emerged from the tube into the ionization region of a Bendix time-of-flight mass spectrometer. The conditions were chosen to give rapid escape of unstable species from the quartz tube into the mass spectrometer, but thermodynamic equilibrium was not established within the tube.

As the tube temperature was raised from 25 to 900°, the mass spectrum of the effluent gas, taken at 20 ev, showed only peaks normally present in the spectrum of P_2F_4, but their relative intensities

† Present address: School of Chemistry, University of Bristol, Bristol 8.

changed. Above 350°, the intensity of $P_2F_3^+$ and $P_2F_4^+$ was observed to decrease, and that of PF_2^+ to increase with temperature. By 700°, the ratios of the intensities $PF_2^+ : P_2F_3^+$ and $PF_2^+ : P_2F_4^+$ had each increased ten-fold over their value in the spectrum of P_2F_4.

At 13 ev, no spectrum was seen for the effluent gas with the tube temperature below 350°. Above 350°, PF_2^+ appeared and increased in intensity with temperature. Up to 900° no other ions were detected.

These results indicate that the $\cdot PF_2$ radical was being formed by dissociation of P_2F_4 at high temperatures and low pressures, and that it was probably the only new species generated under the experimental conditions.

When gaseous P_2F_4 was passed through a quartz furnace at 900° at a pressure of about 3 torr, and thence by a collision-free path to a liquid-nitrogen cooled surface, a transparent yellow solid collected (the e.s.r. spectrum of such a solid in a parallel experiment, showed it contained up to 1% of a free radical, possibly $\cdot PF_2$). On warming the deposit to room temperature, PF_3 and P_2F_4 were pumped off, followed by several highly unstable fractions which deposited yellow phosphorus–fluorine polymers on the walls of the vacuum system wherever they were condensed. From this mixture, low temperature fractional distillation eventually yielded a small amount of a less unstable colourless liquid.

The mass spectrum of this liquid showed that it contained only phosphorus and fluorine. The highest molecular weight ion appeared at *m/e* 238, corresponding to $P_4F_6^+$, and the PF_2^+ ion was the most intense in the spectrum at 50 ev.

The ^{19}F n.m.r. spectrum (94·1 MHz) of the liquid at −30°, showed a doublet of doublets centred at +88 p.p.m. relative to CCl_3F. The ^{31}P n.m.r. spectrum (40·5 MHz) showed a triplet of doublets of triplets, and a less intense quartet of septets 245 p.p.m. upfield. The area ratio of these two features was three to one. The spectra were those expected for first order P–F, P–P–F, P–P, and P–P–P splittings in a structure $P(PF_2)_3$. However, neither spectrum was simple first-order, as each had impressed upon the above first-order form many other lines of lesser intensity. Fortunately, this second-order form was much less dominant than has been described for P_2F_4,[5] where it was due to the magnetic non-equivalence of the phosphorus and fluorine nuclei. The observed splittings in the ^{19}F and ^{31}P spectra were in agreement, giving approximate coupling-constants (considering only first order interactions), J_{PPP} 36 Hz, J_{PPF} 61 Hz, J_{PP} 323 Hz, and J_{PF} 1225 Hz.

The compound $P(PF_2)_3$ melts at −68°. It decomposes very rapidly in the vapour phase, and in the liquid phase above 10°.

A more detailed study of the high temperature decomposition of P_2F_4 and of the properties of $P(PF_2)_3$ is in progress.

This research was supported by the U.S. Army Research Office at Durham, North Carolina. A Fellowship from the National Science Foundation helped support one of the authors (D.S.).

(*Received, October 7th*, 1968; *Com.* 1368.)

[1] F. A. Johnson and C. B. Colburn, *J. Amer. Chem. Soc.*, 1961, **83**, 3043.
[2] R. W. Rudolph, R. C. Taylor, and R. W. Parry, *J. Amer. Chem. Soc.*, 1966, **88**, 3729.
[3] M. Lustig, J. K. Ruff, and C. B. Colburn, *J. Amer. Chem. Soc.*, 1966, **88**, 3875.
[4] K. W. Morse and R. W. Parry, *J. Amer. Chem. Soc.*, 1967, **89**, 172.
[5] F. A. Johnson and R. W. Rudolph, *J. Chem. Phys.*, 1967, **47**, 5449.

LIST OF REFERENCES

1. M. Gomberg, J. Amer. Chem. Soc. 22, 757 (1900).

2. P. L. Timms, J. Amer. Chem. Soc. 89, 1629 (1967).

3. A. G. Anastassiou and H. E. Simmons, J. Amer. Chem. Soc. 89, 3177 (1967).

4. P. S. Skell, L. D. Wescott, Jr., J. P. Golstein and R. R. Engel, J. Amer. Chem. Soc. 87, 2829 (1965).

5. P. S. Skell and E. J. Goldstein, J. Amer. Chem. Soc. 86, 1442 (1964).

6. R. A. Mitsch, J. Heterocyclic Chem. 1, 59, 225 (1964); J. Amer. Chem. Soc. 87, 758 (1965).

7. P. S. Skell and R. C. Woodworth, J. Amer. Chem. Soc. 78, 4496 (1956).

8. G. N. Lewis, T. T. Magel and D. Lipkin, J. Amer. Chem. Soc. 64, 1774 and 2801 (1942).

9. G. Porter and I. Norman, Nature 174, 508 (1954).

10. E. Whittle, D. A. Dows and G. C. Pimentel, J. Chem. Phys. 22, 1943 (1954).

11. E. D. Becker and G. C. Pimentel, J. Chem. Phys. 25, 224 (1956).

12. E. D. Becker, G. C. Pimentel and M. Van Thiel, J. Chem. Phys. 26, 145 (1957).

13. A. Stock, Hydrides of Boron and Silicon, Cornell University Press, Ithaca, New York, 1933.

14. J. Trotter, M. Akhtar and N. Bartlett, J. Chem. Soc. - Inorg., Phys. and Theoret. 1966(A), 30.

15. R. F. Porter, Private Communication, 1968.

16. L. M. Dennis and R. W. Work, J. Amer. Chem. Soc. 55, 4486 (1933).

17. P. L. Timms, C. S. G. Phillips and C. C. Simpson, J. Chem. Soc. 1964, 1467.

18. D. C. Pease, U. S. Patent 2,840,588, 1958.

19. P. L. Timms, Preparative Inorganic Reactions, Vol. 4, ed. W. L. Jolly, Interscience Publishers, New York, 1968, pp. 59-83.

20. R. W. Randolph, R. C. Taylor and R. W. Parry, J. Amer. Chem. Soc. 88, 3729 (1966).

21. M. Lustig, J. K. Ruff and C. B. Colburn, J. Amer. Chem. Soc. 88, 3875 (1966).

22. F. A. Johnson and C. B. Colburn, J. Amer. Chem. Soc. 83, 3043 (1961).

23. A. O. Diallo, Compt. Rend. 261 (25-6), 5386 (1965).

24. A. Stock and P. Praetorius, Ber. 45, 3568 (1912).

25. See, for instance, H. Poppa, J. Appl. Phys. 38, 3883 (1967).

26. H. S. Peiser, Formation and Trapping of Free Radicals, Chap. 9, eds. A. M. Bass and H. P. Broida, Academic Press, New York, 1960.

27. H. J. De Nordwall and L. A. K. Stavely, Trans. Faraday Soc. 52, 1061 and 1207 (1956).

28. J. L. Jackson, J. Chem. Phys. 28, 1101 (1958).

29. G. E. Leroi, G. E. Ewing and G. C. Pimentel, J. Chem. Phys. 40, 2298 (1964).

30. G. C. Pimentel, Private Communication, 1968.

31. M. M. Rochkind, Anal. Chem. 39, 567 (1967) and Science 160, 196 (1968).

32. P. L. Timms, Inorg. Chem. 7, 387 (1968).

33. P. L. Timms, Private Communication, 1968.

34. H. Staudinger and W. Kreis, Helvetica Chimica Acta 8, 71 (1925).

35. F. O. Rice and C. Sparrow, J. Amer. Chem. Soc. 75, 848 (1953).

36. J. C. Thompson and J. L. Margrave, Science 155, 669 (1967).

37. P. Harteck and V. Kopsch, Z. Physik. Chem. B12, 327 (1931).

38. K. H. Geib and P. Harteck, Trans. Faraday Soc. 30(1), 131 (1934).

39. I. Haller and G. C. Pimentel, J. Amer. Chem. Soc. 84, 2855 (1962).

40. R. Klein and M. D. Scheer, J. Phys. Chem. 62, 1011 (1958).

41. K. Stewart, Trans. Faraday Soc. 41, 663 (1945).

42. F. O. Rice and M. Freamo, J. Amer. Chem. Soc. 73, 5529 (1951).

43. P. S. Skell and R. R. Engel, J. Amer. Chem. Soc. 88, 3749 (1966).

44. P. S. Skell and R. R. Engel, J. Amer. Chem. Soc. 88, 4883 (1966).

45. G. Herzberg, Molecular Spectra and Molecular Structure I, Spectra of Diatomic Molecules, D. Van Nostrand Co., Inc., Princeton, New Jersey, 1950.

46. G. Herzberg, Molecular Spectra and Molecular Structure II, Infrared and Raman Spectra of Polyatomic Molecules, D. Van Nostrand Co., Inc., Princeton, New Jersey, 1945.

47. J. W. Linnett and D. F. Heath, Trans. Faraday Soc. 48, 592 (1952).

48. F. A. Cotton, Chemical Applications of Group Theory, John Wiley and Sons, Inc., New York, 1963, pp. 270-275.

49. A. S. Davydov, Quantum Mechanics, NEO Press, Ann Arbor, Michigan, 1966, pp. 516-516b.

50. G. N. Lewis and M. Randall, Thermodynamics, 2nd ed., rev. by K. S. Pitzer and L. Brewer, McGraw-Hill Book Company, New York, New York, 1961.

51. F. J. Adrian, J. Chem. Phys. 36, 1692 (1962).

52. F. O. Rice and M. Freamo, J. Amer. Chem. Soc. 75, 548 (1953).

53. I. L. Mador and M. C. Williams, J. Chem. Phys. 22, 1627 (1954).

54. D. A. Dows, G. C. Pimentel and E. Whittle, J. Chem. Phys. 23, 1606 (1955).

55. M. M. Rochkind, Anal. Chem. 40, 762 (1968).

56. G. C. Pimentel, Spectrochimica Acta 12, 95 (1958).

57. P. H. Kasai and E. B. Whipple, Molecular Physics 9(5), 497 (1965).

58. G. D. Brabson, Ph.D. Thesis, Lawrence Radiation Laboratory, (UCRL-11976), August, 1965.

59. H. S. Booth and A. R. Bozarth, J. Amer. Chem. Soc. 61, 2930 (1939).

60. S. Dushman, Scientific Foundations of Vacuum Technique, 2nd ed., John Wiley and Sons, New York, New York, 1962, pp. 80-107.

61. R. Kirk, Private Communication, 1969.

62. B. A. King, Ph.D. Thesis, Lawrence Radiation Laboratory (UCRL-18618), p. 67 (November, 1968).

63. R. C. Petry, J. Amer. Chem. Soc. 82, 2400 (1960).

64. R. W. Rudolph, Private Communication, 1969.

65. W. F. Hillebrand and G. E. F. Lundell, Applied Inorganic Analysis, 2nd ed., John Wiley and Sons, Inc., 1953, p. 945.

66. Values taken from C. E. Moore, Atomic Energy Levels, Vol. 3, Nat. Bur. Std. Circ. 467, Washington, D. C., 1958.

67. G. Herzberg, Proc. Roy. Soc. 262A, 291 (1961).

68. P. J. Fensham, K. Tamaru, M. Boudart and H. Taylor, J. Phys. Chem. 59, 806 (1955).

69. S. N. Glarum and C. A. Kraus, J. Amer. Chem. Soc. 72, 5398 (1950).

70. R. M. Dreyfuss and W. L. Jolly, Inorg. Chem. 7, 2645 (1968).

71. E. Amberger, Angew. Chem. 71(11), 372 (1959).

72. F. O. Rice and K. F. Herzfeld, J. Amer. Chem. Soc. 56, 284 (1934).

73. K. Stokland, Trans. Faraday Soc. 44, 545 (1948).

74. F. X. Powell and D. R. Lide, J. Chem. Phys. 45, 1067 (1966).

75. P. L. Timms, R. A. Kent, T. C. Ehlert and J. L. Margrave, Nature 207, 188 (1965).

76. See M. E. Volpin, Yu. D. Koreshkov, V. G. Dulova and D. N. Kursanov, Tetrahedron 18, 107 (1962); and F. Johnson and R. S. Gohlke, Tetrahedron Letters 26, 1291 (1962).

77. J. M. Bassler, P. L. Timms and J. L. Margrave, Inorg. Chem. 5, 729 (1966).

78. D. Solan and P. L. Timms, Inorg. Chem. 7, 2157 (1968).

79. E. A. V. Ebsworth, Volatile Silicon Compounds, Pergamon Press, 1963.

80. L. M. Dennis and A. W. Laubengayer, Z. Physik. Chem. 130, 530 (1927); and N. Bartlett and K. C. Yu, Canad. J. Chem. 39, 80 (1961).

81. K. W. Morse and R. W. Parry, J. Amer. Chem. Soc. 89, 172 (1967).

82. T. P. Fehlner, J. Amer. Chem. Soc. 89, 6477 (1967).

83. Joseph G. Morse, Private Communication, 1968.

84. J. K. S. Wan, J. R. Morton and H. J. Bernstein, Canad. J. Chem. 44, 1957 (1966).

85. R. W. Fessenden and R. H. Schuler, J. Chem. Phys. 45, 1845 (1966).

86. J. Gendell, M. S. Wei and J. H. Current, Abstracts of Papers, Minneapolis ACS Meeting, Paper Phys 41, April, 1969.

87. J. H. Current, Private Communication, 1969.

88. R. W. Rudolph and R. W. Parry, Inorg. Chem. 4, 1341 (1965).

89. J. W. Emsley, J. Feeney and L. H. Sutcliffe, High Resolution Nuclear Magnetic Resonance Spectroscopy, Vol. 1, Pergamon Press, 1965, pp. 283-287.

90. F. A. Johnson and R. W. Rudolph, J. Chem. Phys. 47, 5449 (1967).

91. S. L. Manatt, D. D. Elleman, A. H. Cowley and A. B. Burg, J. Amer. Chem. Soc. 89, 4544 (1967).

92. T. P. Fehlner, J. Amer. Chem. Soc. 90, 6062 (1968).

93. T. P. Fehlner, Private Communication, 1969.

94. M. K. Wilson and S. R. Polo, J. Chem. Phys. 20, 1716 (1952).

95. D. M. Yost and T. F. Anderson, J. Chem. Phys. 2, 624 (1934).

96. H. S. Gutowsky and A. D. Liehr, J. Chem. Phys. 20, 1652 (1952).

97. J. E. Griffiths and A. B. Burg, J. Amer. Chem. Soc. 82, 1507 (1960).

98. For instance, see A. B. Burg and K. K. Joshi, J. Amer. Chem. Soc. 86, 355 (1964).

99. R. D. Brown and R. D. Harcourt, Aust. J. Chem. 16, 737 (1963).

100. S. G. Frankiss and F. A. Miller, Spectrochim. Acta 21(7), 1235 (1965).

101. D. R. Lide, Jr. and D. E. Mann, J. Chem. Phys. 31, 1129 (1959).

102. E. R. Nixon, J. Phys. Chem. 60, 1054 (1956).

103. D. W. J. Cruickshank, B. C. Webster and D. F. Mayers, J. Chem. Phys. 40, 3733 (1964).

104. D. P. Craig and E. A. Magnussen, Disc. Faraday Soc. No. 26, 116 (1958).

105. A. B. Burg and J. F. Nixon, J. Amer. Chem. Soc. 86, 356 (1964).

106. P. M. Morse, Phys. Rev. 34, 57 (1929).

107. A. E. Douglas and M. Frackowiak, Canad. J. Phys. 40, 832 (1962).

108. P. Geuter, Zeits. fur Wiss. Phot. 5, 1 (1907).

109. The Dow Chemical Company, JANAF Thermochemical Data, Midland, Michigan, 1961-1965.

110. B. G. DeBoer, A. Zalkin and D. H. Templeton, Inorg. Chem. 8, 386 (1969).

111. R. B. Callen and T. P. Fehlner, Preprint of paper submitted to J. Amer. Chem. Soc. for publication, 1969.

112. Thermodynamic Properties of Individual Substances, Academy of Sciences of the U.S.S.R., Moscow, 1962.

113. P. A. G. O'Hare, The Thermodynamic Properties of P_2, P_4, and Some Phosphorus Fluorides, ANL-7459, December, 1968.

114. H. C. Duus and D. P. Mykytiuk, J. Chem. Eng. Data 9, 585 (1964).

115. D. D. Wagman, W. H. Evans, V. B. Parker, I. Halow, S. M. Bailey and R. H. Schumm, NBS Technical Note 270-3, January, 1968.

116. P. A. G. O'Hare, Private Communication, 1969.

117. P. A. G. O'Hare and W. N. Hubbard, Trans. Faraday Soc. 62(10), 2709 (1966).

118. L. C. Martin, Proc. Roy. Soc. A89, 127 (1913).

119. W. H. Smith and G. E. Leroi, J. Chem. Phys. 45, 1778 (1966).

LEGAL NOTICE